REPORT OF INVESTIGATION

UTAH GEOLOGICAL AND MINERAL SURVEY

NO. 179

EVALUATION OF LOW-TEMPERATURE GEOTHERMAL POTENTIAL IN UTAH AND GOSHEN VALLEYS AND ADJACENT AREAS, UTAH

PART I: GRAVITY SURVEY

by
Deborah Ann Davis and Kenneth L. Cook

April 1983

FOREWORD

Under contract with the U.S. Department of Energy (DOE) the Utah Geological and Mineral Survey (UGMS) has been conducting research to advance the utilization of low-temperature geothermal resources in the State of Utah. Activities related to the contract (originally EG-77-5-7-1679 but later changed to DE-AS07-77ET 28393) began on July 1, 1977.

As part of this ongoing study, Deborah Ann Davis was funded to conduct a gravity survey with emphasis on geothermal areas for Utah and Goshen Valley and adjacent areas, Utah. This work was done for the partial fulfillment of requirements for a Master of Science degree in geophysics from the University of Utah.

Robert H. Klauk
Principal Investigator

ABSTRACT

During 1980 and 1981 a total of 569 new gravity stations were taken in Utah and Goshen Valleys and adjacent areas, Utah. The new stations were combined with 530 other gravity stations taken in previous surveys which resulted in a compilation of 1099 stations which were used in this study. The additional surveys were undertaken to assist in the evaluation of the area for the possible development of geothermal resources by providing an interpreted structural framework by delineating faults, structural trends, intrusions, thickness of valley fill, and increased density of host rock.

The gravity data are presented as (1) a complete Bouguer gravity anomaly map with a 2 mgal contour interval on a scale of 1:100,000 and (2) five generally east-trending gravity profiles. A geologic interpretation of the study area was made from the gravity map and from the interpretive geologic cross sections which were modeled along the gravity profiles.

Two dominant trends of gravity contours are evident on the complete Bouguer gravity anomaly map -- northwest-southeast in the northern part of the study area and northeast-southwest in the southern part; these trends may be related to structural trends of the Sevier orogeny. In addition, the complete Bouguer gravity anomaly map exhibits a pattern of alternating gravity lows and highs over grabens and horsts, respectively, which are separated from each other by bands of closely spaced

gravity contours indicative of large Basin and Range faults. The largest gravity gradients occur along the Utah Lake fault zone and the Wasatch fault zone -- 9 mgal/km over the former in the Saratoga Hot Springs and Crater Hot Springs area and 10 mgal/km over the latter southeast of Provo, Utah.

The gravity data indicate that the Utah Valley graben and the Goshen Valley graben (the two major grabens within the study area) are part of the Wasatch structural trough and as such were displaced downward relative to (1) the Wasatch Range horst on the east, (2) the West Mountain and Warm Springs Mountain horsts in the central part of the study area, and (3) the Oquirrh-Boulter-Tintic fault block on the west. The greatest vertical displacement between the large fault blocks within the survey area is in the southern part of the Utah Valley graben where depth to Paleozoic bedrock is interpreted to be somewhat greater than 4.2 km (13,690 ft). The Goshen Valley graben is interpreted to be complexly faulted and composed of several smaller blocks which exhibit differential displacement along faults or fault zones and whose depth to Paleozoic bedrock is interpreted to be somewhat greater than 1.9 km (6230 ft).

The association of (1) several thermal springs (Saratoga Hot Springs, Lincoln Point Warm Springs, Crater Hot Springs, etc.) with the Utah Lake fault zone, (2) Goshen Warm Springs with the Long Ridge fault, and (3) other springs with other fault zones substantiates the fact that many of the these springs are fault controlled; whereas the interpretive cross sections modeled from the residual gravity anomalies indicate the minimum vertical displacements of the faults. Furthermore, the association of thermal springs with the faults or fault zones suggests that the vertical displacements of the faults or fault zones may be greater than modeled in order for the faults to tap a geothermal reservoir which may exist at depth where the water is heated by the normal geothermal gradient. Alternatively, the greater definition of the underlying structure within the survey area aids in tracing faults through which warm waters are migrating. A small positive residual gravity anomaly associated with Saratoga Hot Springs and Crater Hot Springs is evident on profile A-A' and suggests an increase in density of alluvium and/or underlying Paleozoic bedrock as a result of cementation as the result of circulating hot brines. Although the gravity data apparently, do not delineate any deep intrusive bodies which may represent heat sources, this does not preclude the possibility that these features may exist.

CONTENTS

LIST OF FIGURES

PLATES

LIST OF TABLES

INTRODUCTION

Location and Purpose of Survey

The gravity survey discussed in this report (Fig. 1) is approximately 3,340 km^2 (1,350 mi^2) bounded by latitudes $39^{o}52.5'$ N. and $40^{o}30.0'$ N. and longitudes $111^{o}30'$ E. and $112^{o}7.5'$ E. The study area is located about 56 km (35 mi) southeast of the Great Salt Lake and comprises principally Utah Valley (including Utah Lake), Goshen Valley, and the mountains adjacent to these valleys (Fig. 2). The mountains include the Traverse Mountains, the Lake Mountains, West Mountain, the eastern margin of the East Tintic Mountains, and the western margin of the central Wasatch Range.

A gravity survey was undertaken to assist in the evaluation of the area for the possible development of geothermal resources. The area lies within the Basin and Range province, which is characterized by: 1) high heat flow; 2) Tertiary volcanism; and 3) a thin crust of 20 to 25 km (15 mi) thickness (in comparison with 40 to 50 km (25 to 31 mi) in the Middle Rocky Mountains province). Indeed, the presence of low-temperature (less than $90^{o}C$; Muffler and others, 1981) geothermal activity within the valleys (i.e., Goshen Warm Springs near Goshen, Saratoga Hot Springs at the northwestern margin of Utah Lake, and Crystal Hot Springs in southern Jordan Valley) and warm temperatures obtained from wells in the southern portion of Utah Valley (Goode, 1978 and unpublished Utah Geological and Mineral Survey data) in con-

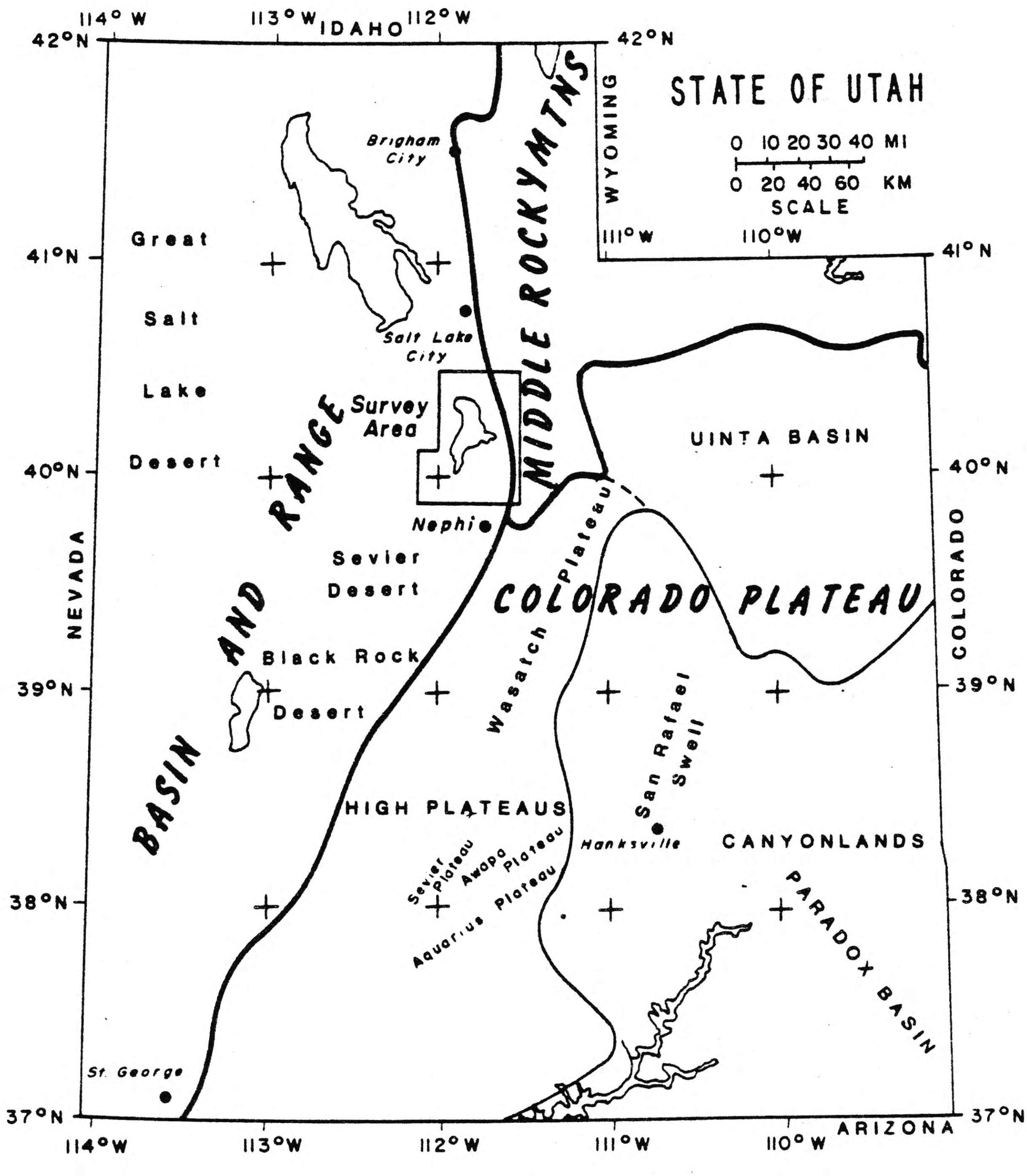

Figure 1. Map of Utah showing location of survey area.

junction with Basin and Range normal faulting and minor east-west faulting, indicate the possibility of low-temperature geothermal resources within the study area.

A gravity survey is helpful in geothermal prospecting by providing a structural framework which may define geothermal targets by delineating faults, structural trends, intrusions, and thickness of valley fill that may be directly or indirectly related to a geothermal resource. Gravity anomaly patterns (gravity highs, gravity lows, and bands of closely spaced gravity contours) usually associated with geothermal systems in the Basin and Range province are generally not any different from those gravity anomalies associated with interpreted structural phenomena (Thangsuphanich, 1976). Geothermal manifestations associated with gravity patterns are as follows: 1) an increased density of sediments or host rock as a result of cementation and/or thermal metamorphism by circulation of hot brine in a liquid dominated hydrothermal system could result in a gravity high (the emplacement of higher density material into lower density material, such as the emplacement of a rhyolite dome into valley sediments may also result in a gravity high); 2) a shallow magma chamber, which might be the direct heat source of the geothermal system, may result in a gravity low; 3) a fault or fault zone, that may serve as a network for the fluid migration, may result in a band or bands of closely spaced gravity contours; and 4) the intersection of faults that may indicate the location of a geothermal reservoir, may result in an intersection of bands of closely spaced contours.

In the Imperial Valley Known Geothermal Resource Area (KGRA) in California south of the Salton Sea, a residual gravity high with a closure of 4 mgal over an area of about 2.5 km^2 (0.9 mi^2) encompasses a region of high heat flow (Coombs and Muffler, 1973) and is believed to be due to an increased density of the sediments due to cementation and/or local thermal metamorphism by the circulation of hot brines within the area (Biehler and Coombs, 1972). The Wairakei Broadlands geothermal field exhibits a gravity high with a 10 mgal closure over an area of 4 km^2 (1.5 mi^2) (Hochstein and Hunt, 1970). In addition, the Glass Mountain KGRA in Siskiyou County, California is centered over a concealed caldera of Miocene age and exhibits a gravity high with a 4 mgal closure over 20 km^2 (7.6 mi^2) (Anderson and Axtell, 1972).

A gravity low associated with geothermal phenomena may be attributed to the presence of a less dense magma chamber surrounded by a higher density volcanic field as in the Geysers geothermal field. The gravity low associated with this field exhibits a 15-20 mgal closure over 525 km^2 (200 mi^2) (Peters, 1974) and indicates a silicic magma chamber at a shallow depth beneath the Clear Lake volcano field (Isherwood, 1975; Anderson and Axtell, 1972).

A band of closely spaced gravity contours associated with geothermal phenomena in the Basin and Range province usually indicates a fault or fault zone through which thermal waters may migrate. For instance, an east-west band of closely spaced gravity contours occurs over Crystal Hot Springs in Jordan Valley, Utah and is interpreted to indicate faults which control the convective system of the springs (Murphy and Gwynn, 1979; Utah Energy Office, 1981). Thus, gravity anomalies are useful in locating the heat source (indirectly), increased density of sediments due to circulation of hot brines, or delineating the geologic structure associated with thermal resources. However, the relationship between the geothermal prospect and the gravity data may not be direct. Therefore, the interpretation of gravity data must take into account geological considerations and obvious geothermal attributes (such as hot springs). In addition, gravity data may aid in a more refined interpretation of subsurface geology and the design of future surveys in the area.

Topography and Physiography

The study area lies within the transition zone between the Basin and Range and Middle Rocky Mountains physiographic provinces (Fenneman, 1928, 1946; Stokes, 1977). Consequently, the Wasatch Range, bordering the Cordilleran Hingeline, is typical not only of the Middle Rocky Mountains physiographic province as defined by Fenneman (1928, 1946), but also of the Wasatch Range and Wasatch Hinterland subdivisions as defined by Stokes (1977). These mountains exhibit extremely rugged relief and trend approximately north-south along the eastern edge of the survey area (Plate 1, in pocket). The highest of the peaks in the Wasatch Range are Mount Timpanogos rising to an elevation of 3570 m (11,722 ft) and Provo Peak at an altitude of 3370 m (11,068 ft) from a base of about 1460 m (4800 ft).

West of the Cordilleran Hingeline, Utah Valley, Jordan Valley, and Juab Valley comprise part of the Wasatch Front Valley physiographic subdivision (Stokes, 1977) which averages only 1460 m (4800 ft) in elevation. Goshen Valley, West Mountain, and the western part of the East Tintic Mountains lie in the Thomas Mountains-Tintic Mountains subdivision (Stokes, 1977); whereas the Lake Mountains and the adjoining area comprise part of the Uinta Extension subdivision. All of these features are part of the Bonneville Basin section of the Basin and Range province (Fenneman; 1928,1946).

Utah Valley is approximately 45 km (28 mi) long and 19 km (12 mi) wide and trends roughly north-south parallel to the Wasatch Range. Located east of the East Tintic Mountains and also trending north-south, Goshen Valley is 19 km (12 mi) long and 13 km (8 mi) wide. Both Utah Valley and Goshen Valley are partly inundated by Utah Lake, which is approximately 10 km (16 mi) wide and 32 km (51 mi) long. Utah Lake is a fresh-water lake recharged primarily by the Provo and American Fork rivers, as well as Dry Creek, and ground water. The lake forms the head waters of the Jordan River which flows northward through the Jordan Narrows into the Jordan River Valley and finally into the Great Salt Lake.

West Mountain and the Lake Mountains trend north-south and rise to 2070 m (6800 ft) and 2320 m (7600 ft), respectively, from 1460 m (4800 ft) at their bases. West Mountain forms the border between Utah Valley and Goshen Valley and is approximately 13 km (8 mi) long. The Lake Mountains form the northwestern boundary of Utah Valley and are also 13 km (8 mi) long.

The East Tintic Mountains rise to an elevation of 2500 m (8200 ft) and form the southwestern boundary of the survey area. The Traverse Mountains are the only east-west trending mountains in the study area and rise to an elevation of 2010 m (6600 ft); these mountains exhibit a more rounded topography and are believed to reflect a mature topographic surface (Hunt and others, 1953).

GENERAL GEOLOGY

Sedimentary and Igneous Rocks

Located within the transition zone between the Middle Rocky Mountains and the Basin and Range provinces, the rocks in the study area reflect a complex history of sedimentation (Plate 2, in pocket). Early in the history of the area, sedimentary rocks were primarily miogeosynclinal in origin; later, sediments varied from continental to transitional shelf deposits (Hintze, 1973).

Precambrian

Rocks of Precambrian age are exposed along the Wasatch Range in isolated localities and are primarily made up of the Big Cottonwood Formation, the Mineral Fork Tillite, and the Mutual Formation. The Big Cottonwood Formation and the Mutual Formation are composed of medium-to-fine-grained clastics (quartz arenites, siltstones). The Mineral Fork Tillite is a glacial deposit composed primarily of gravel. The total thickness of the Precambrian strata varies and is unknown -- the Big Cottonwood formation is 510 m (1675 ft) thick (Morris and Lovering, 1961) in the East Tintic Mountains; and an exposure in Slate Canyon east of Provo reveals more than 300 m (910 ft) of Precambrian strata (Baker, 1947) (Plate 1). The Big Cottonwood Formation and the Mutual Formation are both slightly metamorphosed and represent sediments which accumulated in a major northeast-trending geosynclinal belt more than 1.5 billion years ago.

Paleozoic

Generally, Paleozoic formations are more calcic in character (Fig. 4A) and exhibit a sedimentation pattern consistent with the Cordilleran miogeosynclinal environment and whose depositional extent was primarily governed by the Cordilleran Hingeline. Deposition west of the Hingeline was generally characterized by thick continuous suites of shallow marine sediments (i.e., limestones, shales, and sandstones); whereas eastern Utah was only intermittently covered by marine shelf sediments. Rocks from all periods of this era are exposed along the Wasatch Range, West Mountain, the Lake Mountains, the East Tintic Mountains, and Long Ridge; and total approximately 12,200 m (40,000 ft) in thickness (Baker, 1947).

Middle Cambrian to Middle Devonian sedimentary rocks exemplify this type of environment and are characteristically continuous and of wide areal extent. The Tintic Quartzite represents a marine transgressive series, and the Manning Canyon Shale and the Great Blue Limestone represent marine facies. The Stansbury Disturbance, in Late Devonian time, however, led to deposition of coarse clastic material -- sandstone and conglomerate typified by the Victoria Formation which crops out on Long Ridge near Santaquin and in Rock Canyon near Provo. By Mississippian time, the geosynclinal environment was again dominant and great carbonate banks were built up as exemplified in the Tintic mining district by the Gardison Limestone, the Fitchville Formation, and the Deseret Limestone. Basinal downwarping and cyclothemic sedimentation patterns in the Late Pennsylvanian and Early Permian time resulted in an accumulation of over 7600 m (25,000 ft) (Hintze, 1973) of interfingering carbonates, sands, and shales as seen in the Oquirrh Formation.

Figure 2. Columnar section of (A) Paleozoic rocks and (B) layered Cenozoic rocks, East Tintic mining district (Morris and Lovering, 1979).

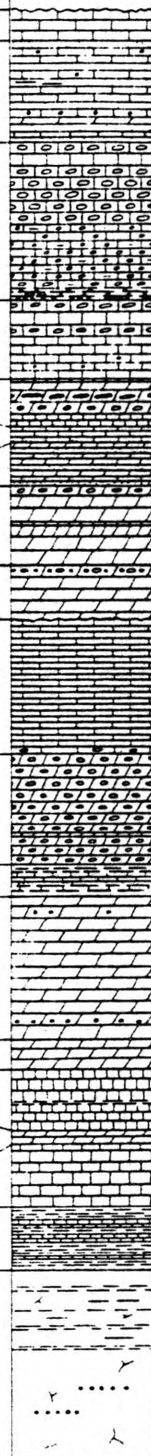

SYSTEM or SERIES	FORMATION	LITHOLOGIC CHARACTER	THICKNESS (FEET)	DESCRIPTION
Upper Mississippian	Great Blue Formation		+100	Topliff Limestone Member: blue-gray limestone
	Humbug Formation		650	Interbedded blue-gray sparsely cherty limestone and persistent lenses of buff sandstone
	Deseret Limestone		1,000-1,100	Uncle Joe Member: light-gray massive cherty coquinoid limestone about 550 feet thick Tetro Member: medium-gray, cherty, sandy, and argillaceous limestone about 475 feet thick Phosphatic shale member: sooty black phosphatic shale and silty limestone 5 - 150 feet thick
Lower Mississippian	Gardison Limestone		500	Upper member, about 125 feet thick, is blue-gray massive cherty limestone. lower member, about 375 feet thick, is blue-gray medium-bedded fossiliferous limestone
Lower Mississippian and Upper Devonian	Fitchville Formation		300	Eight distinctive units of limestone and dolomite, some cherty. Stromatolitic limestone at top
Upper Devonian	Pinyon Peak Limestone		70-125	Blue-gray silt-streaked limestone
	Victoria Formation		250-300	Interbedded gray dolomite and buff quartzite; some lenses of penecontemporaneous breccia
Devonian, Silurian, and Upper Ordovician	Bluebell Dolomite		335-600	Dusky-gray massive dolomite, cherty near top. Prominent stromatolitic dolomite unit 275 - 300 feet above base
Upper Ordovician	Fish Haven Dolomite		200-345	Dusky-gray massive dolomite; mottled and cherty near top
Lower Ordovician	Opohonga Limestone		300-850	Light-blue-gray thin-bedded argillaceous limestone with many thin layers of flat-pebble conglomerate. Cherty and sandy at base
Upper Cambrian	Ajax Dolomite		650	Mostly dusky-blue-gray medium-bedded cherty dolomite. Emerald Member, a thin unit of grayish-white, mottled dolomite, 90 - 180 feet above base
	Opex Formation		145-245	Interbedded sandy limestone, shale, and sandstone
Middle Cambrian	Cole Canyon Dolomite		830-900	Interbedded dusky blue-gray dolomite like Bluebird Dolomite, and creamy white laminated dolomite like Dagmar Dolomite. Sparsely cherty
	Bluebird Dolomite		185	Dusky-gray dolomite with short white markings
	Herkimer Limestone		350-430	Blue-gray argillaceous limestone; zone of gray-green shale about 180 feet above base
	Dagmar Dolomite		65-100	Creamy-white laminated dolomite
	Teutonic Limestone		390-420	Blue-gray argillaceous limestone with pisolitic beds in lower part
	Ophir Formation		375-425	Upper shale member: gray-green shale Middle limestone member: limestone and shale Lower shale member: shale, sandy at base
Lower Cambrian	Tintic Quartzite		+1,200 (Base not exposed)	Buff, prominently bedded quartzite, gray-green phyllitic shale beds in upper 500 feet. Chloritized basalt flow 980 feet above base, and lower 500 feet or so conglomeratic in adjacent areas Total thickness in adjacent areas is 2,300 - 3,200 feet

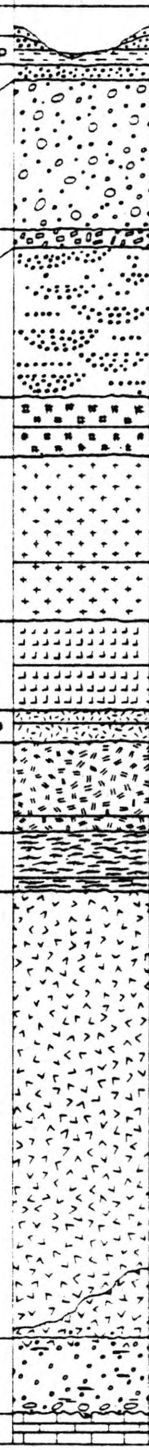

SERIES	GROUP, FORMATION, OR UNIT		LITHOLOGIC CHARACTER	THICKNESS (FEET)	DESCRIPTION
Holocene	Younger alluvium			0 - 50	Alluvium in most modern stream valleys
Pleistocene	Lake Bonneville Group			0 - 200	Lacustrine deposits of Alpine and Bonnevile Formations
	Terrace gravel			0 - 100	Gravel and sand in partly dissected benches
	Older alluvium			0-1,000+	Chiefly fanglomerate underlying thin alluvium and lacustrine deposits in Goshen Valley and the larger stream valleys that extend into the range
Miocene	Silver Shield Quartz Latite			0 - 125	Dark-gray coarse-grained quartz latite porphyry
	Pinyon Creek Conglomerate			0-1,000+	Poorly sorted moderately well stratified conglomerate consisting of boulders and cobbles of volcanic rock embedded in grit and sand; many channeled contacts
Oligocene	Laguna Springs Volcanic Group	Tintic Delmar Latite		0-400+	Flow member is gray to dark-reddish-brown medium-grained latite porphyry, tuff member is buff to white fine- to coarse-grained tuff
	Laguna Springs Volcanic Group	Pinyon Queen Latite		0-1,100+	Flow member is dark-reddish-brown medium- to coarse-grained latite porphyry characterized by large white plagioclase phenocrysts. tuff member consists of intermixed fine-grained and boulder tuff, and agglomerate
	Laguna Springs Volcanic Group	North Standard Latite		0-600	Flow member is purplish-gray medium-grained latite vitrophyre, tuff member is gray to white heterogeneous boulder tuff
	Tintic Mountain Volcanic Group	Big Canyon Latite		0 - 200	Flow member is dark-gray fine-grained latite; tuff member is buff to white fine-grained tuff
	Tintic Mountain Volcanic Group	Latite Ridge Latite		0 - 600	Welded tuff member is reddish-brown densely welded tuff and breccia, airfall tuff member is fine-grained white tuff
	Tintic Mountain Volcanic Group	Copperopolis Latite		0-400+	Flow member is black to reddish-brown fine-grained latite; tuff member is white fine-grained vitric tuff
	Packard Quartz Latite			0-3,000+	Chiefly pinkish- or lavender-gray medium-grained quartz latite porphyry. Generally divisible into an upper unit of dark-green to black vitrophyre and tuff as much as 500 feet thick; a middle unit of quartz latite porphyry locally more than 2,700 feet thick; a lower unit of dark-green to black vitrophyre as much as 200 feet thick, and a basal unit of fine-grained tuff as much 700 feet thick
	Apex Conglomerate			0 - 500	Prelava soil and rubble, ranging from claystone to coarse conglomerate
Paleozoic rocks					Folded, faulted, and deeply eroded sedimentary strata

B

During the later portion of the Early Permian, the area gradually became unstable. Eolian sediments (e.g., Diamond Creek Sandstone) were deposited as the area became emergent. Later, the area again submerged and a great marine transgression deposited the Phosphoria Formation.

Mesozoic

Mesozoic rocks are exposed locally on Long Ridge, at the mouth of Spanish Fork Canyon, and in the southeastern and northeastern margins of the survey area. These rocks reflect a radical change which occurred along the Cordilleran Hingeline in the configuration of sedimentation patterns, during the Triassic. Throughout most of the Mesozoic, erosion occurred west of the Hingeline and deposition occurred east of the Hingeline, which resulted first in the Triassic red beds (Shinarump, Chinle, and Moenkopi formations) and later in a variety of marine (Twin Creek Limestone) and non-marine sediments (Nugget Sandstone). Total thicknesses for these strata vary. However, Baker (1947) measured up to 3050 m (10,000 ft) of Mesozoic strata in the southeastern part of the survey area.

Tertiary

In Oligocene time, volcanic activity produced thick volcanic piles of pyroclastic debris and quartz latite and andesite flows which overlie the Apex Conglomerate and the pre-Tertiary erosional surface (Fig. 4B). The Apex Conglomerate is a colluvial sediment which probably covered the pre-Tertiary surface and has a thickness of possibly 1500 ft (457 m) in the valley areas (H. T. Morris, oral commun., 1982). The volcanic rocks are: the Packard Quartz Latite with a thickness of over

3000 ft (914 m) (H. T. Morris, oral commun., 1982); the Tintic Mountain Volcanic Group with a thickness of 1800 ft (549 m); the Laguna Springs Volcanic Group with a thickness of over 2100 ft (640 m); the West Traverse Mountains latite and andesite volcanics with a total thickness of 3000 ft (914 m) (Moore, 1973); and the East Traverse Mountains andesite flows whose thicknesses total more than 2000 ft (610 m) (Bullock, 1958).

Quaternary

Quaternary sediments dominate the valley floors and consist primarily of colluvium, loess, glacial deposits, and lacustrine deposits. Pre-Lake Bonneville fan deposits bordering the mountains extend far into the valleys, are cut by the wave terraces of Lake Bonneville, and locally contain a paleosol which formed prior to the rise of the lake (Bissell, 1963). Lake Bonneville at its highest stage covered approximately 52,000 km^2 (20,077 mi^2) and had a maximum depth of about 350 m (1148 ft) (Currey, 1980). Pleistocene sediments consist chiefly of clay, silt, and sand which make up the Lake Bonneville sediments. It should be noted that previous interpretations of Lake Bonneville stratigraphy should be modified based on studies done by Donald R. Currey (1980), W. E. Scott (1980), and W. E. Scott and others (1981).

Previous investigators of Lake Bonneville in Utah and Goshen valleys (Hunt and others, 1953; Bissel, 1963) intepreted the various shorlines of Lake Bonneville to consist of three major deposits which they considered to make up the Lake Bonneville Group: Alpine (oldest), Bonneville, and Provo (youngest). The Alpine Formation was believed to signify the first deep-lake cycle which rose to about 5100 ft (1554 m).

in altitude -- the intermediate terrace deposit of the group. The highest shoreline was represented as the Bonneville Formation, which is evident at an altitude of about 5135 ft (1565 m). The Provo Formation was believed to mark the last of the major deep-lake cycles in this area and represented the lowest major level of the lake at 4760 ft (1451 m).

Donald R. Currey (1980) and W. E. Scott and others (1981) have modified the above interpretation based on new radiocarbon dates. Their conclusions are as follows: 1) many of the deposits mapped as Alpine Formation were deposited during the Bonneville Lake cycle, rather than during an older lake cycle; and 2) the Bonnevill Lake cycle consisted of a gradual increase in lake level starting perhaps 25,000 years ago reaching the Bonneville level approximately 17,500 years ago. The lake level fluctuated several times on the perimeter of the Bonneville basin until about 14,300 years ago, when a final transgression resulted in headward erosion at Red Rock Pass in southern Idaho which resulted in the catastrophic Bonneville flood. The Provo level (4760 ft; 1451 m) of the lake was reached as a result of the flood reaching resistant bedrock in Red Rock Pass. Approximately 14,000 years ago (several hundred years later), another episode of downcutting resulted in a final altitude of about 4724 ft (1440 m). This level was maintained until approximately 12,500 years ago when the Pleistocene decline of the lake reduced Lake Bonneville to basin-floor levels about 11,000 years ago.

Utah Lake is a geomorphological remnant of Lake Bonneville. The more recent sediments along the shores of the lake consist chiefly of deposits of silt and clay and other colluvial, eolian, and alluvial deposits. The elevation of the Utah Lake shoreline was about 4462 ft (1360 m) during 1980. The level of the Utah Lake is maintained by the Jordan River through locks in a dam located at the north end of the statute and is controlled each year by the amount of flow allowed into the lake.

Structural Features

The structural features observed in the survey area are complex, but the general patterns of many of the structural features are now recognized and understood. From Late Precambrian into Permian time more than 30,000 ft (9140 m) (Morris and Lovering, 1961) of sedimentary rocks accumulated in the miogeosyncline west of the Cordilleran Hingeline. Collision between the North American and the Pacific plates during Triassic time resulted in uplift west of the Hingeline and thus a reversal in the past sedimentary pattern in the area. Continued collision of these plates resulted in the Sevier (Late Jurassic to Late Cretaceous) and Laramide (Late Cretaceous to Late Eocene) orogenies which created a series of superimposed thrust faults. Mesozoic and older strata from eastern Nevada were moved as much as 160 km (99 mi) (Morris and Lovering, 1979) over Mesozoic and older strata into central Utah. The Sevier orogeny is not only associated with thrust faulting, but is also associated with tear faulting and folding. The amount of shortening of the Sevier orogenic belt by folding and faulting is postulated to be between 60 and 100 km (37 and 62 mi) (Armstrong, 1968).

The major mapped thrust faults in the survey area are (Plate 2): 1) the Charleston thrusts; 2) the Deer Creek thrust; 3) Big Baldy thrust; and 4) the East Tintic thrust. The Charleston thrusts, which consist of the Charleston thrust and the Upper Charleston thrust, are located in the northeastern part of the area, trend east-west locally, dip about 20° S. (Baker, 1959), and can be followed from the north end of Deer Creek up Bear Canyon and into Mill Creek Canyon. It has been postulated that the Corner Creek fault was originally part of the Charleston thrust which during the Basin and Range faulting became a normal fault. The Charleston thrust, which is thought to have involved a horizontal displacement of over 160 km (99 mi) (Morris and Lovering, 1979), forms the main basal thrust system of the Wasatch Range. This thrust involves Pennsylvanian strata overthrust by Tintic Quartzite (of Cambrian age), which in turn, has been overthrust by Mississippian strata (Baker, 1959). The Deer Creek thrust is believed to trend east-west and dip south along the valley of the South Fork of Deer Creek, where it is concealed by the Tibble Formation (Tertiary in age) and where bedrock outcrops provide evidence for projecting the location of the fault. On the west side of Mount Timpanogos and trending north-south, the Big Baldy thrust extends south across the Provo River, where the trend becomes east-west, and terminates against normal Basin and Range faulting associated with the Wasatch fault zone. The thrust plane is nearly horizontal and is offset by numerous vertical normal faults (Baker, 1959). The East Tintic thrust is in the southwestern part of the survey area in the East Tintic Mountains and strikes roughly north-south. The inferred location of this fault in the Big Canyon area is based on the exposures in the Burgin mine and exploratory drill holes. This thrust is believed to terminate in the vicinity of the Inez tear fault, where the thrust dips about 20° W. In the area of the Silver Shield mine the East Tintic thrust exhibits a throw of 2,130 m (7000 ft) displacing the Tintic Quartzite over Upper Mississippian strata (Morris and Lovering, 1979).

The major folds associated with the Sevier orogeny (Armstrong, 1968) in the survey area are the Lake Mountain syncline and the East Tintic anticline. The Lake Mountain syncline, which involves the whole of the Lake Mountains (Plate 2), is faulted by at least two large tear faults trending northeast-southwest. Slightly asymmetrical and trending roughly north-south in a sinuous bend, the Lake Mountain syncline can be traced approximately 18 km (11 mi) (Bullock, 1951). The East Tintic anticline is largely concealed by lava in the East Tintic Mountains and is known from sparse surface exposures and drill hole data. The East Tintic anticline is a north-trending structure believed to be part of the Tintic-Oquirrh fold belt and is believed to be flanked on the west by the Tintic syncline which is also covered by lava. The amplitudes of the anticline and syncline are believed to be about 3,050 m (10,000 ft) (Morris and Lovering, 1979).

Major shear and tear faults which form a conjugate fracture system in the East Tintic mining district originated during the Sevier orogeny. The major tear faults are: 1) the Homansville fault; 2) the Inez fault; and 3) the Ballpark fault. The Homansville fault is on the north side of Homansville Canyon and trends northeast continuing under Tertiary volcanics. The fault has an average throw of about 920 m (3000 ft), is downthrown on the north, and has an average dip of 80° N. (Morris and Lovering, 1979). The Ballpark fault, which is known only locally about 1 km north of the Burgin No. 2 shaft, apparently trends N. 30° E., dips 75° W., and has a vertical displacement of about 300 m (1000 ft) (Morris and Lovering, 1979). Drill hole data and exposures of sedimentary rock near the Burgin mine are indicative of a totally concealed northeast-trending tear fault known as the Inez fault. The drill data indicate that the East Tintic thrust terminates against this fault. Furthermore, this regional tear fault may be the westward continuation of a fault exposed in the southern part of West Mountain (Morris and Shepard, 1964). The trend of this tear fault is about N. 40° E. with nearly vertical dip but varied displacement.

Between 35 and 19 m.y. ago (Hintze, 1973), quartz monzonitic stocks were intruded in this area accompanied by andesitic-latitic volcanism. Approximately 20 m.y. ago, extensional tectonics resulted in Basin and Range faulting accompanied by basaltic and rhyolitic volcanism which now characterizes the survey area. The dominant feature is the Wasatch fault zone which marks the boundary between the Basin and Range and the Middle Rocky Mountains provinces and which is characterized by earthquakes and is located within the Intermountain Seismic Belt.

Thermal Springs

In the survey area, the known thermal springs, or groups of springs, are listed in Table 1 (a total of nine springs) and are shown, by letter designation, on Plate 2. In some areas the springs occur as a cluster of individual warm springs which form an alignment indicating that the springs may be fault controlled. Indeed, most of the thermal springs in the study area are associated with major faults which bound large grabens and horsts and act as conduits for deep circulation of meteoric water. In general, the springs are considered to be favorable as local sources of low-temperature ground water which may be used for direct heat applications, such as space heating and greenhouse agriculture.

Table 1. -- Summary of characteristics of principal thermal springs in survey area[4].

	Name	Location	Temperature (°C)	Geologic Notes
a	Bird Island Warm Springs[1]	Off the tip of Lincoln Point lat 40° 10.6' long 111° 48.0'	30	Valley fill
b	Burgin Mine[2]	sec.22, T. 10 S., R. 2 W. Lat 39° 57.0' long 112° 2.7'	54.5	Fault-controlled
c	Castilla Hot Springs[3]	sec. 18, T. 9 S., R. 4 E. lat 40° 2.3' long 111° 32.7'	42-44	Sandstone; fault-controlled
d	Crater Hot Spring[3]	sec. 25, T. 5 S., R. 1 W. lat 40° 21.2' long 111° 53.7'	38	Valley fill; fault-controlled
e	Crystal Hot Springs[3]	sec. 12, T. 4 S., R. 1 W. lat 40° 29.1' long 111° 53.9'	21-54	Valley fill; fault-controlled
f	Goshen Warm Springs[3]	sec. 8, T. 10 S., R. 1 E. lat 39° 57.5' long 111° 51.3'	21	Colluvium; fault-controlled
g	Lincoln Point Warm Springs[3]	sec. 2, T. 8 S., R. 1 E. and	21-32	Valley fill
		sec. 3, T. 8 S., R. 1 E. lat 40° 21.0' long 111° 48.8'	Do	Do

Table 1. -- (cont.)

Name	Location	Temperature (°C)	Geologic Notes
h Saratoga Hot Springs[3]	sec. 5, T. 5 S., R. 1 W. lat 40° 21.0' long 111° 54.4'	44	Valley fill; fault-controlled
i Warm Springs at Goose Point[3]	sec. 5, T. 7 S., R. 1 E. and	21-24	Valley fill
	sec. 8, T. 7 S., R. 1 E. lat 40° 5.6' long 111° 52.0'	Do	Do

[1]Milligan and others, 1966. Although these authors do not give a specific name for the warm springs on Bird Island, the designation "Bird Island Warm Springs" will be used for convenience in this report to identify these warm springs.

[2]Morris and Lovering, 1979.

[3]Mundorff, 1970.

[4]The letter designations "a","b", etc. before the names of the springs in this table are used on the map in Figure 3 to identify the locations of the springs.

DATA PRESENTATION

Gravity Data

The gravity data used in this report consist of a compilation of data from 1099 stations obtained in four surveys by the following: 1) Cook and Berg (1961 and 1972); 2) Applied Geophysics Inc. (1978); 3) Meiiji Resource Consultants (1980); and 4) Davis (1981). Figure 3 shows the areal extent of each survey and Table 2 gives the number of gravity stations taken in each survey. A listing of the principal facts of all gravity stations is given in Appendix A. A total of 37 of the 1099 stations are omitted from the complete Bouguer gravity anomaly map (Plate 2) in order to facilitate drafting because in some areas (as, for example, along certain profiles) the stations were more closely spaced[1]. Also, 7 additional stations are omitted from the complete Bouguer anomaly gravity map (Plate 2) and the listing of principal facts (Appendix A) because the gravity values of these stations are considered in error due to mislocation of stations, erroneous elevation determinations, or possible instrument reading errors in the field.

---

[1] It should be noted that these 37 stations are included in the listing of the principal facts of gravity stations (Appendix A) and were used as needed in the analysis and intepretation of the gravity profiles.

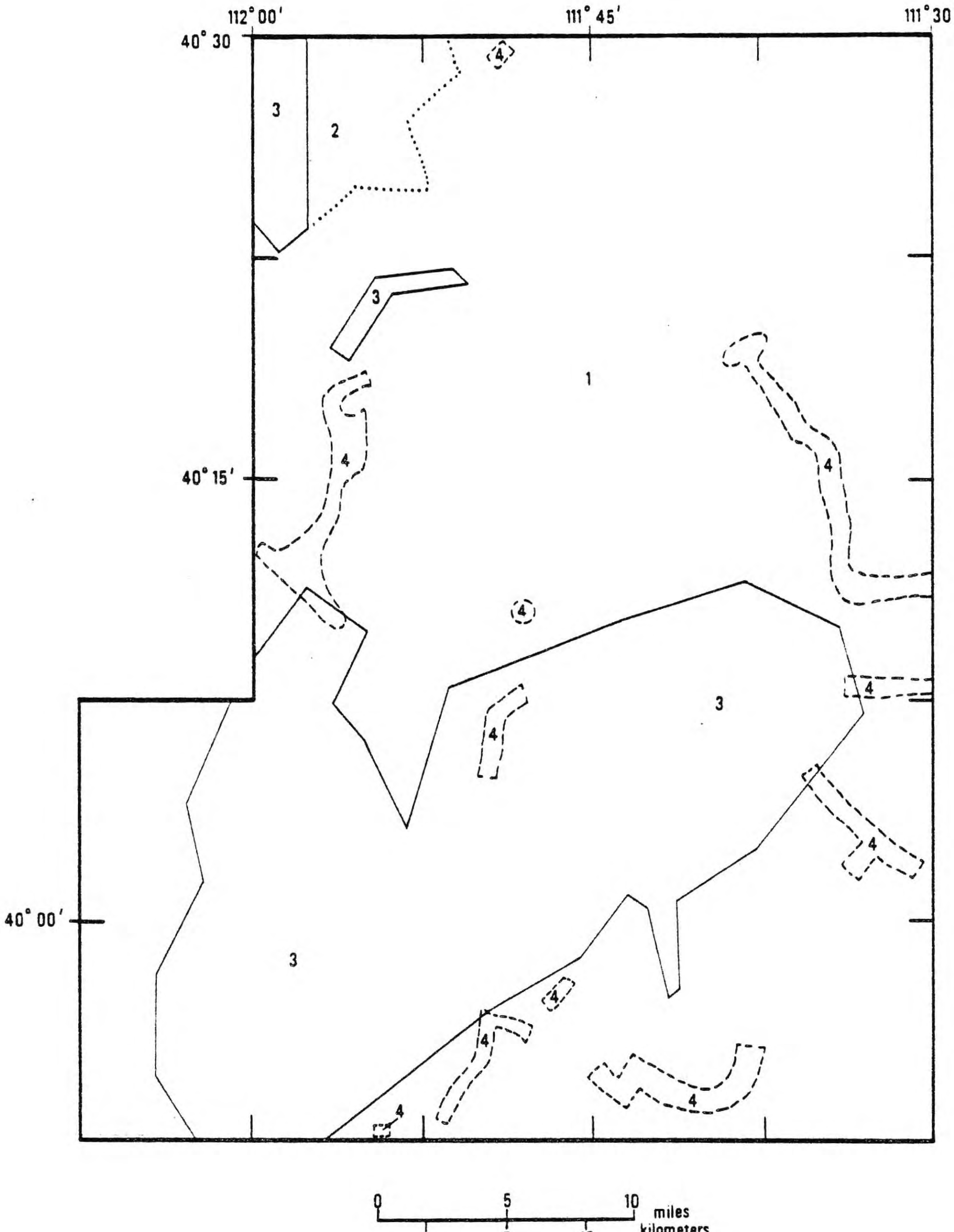

LEGEND

Symbol	Index No.	Investigators
——— (heavy solid)	1	Cook and Berg (1961 and 1972)
········ (dotted)	2	Applied Geophysics Inc. (1978)
——— (solid)	3	Meiiji Resources Consultants (1980)
- - - - (dashed)	4	Davis, D.A. (1981)

Figure 3. Map of survey area showing sources of gravity data.

Table 2. -- Sources of gravity data in the study area.

Investigator or Project	Number of Stations
Cook and Berg, 1961 and 1972	357
Applied Geophysics Inc., 1978	206
Meiiji Resource Consultants, 1980	478
Davis, D. A., 1981	58

Standard techniques were used in obtaining the gravity data and in standard techniques were used in the compilation and reduction of data to give complete Bouguer gravity anomaly values. The details of these methods are given in Appendix B. Plate 2 shows the resulting complete Bouguer gravity anomaly map, with a contour interval of 2 mgal.

Discussion of Errors

Errors associated with gravity data compilation and reduction in this study are as follows: 1) instrument error; 2) instrument drift and tidal variation; 3) elevation determination; 4) horizontal control; 5) assumed mean rock density; and 6) errors inherent in using the terrain correction program. A more detailed discussion of these errors is given in Appendix C. In this study, an estimated maximum error of about 0.65 mgal to 1.0 mgal (Appendix C) in the complete Bouguer gravity anomaly value could result if all sources of error were to accumulate at one station. However, it should be noted that the accumulation of these errors at one station is unlikely.

Density Measurements and Sample Collections

Eleven rock samples were collected from outcrops within the study area in order to ascertain the rock densities of the pre-Mesozoic sedimentary formations. Table 4 (Appendix D) is a compilation of the location, rock type, and density of the rock samples collected. Eight of the samples were limestone, two were sandstone, and one was quartzite. The average density for the limestone samples is 2.61 gm/cc, the average density for the sandstone samples is 2.42 gm/cc, and the density for the quartzite sample is 2.70 gm/cc. In the modeling of the gravity profiles, a mean rock density value of 2.67 gm/cc was used for Paleozoic and older formations.

Also, density measurements of the Packard Quartz Latite (Tertiary in age) were made in order to facilitate the modeling in Goshen Valley (see Table 4, Appendix D). Four samples were selected within a few meters of each other. The average density of these samples is 2.475 gm/cc. It should be noted that this average density value agrees well with the dry density value of 2.47 gm/cc for the Packard Quartz Latite as determined by Morris and Lovering (1979, Table 2, p. 32). Consequently, an assumed rock density value of 2.47 gm/cc was used for the Packard Quartz Latite in the modeling of the gravity profiles in this report.

Drill Hole Information

The drill hole information utilized for geologic control in the study area was obtained from: 1) 12 selected water wells with depths greater than 240 m (800 ft); 2) a deep wildcat oil and gas test well drilled by Gulf Energy and Minerals Company near Spanish Fork, Utah in 1977; and 3) a deep drill hole for ore exploration in the East Tintic mining district (Morris and Lovering, 1979). The locations of all of these wells are shown in Figure 2. The 12 water wells were selected from a large number of wells because they are among the deepest in the area and are located near the profiles discussed in this report. The simplified lithologic logs of these wells are summarized in Appendix E.

The Gulf Energy and Minerals Company #1 Bank exploration well was drilled to a total depth of 13,000 ft (3962 m) and bottomed in Miocene sedimentary rock. The drill hole information from this well included: 1) a lithologic log; 2) a compensated formation density log (gamma-gamma); and 3) a simultaneous compensated neutron-formation density log. As a result, the density profile and composition of the valley fill, as shown by this particular well (Fig. 9, Appendix E), was utilized in determining the geologic cross sections of all profiles in this study. It should be noted that: 1) in the depth range 0 to 500 ft (0 to 152 m) no lithology log was available, and in the depth range 3300 to 3400 ft (1005 to 1036 m) the bit was damaged, resulting in a misinterpretation of hole samples as noted by the lithology log; and 2) in the depth range 0 to 500 ft (0 to 152 m) and 2000 to 6000 ft (610 to 1830 m), no compensated formation density or simulataneous compensated neutron-formation density log was available.

The deep ore exploration drill hole [total depth of about 820 m (2700 ft)] in the East Tintic mining district was begun in Packard Quartz Latite. The hole bottomed in Packard Quartz Latite without encountering any other formation (Morris and Lovering, 1979).

Gravity Map and Gravity Profiles

The reduced gravity data are presented as a hand-contoured complete Bouguer gravity anomaly map with a 2-mgal contour interval (Plate 2). In addition, 5 gravity profiles and associated interpretive geologic cross sections, all of which trend generally east-west, are presented. The geologic control for the geologic cross sections comprises: 1) the generalized geology map (Plate 2); 2) the columnar section of Paleozoic and layered Cenozoic rocks in the East Tintic mining district

(Fig. 4); 3) 12 water wells located throughout the survey area (Plate 1); 4) The Gulf Energy and Minerals Company #1 Bank well (Appendix E, Fig. 9); and 5) a mineral exploration hole located in the East Tintic mining district (Morris and Lovering, 1979). The basis for the assumed densities in the interpretive geologic cross sections was discussed in the previous sections titled: 1) "Density measurements and sample collections" and 2) "Drill hole information".

DATA INTERPRETATION

Gravity Map

General Features

The complete Bouguer gravity anomaly map of the study area (Plate 2), which has a 2 mgal contour interval, shows a pattern of alternating gravity lows and highs over grabens and horsts, respectively, which is characteristic of the Basin and Range province (Stewart, 1971). Also, the zones or belts of closely spaced gravity contours, which define steep gravity gradients, indicate large Basin and Range faults which occur between adjacent grabens and horsts. In the survey area, the gravity contours have two dominant trends -- northwest-southeast and northeast-southwest, with minor gravity lineations which trend north-south and east-west. In the northern portion of the survey area, the pattern consists of widespread elongate northwest-southeast trending gravity highs over the Lake Mountains and the Wasatch Range separated by a large similar-trending gravity low over the northern part of Utah Valley; and in the southwestern portion of the survey area, the pattern consists of elongate northeast-southwest trending gravity highs over the East Tintic Mountains and Warm Springs Mountain separated by a large gravity low over Goshen Valley. Furthermore, these two dominant trends roughly parallel Sevier orogenic trends mapped in this area by Eardley (1939), indicating that the Basin and Range normal faulting pattern may, in part, be controlled by Sevier orogenic trends.

The complete Bouguer gravity anomaly values range from a maximum of about -168 mgal over the southern portion of the Lake Mountains on the west side of the survey area to a minimum of about -224 mgal over the area just northwest of Spanish Fork in Utah Valley. It should be noted that local anomalies are superimposed on the eastern margin of a regional Bouguer gravity high over the Lake Bonneville Basin; and that regional Bouguer gravity anomalies exhibit an inverse correlation with the regional elevation which apparently is the result of a complex density distribution involving an increase in crustal thickness toward the east and variations in density of the lower crust and upper mantle (Montgomery, 1973; Eaton and others, 1978). In particular, the regional gravity is assumed to decrease about 5 to 6 mgal from the East Tintic Mountains to West Mountain along profiles C-C' and D-D', and to decrease about 16 mgal from West Mountain to the Wasatch Range along profile B-B'.

The major gravity lows occur in the southern part of Utah Valley and in the central part of Goshen Valley with minimum gravity anomaly values of about -224 mgal and -204 mgal, respectively. The major gravity highs occur over the Lake Mountains, West Mountain, and the Wasatch Range with maximum gravity anomaly values of about -168 mgal, -180 mgal, and -189 mgal, respectively. The steepest measured gravity gradients occur over the Wasatch fault zone in the area southeast of Provo with a gradient of about 10 mgal/km and over the Utah Lake fault zone in the area of Saratoga Hot Springs with a gradient of about 9 mgal/km.

Wasatch Fault Zone

The Wasatch fault zone is a typical Basin and Range normal fault system which consists of complexly braided faults which dip approximately 50-70^{o} W (Eardley, 1939). Near the mouth of Santaquin Canyon, one of the faults associated with this fault zone exhibits a vertical throw of 1680-2140 m (5500-7000 ft) (Eardley, 1939). The Wasatch fault zone is one of the dominant structural features within the study area and coincides with a band of closely spaced gravity contours which defines a large gravity gradient along the western margin of the Wasatch Range within the survey area. In the area southeast of Provo, a gravity gradient of 10 mgal/km is observed. The band of closely spaced gravity contours associated with the Wasatch fault zone trends northwest-southeast along the Wasatch Range from Springville to Alpine. However, at the mouth of Hobble Creek Canyon just south of Springville, the band of closely spaced gravity contours abruptly changes in trend from northwest-southeast to northeast-southwest parallel to the Wasatch fault zone. At the mouth of Spanish Fork Canyon, the gravity contours are sharply offset toward the north because of a juxtaposition of east-west and northeast-southwest trending faults which result in a small spur of bedrock jutting out into the Utah Valley. From the mouth of Payson Canyon to the mouth of Santaquin Canyon, the trend of the gravity contours associated with the Wasatch fault zone is not only influenced by the Wasatch fault zone but also by a zone of east-west faults as mapped by Eardley (1933) which are believed to indicate a zone of weakness which existed before Basin and Range faulting. The combination of these two structural features delineate the northern boundary of the "Santaquin spur", which is a bedrock spur projecting westward from the Wasatch Range and which was first recognized and designated by Gilbert (1928). According to Gilbert, this spur is a large faulted block which separated from the main mountain block and became lodged at an intermediate level between the mountain block and the valley block to the north. From Santaquin Canyon south within the study area, the Wasatch fault zone shows little or no effect on the gravity data; however, it should be noted that the gravity data are sparse in this area.

Utah Lake Fault Zone

The Utah Lake fault zone, first designated by Cook and Berg (1961), is indicated by one of the most dominant belts of gravity contours in the survey area which trends north from Santaquin, through Holladay Springs, along the eastern margin of West Mountain, through the thermal springs at Lincoln Point, through the Bird Island Warm Springs, and then continues with a northwest-southeast trend through Saratoga Hot Springs and Crater Hot Springs. The exact location of the Utah Lake fault zone beneath the central and northwestern parts of Utah Lake is unknown due to the lack of gravity data over the lake. The continuation of the gravity contours -- and hence the Utah Lake fault zone -- from Bird Island through the Saratoga Hot Springs and Crater Hot Springs area is supported by the following: 1) the existence of thermal springs along this band of gravity contours; 2) the gravity gradient which is firmly established by many gravity stations on or near the shores of Utah Lake; 3) a fault scarp along the eastern margin of West Mountain (Eaton, 1929); and 4) a mapped fault in the Pelican Hills on the east margin of the Lake Mountains (Bullock, 1951). It should be noted that the location of the thermal springs along the Utah Lake fault zone is generally along the western margin of the belt of closely spaced gravity contours.

North of Saratoga Hot Springs the Utah Lake fault zone divides into two different branches which are indicated by two separate bands of gravity contours. One band of gravity contours continues first northwestward over the Beverly Hills area, where high-angle faults occur (Madsen, 1952), and over the western part of the Traverse Mountains, and then northward (off the map in Plate 2), eventually to become part of a band of closely spaced gravity contours (Cook and Berg, 1961) which are associated with a fault zone which separates the Jordan Valley graben from the Oquirrh-Boulter-Tintic fault block. The other band of gravity contours trends northerly along the western margin of the Traverse spur (i.e., the eastern segment of the Traverse Mountains). Then, this band of gravity contours trends northwesterly in an arcuate manner to eventually join the band of east-trending gravity contours which delineate the fault zone which forms the southern boundary of the Jordan Valley graben. It should be noted that the Crystal Hot Springs, shown on Plate 2 near the Utah State Prison in Jordan Valley, are controlled by this fault zone.

Utah Valley Graben

The Utah Valley graben is indicated by an elongate north-south to northwest-southeast trending pattern of two gravity lows and two bounding sets of gravity contours associated with the Utah Lake fault zone on the west and the Wasatch fault zone on the east. It should be noted that because there were no gravity data available over Utah Lake, the contours were evenly spaced between known gravity data; and this resulted in the contouring of two gravity lows instead of the one gravity low contoured by Cook and Berg (1961). The northern gravity low, south of American Fork, shows a closure of about 8 mgal and a complete Bouguer gravity anomaly minimum value of -220 mgal; and the southern gravity low, lying north of Spanish Fork, shows a closure of about 12 mgal and a gravity anomaly minimum value of approximately -224 mgal. Together the two gravity lows combine to form a large elongate gravity low approximately 35 mi (55 km) long and 10 mi (16 km) wide with a closure of about 16 mgal. It should be noted that although two gravity lows were contoured over the Utah Valley graben (suggesting the possibility of two blocks instead of one) one large block is assumed. This does not preclude the possibility that the Utah Valley graben is composed of two separate blocks. The block associated with the Utah Valley graben may be tilted toward the southeast as indicated by the complete Bouguer gravity anomaly minimum (-224 mgal) associated with the gravity low lying north of Spanish Fork.

The Utah Valley graben is bounded on the north and south by gravity saddles trending east-west. The gravity saddle delineating the northern margin of this graben has been associated with the Traverse spur, and the southern gravity saddle with the Santaquin spur (Cook and Berg, 1961). These spurs, which were originally recognized and designated by Gilbert (1928), are bedrock salients projecting westward from the Wasatch Range which he interpreted to be blocks downdropped to an intermediate level between the Wasatch Range block and the valley blocks.

The eastern and southeastern margin of the Utah Valley graben is delineated by a band of closely spaced gravity contours indicative of a large gravity gradient associated with the Wasatch fault zone as mapped by Hunt and others (1953). The gravity contours associated with the southern margin of the Utah Valley graben is markedly discontinuous in trend and is probably influenced by three structural elements: 1) the Santaquin spur, which is essentially a series of bedrock blocks separated by at least two north-south trending faults (Gilbert, 1928); 2) a series of east-west faults located between the mouths of Payson Canyon and Santaquin Canyon (Eardley, 1933); and 3) the Wasatch fault zone, which trends roughly northeast in this region.

The western margin of the Utah Valley graben is delineated by the gravity contours associated with the Utah Lake fault zone which extends north from Santaquin, along the eastern margin of West Mountain, through the central part of Utah Lake, and then continues with northwestward trend through Saratoga Hot Springs. Along the western margin of the Utah Valley graben in the Pelican Point area, the gravity anomaly contours show a total relief of approximately 40 mgal.

Only one deep oil and gas well test is known within the Utah Valley graben. This well is the Gulf Energy and Minerals Company #1 Bank well (Appendix E, Fig. 11), northwest of Spanish Fork, which bottomed in rock of Miocene age at a total depth of 13,000 ft (3,900 m).

Goshen Valley Graben

The Goshen Valley graben is indicated on the complete Bouguer gravity anomaly map (Plate 2) by four gravity lows located in the southwestern portion of the survey area, which together trend generally north-south to northeast-southwest. The gravity data indicate that the graben is complex and apparently consists essentially of four structural blocks, each of which is displaced downward at various levels with respect to each other. These structural blocks are herein designated as: 1) the North Goshen platform; 2) the East Goshen platform; 3) the West Goshen bench; and 4) the South Goshen block -- these blocks are designated "a", "b", "c", and "d", respectively, on Plate 2.

The North Goshen platform is the northernmost block and is delineated by the following gravity features: 1) on the north, by a small east-trending band of gravity contours along the southern margin of the gravity saddle which extends southeastward from the Mosida Hills; 2) on the east, by a small band of gravity contours along the southwestern margin of West Mountain and the extreme northwestern margin of Warm Springs Mountain; and 3) on the southwest, by a southeast-trending band of closely space gravity contours which separate this platform from the East Goshen platform and the South Goshen block (both of which will be discussed presently). In addition, within the North Goshen platform, two minor gravity lows define a small east-west lineament. The western gravity low shows a closure of approximately 2 mgal, whereas the eastern gravity low shows a closure of about 4 mgal; this feature suggests a tilting of the North Goshen platform toward the east.

The East Goshen platform is the easternmost block which, lying southeast of the North Goshen platform, has been downdropped relative to the North Goshen platform. The East Goshen platform is bound on the east by the Long Ridge fault, mapped by Eaton (1929), which is indicated by a cresent-shaped band of closely spaced gravity contours which is concave toward the west and which is associated with the Goshen Warm Springs. On the west, the East Goshen platform is delineated by a north-trending band of closely spaced gravity contours which separates this platform from the South Goshen block. In addition, the East Goshen platform contains a minor gravity low with a closure of about 2 mgal which is interpreted to be associated with a small downdropped block within the platform.

The West Goshen bench is a narrow elongate north-northeastern trending structural block along the western margin of the Goshen Valley graben. The block is delineated on the west and east by two north-northeastern trending bands of closely spaced gravity contours which indicate two large fault zones, which are herein designated as the "East Tintic Mountains fault zone" and the "Goshen Valley fault zone", respectively.

The South Goshen block is indicated by the north-northeastern trending gravity low, with a closure of more than 6 mgal, which extends throughout the central part of Goshen Valley. The gravity minimum lies about 2 mi (3.3 km) northeast of the town of Elberta. The asymmetrical shape of the gravity low, with the steepest gravity gradients on the east and northeastern sides, suggests a tilting of the block toward the northeast. It should be noted that the South Goshen block is down-dropped relative to each of the other three structural blocks just discussed: the North Goshen platform (on the north), the East Goshen platform (on the east), and the West Goshen bench (on the west). Furthermore, on the west, the South Goshen block is bound by the fault zone herein previously designated as the "Goshen Valley fault zone".

The deepest boring within the Goshen Valley graben is the mineral exploration hole noted by Morris and Lovering (1979) located on the western margin of the graben in the foothills of the East Tintic Mountains which started in Packard Quartz Latite and bottomed in Packard Quartz latite at a depth of about 2700 ft (820 m). Other borings consist of water wells which bottomed in unconsolidated valley fill except for one well south of Elberta which bottomed in volcanic rock at 344 ft (100 m). A more comprehensive explanation of the geology and depths to bedrock is given in the discussion pertaining to profiles C-C', D-D', and E-E'.

Wasatch Range Horst

The Wasatch Range, which was first designated as a horst by Gilbert (1928), is bounded on the west by the Wasatch fault zone (Plate 2). Only a segment of the western part of the Wasatch Range horst lies within the study area.

Along the northeastern margin of the survey area, a large segment of the Wasatch Range horst coincides with a broad elongate northwest-southeast trending gravity high with a known closure of at least 8 mgal and a maximum Bouguer gravity anomaly value of about -188 mgal. On the northeastern margin of this gravity high, a general parallelism occurs between the gravity contours and the Deer Creek and Charleston thrusts; and on the eastern margin of this gravity high, a general parallelism occurs between the north-south trending gravity contours and the trends of the West Aspen Grove and the Aspen Grove faults. However, in this region, the data are so sparse because of difficulty of access that any direct correlation between the mapped structual features and the gravity contours is uncertain and speculative. Along the eastern and southeastern parts of the survey area, the maximum gravity anomaly values over the Wasatch Range horst range from -200 mgal over the Spanish Fork Canyon region to -192 mgal over the Payson Canyon region.

Lake Mountains Horst

The Lake Mountains horst, which lies along the western margin of the study area, is indicated by a pair of north-south trending gravity highs which overlie the Lake Mountains and which range from -170 mgal on the south to -178 mgal on the north. The Lake Mountains horst consists of Paleozoic rocks which have been folded, then faulted. The decrease in gravity values toward the north represented by the two gravity highs, separated by an east-west trending gravity gradient may be the result of: 1) plunging of the Lake Mountains syncline toward the north; 2) two tear faults on the west side of the Lake Mountains horst which have been downdropped toward the south (Bullock, 1951); 3) thrust faulting which is evident in the Cedar Valley, Pelican Point, and Beverly Hills area (Bullock, 1951); or 4) a combination of all these factors. The northern margin of the Lake Mountains horst is indicated by a northwest-trending band of gravity contours associated with the western branch of the Utah Lake fault zone, whereas the eastern margin of the horst is indicated by the north-south trending band of gravity contours with a steep gravity gradient associated with the Utah Lake fault zone. The southeastern margin of the Lake Mountains horst is delineated by a northeast-southwest trending band of gravity contours with a steep gravity gradient which indicates the bounding fault between the horst and the valley floor. The southern margin of the horst is indicated by a southeast-northwest trending band of gravity contours which form a re-entrant which separates the Lake Mountains horst on the north from two northeast-southwest trending gravity highs associated with the Greeley Hill and Mosida Hills blocks on the south.

Greeley Hill and Mosida Hills Blocks

The Greeley Hill and Mosida Hills blocks are indicated by two small northeast-southwest trending gravity highs which overlie Greeley Hill on the west and the Mosida Hills on the east just south of the Lake Mountains horst. Each of the gravity highs is several kilometers in length and has a closure of at least 4 mgal; each of the gravity highs exhibits a complete Bouguer gravity anomaly value of about -168 mgal. Furthermore, each horst consists essentially of folded and faulted Paleozoic rocks. The elongate north-northeast trending gravity saddle lying between the Greeley Hill block and the Mosida Hills block is essentially coincident with the Tintic Prince fault -- a right-lateral shear fault mapped by Morris and Lovering (1961).

The northern margin of these two blocks is coincident with a gravity gradient associated with the southern margin of the Lake Mountains horst. The band of closely spaced gravity contours with a steep gravity gradient along the east side of the Mosida Hills block indicates a marginal fault zone, herein designated as the "Mosida Hills fault zone", which separates the Mosida Hills block from what is postulated to be a tilted (to the west) block under the southwestern arm of Utah Lake in the area west of West Mountain. The southern margin of the Mosida Hills block is delineated by an east-west trending band of gravity contours which is indicative of the offset faulting that is associated with the en echelon faulting that is interpreted at the northern end of the East Tintic Mountains fault zone and the southern end of the Mosida Hills fault zone. The southern margin of the Greeley Hill block is delineated by an east-southeast trending band of closely spaced gravity contours which indicate a fault zone; but, no fault with this trend was mapped in this area by Morris and Lovering (1961, 1979). It should be noted that the East Tintic Mountains horst, the Lake Mountains horst, the Greeley Hill block, and the Mosida Hills block together apparently form the eastern margin of one of the great structural blocks in the region, designated by Cook and Berg (1961) as the "Oquirrh-Boulter-Tintic fault block" which, according to them, is bounded on the west by the Oquirrh-Boulter-Tintic fault zone.

East Tintic Mountains Horst

The East Tintic Mountains horst is indicated by a prominent north-northeast trending gravity nose in the southwestern portion of the survey area, over which the complete Bouguer gravity values decrease from -176 mgal in the north to -190 mgal in the south. The decrease in gravity values toward the south may be indicative of a thickening of volcanic rocks or a change in the density structure due to thrusting in this region, or a combination of both of these effects. Furthermore, the horst may be considered as a southern continuation of the Greeley Hill and Mosida Hills horsts. The East Tintic Moutains horst is composed essentially of Paleozoic rocks (Plate 2) which have not only been thrust faulted, but also folded, block faulted, and covered by Tertiary volcanic rocks (Morris and Lovering, 1979). A major northeast-southwest trending band of closely spaced gravity contours which extends along the eastern margin of the East Tintic Mountains indicates a fault zone which delineates the eastern boundary of the East Tintic Mountains horst and the western boundary of the Goshen Valley graben. This fault zone has previously been designated herein as the East Tintic Mountains fault zone. South of Highway 50, this band of gravity contours merges with a northeast-trending band of closely spaced gravity contours (which, to the north, is associated with the Goshen Valley fault zone) in such a manner that the individual definition of the East Tintic Mountains fault zone becomes vague because of the essentially constant spacing of the gravity contours in this region. It should be noted that the results of the interpretation along profiles C-C' and D-D' aid in delineating the location of the East Tintic Mountains fault zone.

West Mountain Horst

A gravity high of -180 mgal, trending north-south with a closure of 4 mgal, overlies West Mountain in the central part of the survey area. The horst is bounded on the east by the Utah Lake fault zone and on the west by a fault inferred by Eaton (1929) on the basis of an abrupt scarp on this side of the mountain. It should be noted that the absence of a steep gravity gradient on the west flank of West Mountain is indicative of a thin veneer of sediments over bedrock and does not necessarily negate the presence of a buried fault in this region. The northern boundary of this horst is not well delineated by the gravity data.

A broad gravity low, with a closure of 4 mgal, overlies the southwestern arm of Utah Lake in the area lying west of West Mountain and probably indicates a block which has been downdropped relative to the Mosida Hills on the west and West Mountain on the east. The western margin of the block is delineated by a band of closely spaced gravity contours along the eastern margin of the Mosida Hills, which indicates a fault zone previously designated herein as the Mosida Hills fault zone. The block is bound on the east by the inferred fault along the west side of West Mountain, as previously discussed. Furthermore, the gentle gravity gradient associated with the gravity contours on the eastern margin of the block and the steep gravity gradient associated with the gravity contours on the western margin of the block suggests that the block may be tilted toward the west. The south end of the downdropped block is indicated by a small gravity saddle which lies along the southern margin of the above-mentioned small gravity low. This gravity saddle also indicates that the downdropped block is probably separate and distinct from the structural block lying immediately south of the gravity saddle, which was previously designated herein as the North Goshen platform.

East-West Gravity Trends

On a gravity anomaly contour map, structural trends are often indicated by a systematic arrangement of features or patterns of gravity contours which is related to corresponding contrasts of density in the underlying rocks of the survey area. The gravity features which may indicate such structural trends include: 1) alignment of the gravity contours; 2) systematic offset of the gravity contours; and 3) systematic termination or abrupt changes of gravity anomalies -- either gravity highs or lows.

Two east-west gravity trends are evident in the southern part of the survey area on the complete Bouguer gravity anomaly map (Plate 2). One of these trends lies south of the Greeley Hill horst, the Mosida Hills horst, and the western arm of Utah Lake, between the western margin of the East Tintic horst and West Mountain. Furthermore, the gravity trend is indicated not only by a narrow band of gravity contours which are interpreted to indicate a marginal fault which separates the Greeley Hill and Mosida Hills horsts from the East Tintic Mountains horst, but also by a small gravity saddle between the Goshen Valley graben on the south and a small gravity low on the north. The other east-west gravity trend is indicated by an east-west trending band of gravity contours which coincides with the southern margin of the Utah Valley graben and a zone of east-west faults mapped by Eardley (1933).

Furthermore, the two gravity trends lie within and are parallel to the Deep Creek-Tintic belt, which is a 50-65 km (30-40 mi) wide belt along latitude 40°N. characterized by an east-west alignment of intrusive bodies, and metallic and nonmetallic deposits (Hilpert and Roberts, 1964; Stokes, 1968) which is also coincidental with (1) a much larger regional east-west gravity lineation (Cook and Montgomery, 1972; Montgomery, 1973), (2) a series of east-west trending magnetic highs (Mabey and others, 1964; Zeitz and others, 1969; Stewart and others, 1977), and (3) east-west seismic trends (Kastrinsky, 1977; McKee, 1982). The large regional east-west gravity lineation is also coincident with the north end of the Tintic Mountains, the Santaquin Spur, and the south end of the Utah Valley graben (Montgomery, 1973) and as such is believed to control the offset of the Wasatch Range and the north and south termini of the Basin and Range grabens and horsts located along latitude 40° N. The series of east-west trending aeromagnetic highs are believed to be associated with intrusive bodies several thousand feet below the surface in the East Tintic Mountains (Mabey and others, 1964). The east-west seismic trends were investigated by Kastrinsky (1977) by a microearthquake survey in 1975 in Goshen Valley. The epicentral pattern of microseismicity was found to be perpendicular to typical Basin and Range normal faulting trends with a nodal plane solution of N. 85° E. and was interpreted by Kastrinsky as not necessarily related to the development of the valley. Furthermore, it was postulated by Cook and Montgomery (1972) and Montgomery (1973) that the source of the east-west gravity trends, and aeromagnetic anomalies may be related to a fracture or fracture zone associated with an ancient transform fault extending into the upper mantle.

Gravity Profiles and Interpretive Geologic Cross Sections

In this report, five interpretive geologic cross sections[1] are shown along generally east-west trending gravity profiles, which are designated A-A' through E-E' (Plate 2). All profiles pass through or near thermal springs in the survey area. The data along each profile include the complete Bouguer gravity anomaly values (designated

---

[1]The results of a preliminary analysis of a north-south profile through the town of Elberta are omitted from this report because most of the profile paralleled the main trends of the gravity and geology of the area.

"observed"), the assumed regional gravity, the residual gravity, and the calculated gravity. The regional gravity for all profiles is assumed to be linear, from bedrock outcrop to bedrock outcrop, with gravity decreasing toward the east. As was noted previously, the regional Bouguer gravity anomalies exhibit an inverse correlation with the regional elevation of the survey area; and as a result, the regional gradient is probably not linear along the length of the profiles and could have been related to regional topography. However, this would not have changed the residual anomlies appreciably. The residual gravity is obtained by subtracting the observed gravity from the assumed regional gravity. The calculated gravity is the theoretical gravity computed for the model shown in the geologic cross section. For all the models shown, the difference between the residual and calculated gravity values is generally less than 0.5 mgal.

All profiles were modeled using 2 dimensional and/or 2-1/2 dimensional gravity modeling programs which were developed by Snow (1978) using the 2 dimensional gravity computation algorithm of Talwani and others (1959) and the 2-1/2 dimensional computational algorithm of Cady (1977; 1980). For those models which used 2-1/2 dimensional techniques, a finite (rather than an infinite) strike length for each polygon was assumed in the model. Thus, strike lengths are noted for those polygons within the model when 2-1/2 dimensional techniques were used. The geological cross sections modeled from the gravity data were accepted when the difference between the calculated and residual gravity anomalies was less than 0.4 mgal.

Each profile was modeled assuming a 4-layer sedimentary rock model based on the Gulf Energy and Minerals Company #1 Bank well near Spanish Fork (see Table 3). However, two profiles in the Goshen Valley region include a volcanic rock layer with an assumed density of 2.47 gm/cc based on the density determinations of the Packard Quartz Latite (Table 4) and a conglomerate layer associated with the Apex Conglomerate with an assumed density of 2.40 gm/cc. Horizontal density horizons were assumed for most models for ease of modeling; and it should be noted that vertical as well as horizontal variation in the density of the valley fill probably occurs.

Along each profile in the valley areas, the top layer represents lake deposits with an assumed density of 2.05 gm/cc to a depth of 0.43 km (1400 ft)and consists of clay, gravel, and silt lenses, as exemplified in the water well logs (see Tables 5 to 16). Also, along each profile in the valley areas, the second sedimentary layer has an assumed density of 2.20 gm/cc to a depth of 0.9 km (2950 ft) and consists of essentially the same lithology as the top layer, but is more consolidated. Along profiles A-A' and B-B' in the valley areas, the third layer is assumed to have a density of 2.45 gm/cc and consists of alternating layers of sandstone, claystone, and shale which probably represent Middle Cenozoic sediments to a depth of 3.2 km (10,500 ft). Along profile B-B' in the Utah Valley area, the fourth and bottom layer has an assumed density of 2.55 gm/cc and is composed primarily of shale, sandstone, and siltstone which may indicate rocks of Miocene age or older. Bedrock is assumed to consist of Paleozoic rocks with an assumed mean rock density of 2.67 gm/cc.

Table 3. -- Density values used in modeling -- based on the Gulf Energy and Minerals Company #1 Bank well.

Range of Depth (km)	(ft)	Lithology	Density (gm/cc)
0.0-0.43	0.0-1400	Unconsolidated gravel, clay, silt, and sand.	2.05
0.43-0.9	1400-2950	Consolidated gravel, clay, silt and sand.	2.20
0.9-3.2	2950-10,500	Predominately sandstone, claystone, and shale.	2.45
3.2-3.9	10,500-13,000	Sandstone, siltstone, and shale.	2.55

All depths discussed in the text and shown in the interpretive geologic cross sections are measured with respect to an assumed horizontal surface. It should be understood that the comprehensive geologic cross sections as modeled in this study are not unique, but are modeled to represent the present geology as closely as possible based on drill hole data and known geology. Also, the inherent ambiguity associated with gravity anomalies in many cases necessitates modeling a single steep fault instead of a series of faults or a steep incline.

Profile A-A': Saratoga Hot Springs

The Saratoga Hot Springs profile A-A' (Fig. 4) extends northeastward across the northwestern margin of Utah Valley from the northern margin of the Lake Mountains approximately 12 km (7.4 mi), to about 1.5 km (0.9 mi) northeast of Lehi. The complete Bouguer gravity anomaly values range from -177 mgal over the Paleozoic rocks of the Lake Mountains on the west, to -211 mgal over the sediments covering Utah Valley on the east. The regional gravity associated with this profile is assumed to have a gradient of -0.285 mgal/km toward the east. The geologic cross section was modeled using 2 dimensional techniques.

Along profile A-A', the structure is modeled as the western margin of a graben which was previously designated as the Utah Valley graben (Cook and Berg, 1961); and the modeled maximum depth of the graben is approximately 2.5 km (7620 ft). The graben is bounded on the west by the Utah Lake fault zone, which is indicated by a large residual gravity anomaly with a total gravity relief (with gravity decreasing toward the east) of approximately 32 mgal over a horizontal distance of 12 km (7.5 mi). In the model, the Utah Lake fault zone consists of two

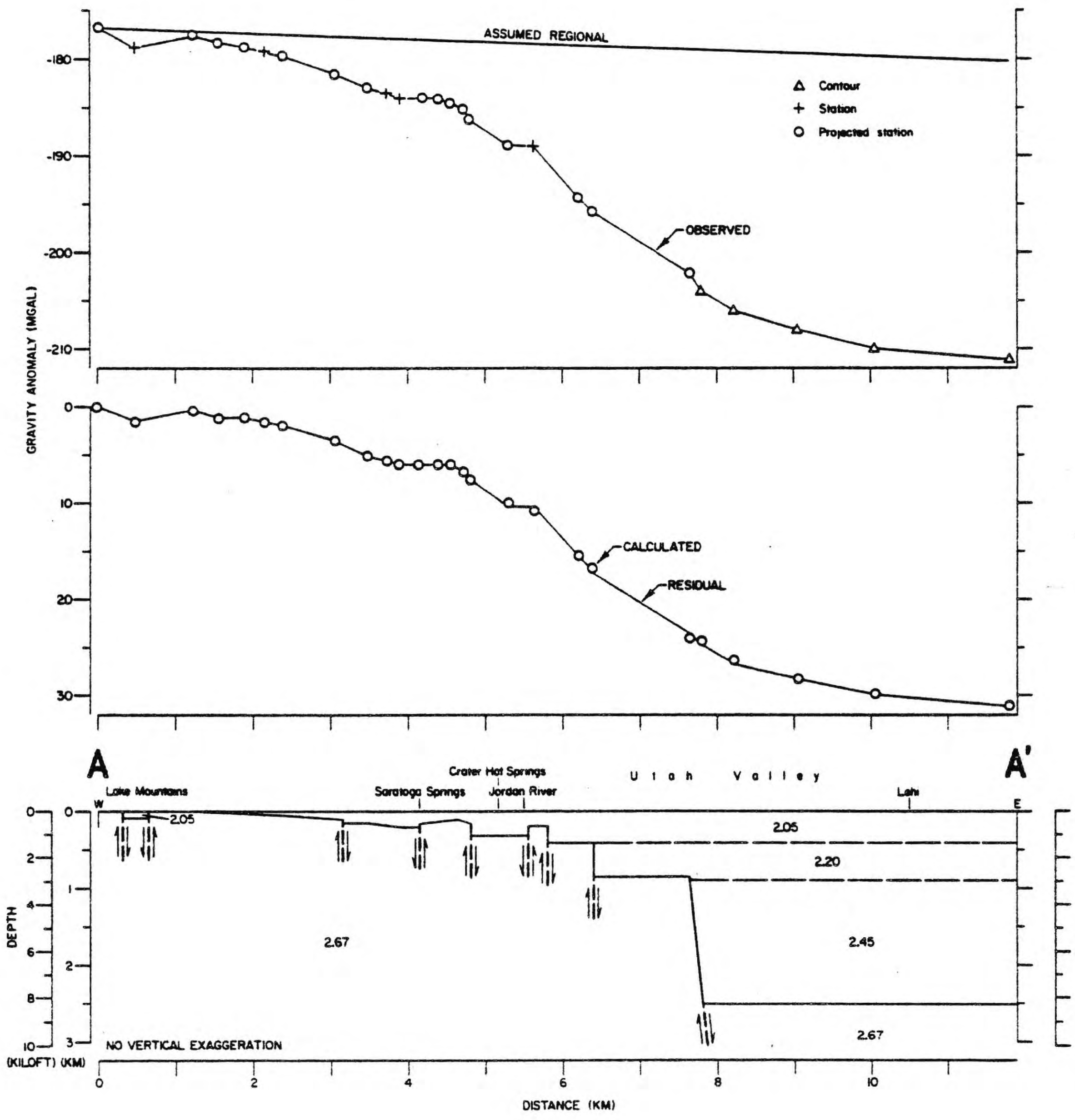

Figure 4. Interpretive geologic cross section along gravity profile A-A'. The number is the density (in gm/cc) of the layer.

major bounding faults, which from west to east, show displacements of 0.46 km (1500 ft) and 1.66 km (5400 ft), respectively. Along the western portion of the profile, the irregular gravity anomaly curve (with gravity decreasing toward the east), is modeled as a broken bedrock surface composed of small blocks buried under a thin, but thickening (toward the east) veneer of alluvial sediments. Along profile A-A', a small residual gravity high over the Saratoga Hot Springs and Crater Hot Springs area (as projected onto the profile) is probably caused by either (1) Paleozoic bedrock blocks which are differentially faulted or (2) an increase of the density of the host rocks -- namely, alluvium and/or undelying Paleozoic bedrock -- as a result of cementation caused by circulating hot brines associated with the hot springs. This interpretation indicates that the fault, or fault zone, which forms the conduit (or conduits) for the hot springs may extend to great depth and are essentially bedrock against bedrock faults. The hot water from Saratoga Hot Springs and Crater Hot Springs, with measured temperatures of 55°C and 38°C, respectively, at the surface (Table 1), may represent leakage from a deep reservior where circulating water is heated by the normal geothermal gradient of the area. Furthermore, if the water is heated by a normal geothermal gradient of 35°C/km (D. S. Chapman, personal commun., 1981), a temperature of 55°C (which is comparable to the surface temperature of the water measured at Saratoga Hot Springs) would be reached at a depth of 1.6 km (5250 ft). Because, the water temperature probably decreases as the water ascends along the faults, this may suggest that the minimum vertical depth of penetration of the faults or fault zone in the vicinity of the hot springs may reach a depth of 1.6 km or more. This reasoning pressumes that the assumed normal geothermal gradient is correct.

Profile B-B': Spanish Fork

The Spanish Fork profile B-B' (Fig. 5), totaling about 25 km (15.6 mi) in length, extends east from West Mountain approximately 12 km (7.4 mi) to the center of Utah Valley, then southeast approximately 13 km (8.0 mi) through Utah Valley and along Spanish Fork Canyon in the Wasatch Range. There is one bend in the profile -- near Spanish Fork. The profile overlies Paleozoic rock in the West Mountain region for about 2 km (1.25 mi), alluvium in Utah Valley for approximately 19 km (11.7 mi), and Paleozoic rocks and alluvium along Spanish Fork Canyon for 3 km (1.8 mi). The complete Bouguer gravity anomaly values range from approximately -181 mgal on the west over West Mountain to approximately -220 mgal over Utah Valley near Spanish Fork, and about -198 mgal over the Wasatch Range. The regional gravity from the Paleozoic rocks of West Mountain to the Paleozoic rocks of the Wasatch Range was assumed to be linear. A regional gravity gradient of 0.66 mgal/km, with gravity decreasing toward the east, was assumed. The geologic cross section was modeled using 2 dimensional and 2-1/2 dimensional techniques -- in particular, polygons "a", "b", and "c" were modeled using 2-1/2 dimensional techniques.

The geologic cross section along profile B-B', as modeled, consists primarily of a single large graben -- the Utah Valley graben -- which is indicated by a minimum residual gravity anomaly of approximately -31 mgal which lies 3 km (2 mi) west of Spanish Fork in the central part of Utah Valley. The Utah Valley graben, as modeled along profile B-B',

Figure 5. Interpretive geologic cross section along gravity profile B-B'. The number is the density (in gm/cc) of the layer. F=mapped fault. Except for polygons a, b, and c (see below), all polygons are assumed 2 dimensional.

Polygon	Strike Length (in km) (north)	(south)
a	12.0	8.5
b	12.0	8.5
c	3.0	0.5

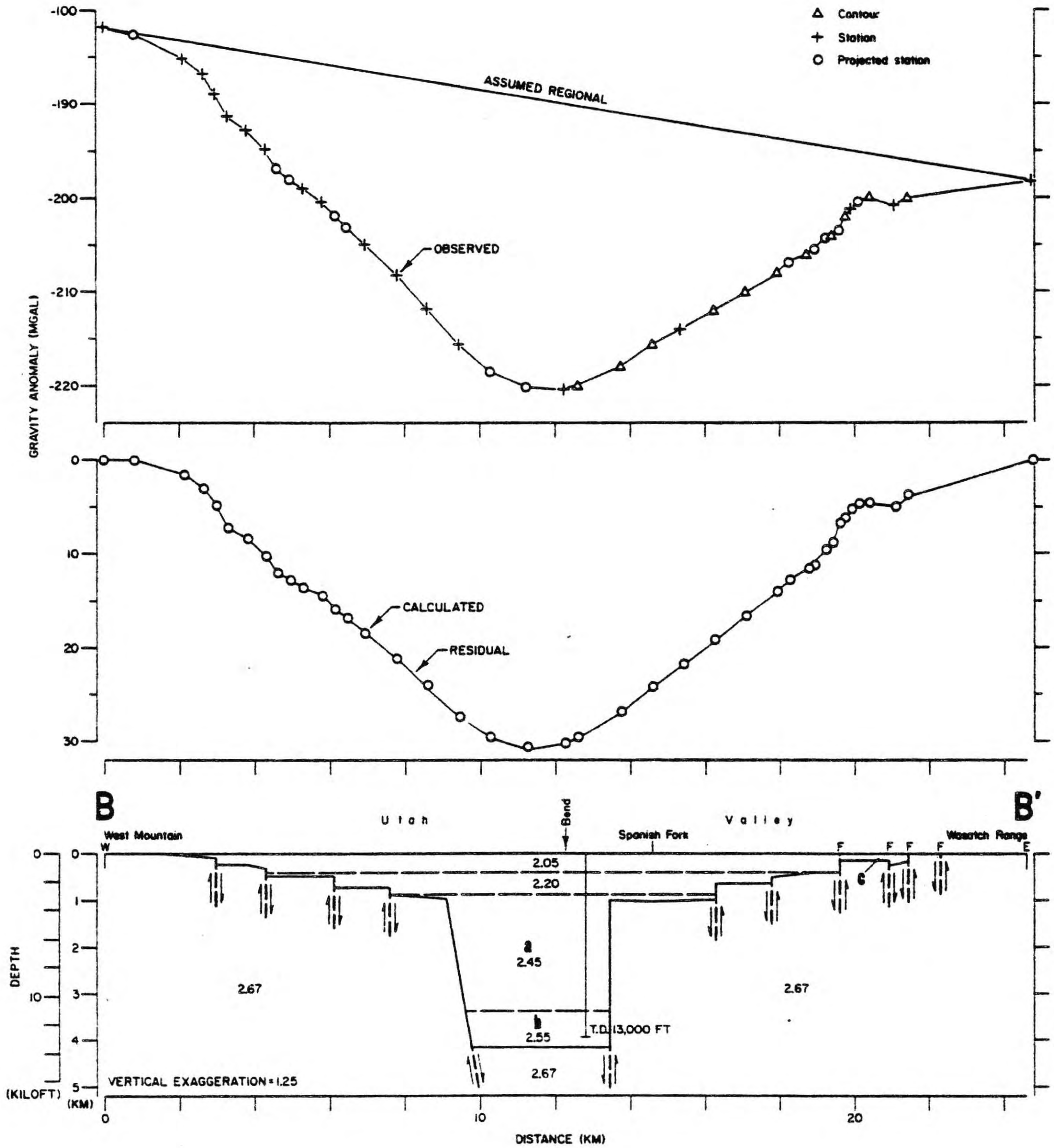

Contour
Station
Projected station
ASSUMED REGIONAL
OBSERVED
CALCULATED
RESIDUAL
GRAVITY ANOMALY (MGAL)
-100
-190
-200
-210
-220
0
10
20
30
B
B'
Utah
Valley
Bend
West Mountain
Spanish Fork
Wasatch Range
W
E
F
2.05
2.20
a
2.45
b
2.55
c
2.67
T.D. 13,000 FT
VERTICAL EXAGGERATION = 1.25
DEPTH
(KILOFT)
(KM)
DISTANCE (KM)

extends for a distance of about 20 km (12.3 mi) between West Mountain and the Wasatch Range; and is modeled as a complexly faulted graben consisting of one large deeply faulted block (about 4 km (2.5 mi) wide) in the central part of the valley, with a series of step faults along the sides. The central block (which consists of polygons designated "a" and "b" in Plate 1) was modeled using 2-1/2 dimensional techniques assuming a strike length of 12 km (7.4 mi) toward the north and a strike length of 8.5 km (5.25 mi) toward the south. As shown in the model, the block is bounded on both sides by large faults, which are indicated by large gravity anomaly slopes and which are modeled to have vertical displacements of approximately 3.3 km (10,000 ft) on the east and 3.2 km (9700 ft) on the west. The series of modeled step faults along each side of the Utah Valley graben, which are indicated by the irregularity of the gravity anomaly slopes along the profile, form a coalition of blocks whose total displacement is approximately 1.0 km (3050 ft) on each side of the Utah Valley graben. The western bounding faults of the Utah Valley graben are interpretated to be associated with the Utah Lake fault zone.

The depth to bedrock (i.e., Paleozoic or older rocks) in the deepest part of the Utah Valley graben is constrained to be greater than 4.0 km (13,000 ft) on the basis of the Gulf Energy and Minerals Company #1 Bank well (which did not completely penetrate rocks of Tertiary age) and is modeled to be approximately 4.2 km (13,780 ft), which is about 0.24 km (800 ft) deeper than the total depth of the Gulf #1 Bank well. However, it should be noted (on the complete Bouguer gravity anomaly map on Plate 2) that this profile does not cross the true gravity minimum (about -224 mgal) within the Utah Valley graben, thus indicating that the depth to bedrock in the area of the true gravity minimum is probably greater than 4.2 km (13,780 ft).

On the east side of the profile, a small shallow horst, which is indicated by a small residual gravity high, is shown adjacent to a small graben, which is indicated by a small gravity minimum; and the modeled associated wedge of alluvium is designated as polygon "c" in Figure 7. For polygon "c", the assumed strike length toward the north is 3.0 km (1.9 mi) and the assumed strike length toward the south is 0.5 km (0.3 mi). It should be emphasized that along the east side of the profile, the marginal faults associated with these structures are mapped (Metter, 1955; Rawson, 1957) faults which are associated with the Wasatch fault zone.

Profile C-C': Genola

The Genola profile C-C' (Fig. 6), totaling about 31 km (19.1 mi) in length, extends generally east from the East Tintic Mountains, across Goshen Valley, over the southern margin of West Mountain, across the constricted southern end of Utah Valley just north of Santaquin, and finally over Dry Mountain. There is one major bend along the profile -- at the southern margin of the western arm of Utah Lake (approximately 6 km [3.7 mi] north of Goshen). From west to east, the profile overlies Paleozoic rocks on the western margin of the profile for approximately 2.5 km (1.5 mi), Tertiary volcanics for 4 km (2.5 mi), alluvium associated with Goshen Valley for 17 km (10.6 mi), Paleozoic rocks on West Mountain for 1 km (0.6 mi), alluvium of Utah Valley for 5 km (3.1 mi), and Paleozoic rocks on Dry Mountain for 1 km (0.6 mi).

Figure 6. Interpretive geologic cross section along gravity profile C-C'. The number is the density (in gm/cc) of the layer. F_1 = East Tintic Mountains fault zone, F_2 = Goshen Valley fault zone, and F=mapped fault. Except for polygons "a", "b", "c", and "d" (see below), all polygons are assumed 2 dimensional.

Polygon	Strike Length (km) (north)	(south)
a	5.0	Infinite
b	5.0	Infinite
c	1.0	Infinite
d	Infinite	0.5

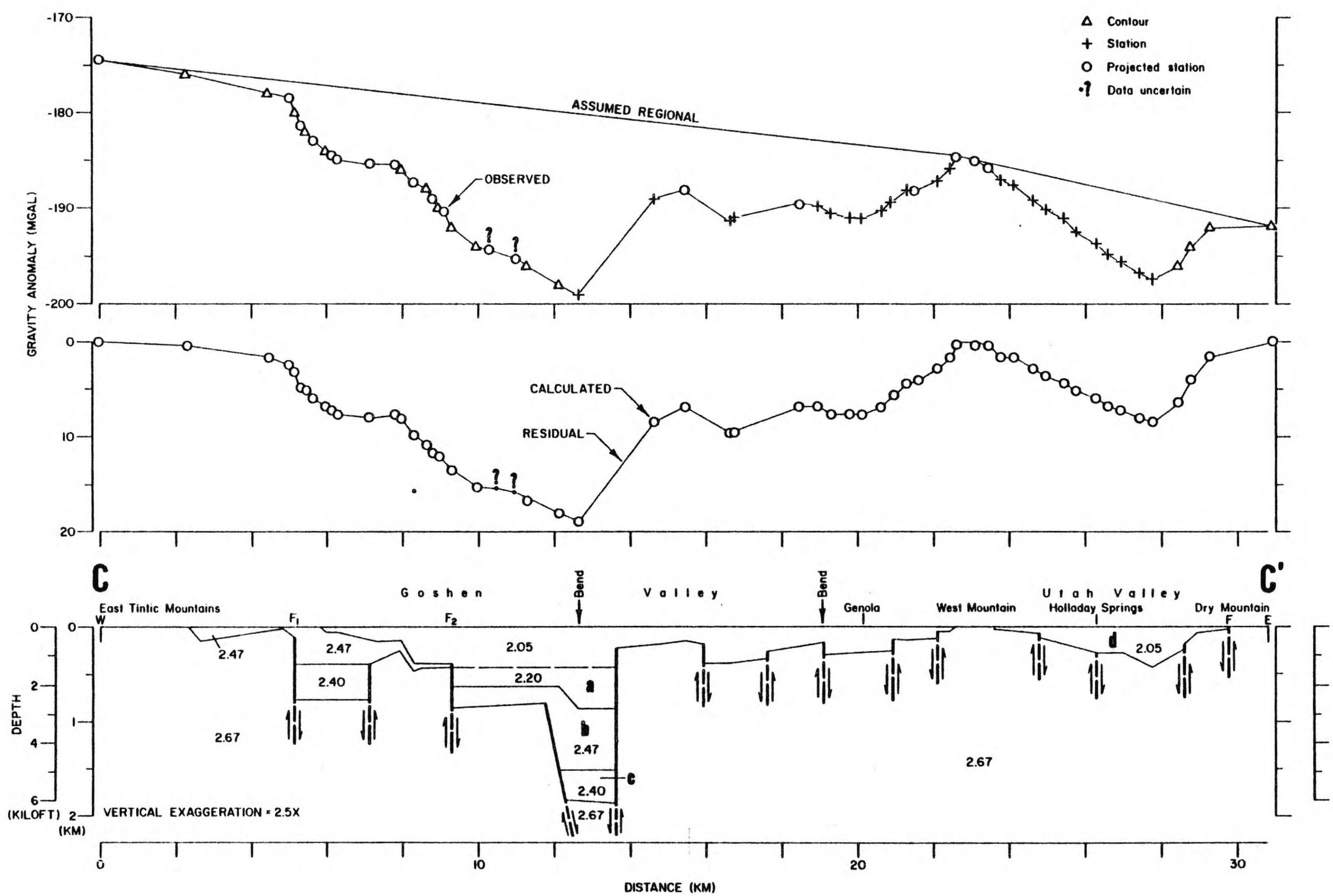

Contour
Station
Projected station
Data uncertain
ASSUMED REGIONAL
OBSERVED
CALCULATED
RESIDUAL
GRAVITY ANOMALY (MGAL)
-170
-180
-190
-200
0
10
20
C
C'
East Tintic Mountains
Goshen
Bend
Valley
Bend
Genola
West Mountain
Utah Valley
Holladay Springs
Dry Mountain
W
E
F
F_1
F_2
2.47
2.47
2.40
2.05
2.20
a
b
2.47
c
2.40
2.67
2.67
2.67
d
2.05
DEPTH
(KILOFT)
(KM)
VERTICAL EXAGGERATION = 2.5X
DISTANCE (KM)
0
10
20
30

Along the profile, the complete Bouguer gravity anomaly values are approximately: -174 mgal over the East Tintic Mountains, -199 mgal over the southern margin of the west arm of Utah Lake, -184 mgal over Goshen Pass, -197 mgal in the area north of Santaquin, and -192 over Dry Mountain. There are two different assumed regional gravity gradients corresponding with two segments of this profile, each of which assumes that the regional gravity decreases toward the east. The assumed regional gravity gradient is 0.443 mgal/km for the western part of the profile, between the East Tintic Mountains and West Mountain; whereas, the assumed regional gravity gradient is 0.896 mgal/km for the eastern part of the profile, between West Mountain and the Wasatch Range. The geologic cross section was modeled using 2 and 2-1/2 dimensional techniques.

The gravity data (which consist primarily of a large residual gravity minimum) along profile C-C' indicate that a broad complexly faulted graben, herein designated as the "Goshen Valley graben", overlies Goshen Valley throughout most of the distance between the East Tintic Mountains and West Mountain. The Goshen Valley graben is interpreted to consist of a main deeply faulted graben block within the central part of the valley that is flanked on both the west and east by a series of subsidary or smaller horsts and grabens in the bedrock.

Along the western part of profile C-C', the westernmost graben, which is shown beneath the eastern flank of the East Tintic Mountains and which was modeled using 2 dimensional techniques, shows a width of about 2 km (1.25 mi) and a depth of about 0.8 km (2600 ft). The graben is modeled as filled primarily by Tertiary volcanic rock with an assumed density of 2.47 gm/cc overlying the Apex Conglomerate with an assumed density of 2.40 gm/cc.

The Goshen Valley graben, as modeled along this profile, is comprised of structural blocks which are herein designated, from west to east: 1) the "West Goshen bench"; 2) the "South Goshen block"; and 3) the "North Goshen platform". The West Goshen bench, which includes the westernmost graben, is bound on the west by the East Tintic Mountains fault zone (previously described and designated as "F_1" in Fig. 6) and on the east by the Goshen Valley fault zone (designated "F_2" in Fig. 6), which are modeled to have vertical displacements of 0.75 km (2500 ft) and 0.5 km (1640 ft), respectively. Along profile C-C', the West Goshen bench has a total width of about 4 km (2.5 mi).

In the central part of profile C-C', the designation "South Goshen block" is herein given to the main deeply faulted graben block within the central part of Goshen Valley. The block was modeled using 2-1/2 dimensional techniques and is composed of polygons "a", "b", and "c". Polygons "a" and "b" represent alluvium younger than Paleozoic in age with a density of 2.20 gm/cc and Tertiary volcanic rocks with a density of 2.47 gm/cc, respectively, and both polygons are assumed to have a north strike length of 5.0 km (3.0 mi) and an infinte south strike length. Polygon "c" represents the Apex Conglomerate which is assumed to have a density of 2.40 gm/cc and a south strike length of 0.5 km (3.0 mi) and an infinite north strike length. The South Goshen block is bound on both sides by large steeply dipping faults: on the extreme west, the block is bound by the Goshen Valley fault zone (designated "F_2" on Fig. 6); and on the east, the block is bound by a fault with modeled vertical displacement of about 4920 ft (1.5 km). This latter fault, which is indicated by a large steep gravity anomaly (with gravity increasing toward the east), delineates the western edge of the North Goshen platform. The South Goshen block is modeled to be about 6230 ft (1.9 km) deep -- the deepest block along the profile. It should be noted that in order for the thickness of the Tertiary volcanic rocks to be constrained to its maximum estimated thickness of 2700 ft (0.82 km) (H. T. Morris, personal commun., 1982), it was necessary to model a thickness of about 1500 ft (0.46 km) of Apex Conglomerate at the bottom of the South Goshen block.

The North Goshen platform was modeled using 2 dimensional techniques and is associated with a broad sinuous gravity anomaly curve that extends from an area located 5 km (3.1 mi) west of the town of Genola to West Mountain. As modeled, this platform has an average depth of about 0.7 km (2300 ft). Furthermore, two separate minor grabens are associated with this platform and are indicated by two minor gravity minima over this region.

Along the eastern part of profile C-C', the West Mountain horst in the Goshen Pass region is bound on both the west and east sides by minor faults which are indicated by small gravity gradients and whose vertical displacements are modeled as 0.04 km (130 ft) and 0.08 km (260 ft), respectively. To the east of West Mountain, profile C-C' crosses only a minor "finger" or narrow southward extension of the southern part of the large gravity minimum associated with the Utah Valley graben (Plate 2). It should be noted that the subsurface geology associated with the Utah Valley graben along profile C-C' (polygon "d", Fig. 6), was modeled using 2-1/2 dimensional techniques, in which the assumed strike length toward the north is infinite and the assumed strike length toward the south is 0.5 km (0.3 mi). This narrow gravity low, with a total relief of approximtely 8 mgal, indicates that a narrow finger of the Utah Valley graben extends southward into this area. The marginal faults which bound the Utah Valley graben along profile C-C' are indicated by a fairly gentle gravity anomaly slope on the west and a fairly steep gravity anomaly slope on the east. The inferred fault associated with Holladay Springs, though not indicated by the residual gravity along the profile, is included in the geologic cross section at the point of intersection of an inclined (toward the east) bedrock surface and a horizontal bedrock surface within the Utah Valley graben. Also, it should be emphasized that the location of the two marginal faults shown on the east side of the Utah Valley graben, which are indicated by the residual gravity anomaly slopes, correspond with the location of mapped (Metter, 1955) faults in this region.

Profile D-D': Goshen

The Goshen profile D-D' (Fig. 7) extends eastward from the East Tintic Mountains along Highway 50 for 32 km (19.9 mi), across Goshen Valley, over the northern margin of Warm Springs Mountain, over the southern margin of Utah Valley (including the town of Santaquin), and finally over Dry Mountain. There are six bends along the profile: one at the mouth of Big Canyon in the East Tintic Mountains; one near Goshen; three minor bends north and northwest of Warm Springs Mountain; and one at Santaquin. The profile overlies exposed Paleozoic rocks for about 1.7 km (1.1 mi) and Paleozoic rocks covered by Packard Quartz

Figure 7. Interpretive geologic cross section along gravity profile D-D'. The number is the density (in gm/cc) of the layer. F_1=East Tintic Mountains fault zone, F_2=Goshen Valley fault zone, F_3=Long Ridge fault, and F=mapped fault.

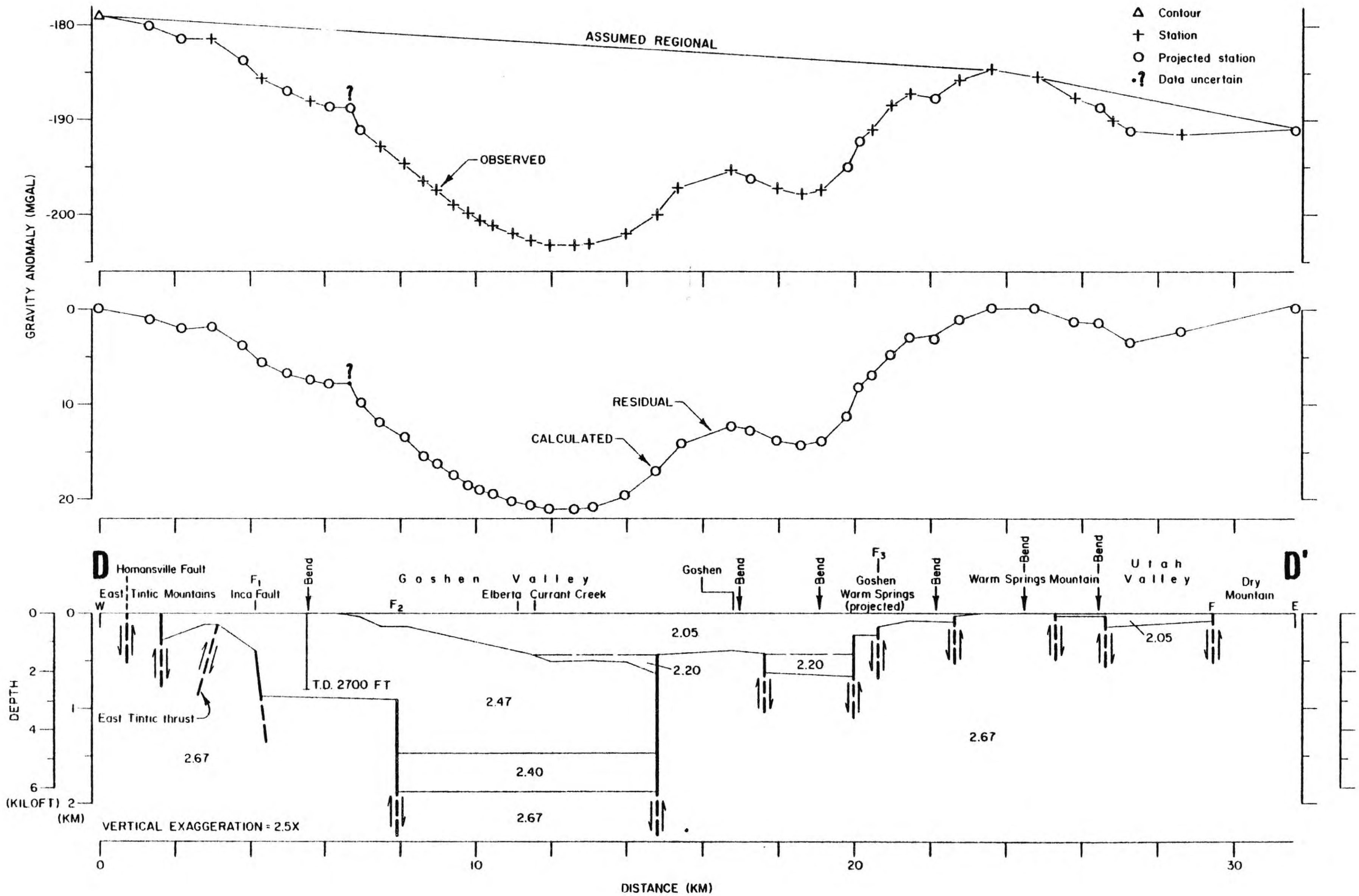

GRAVITY ANOMALY (MGAL)
-180
-190
-200
0
10
20
Contour
Station
Projected station
Data uncertain
ASSUMED REGIONAL
OBSERVED
RESIDUAL
CALCULATED
D
D'
Homansville Fault
East Tintic Mountains
F1
Inca Fault
Bend
Goshen Valley
Elberta
Current Creek
F2
Goshen
F3
Goshen
Warm Springs
(projected)
Warm Springs Mountain
Utah Valley
Dry Mountain
W
E
F
2.05
2.20
2.47
2.40
2.67
T.D. 2700 FT
East Tintic thrust
DEPTH
(KILOFT)
(KM)
VERTICAL EXAGGERATION = 2.5X
0
10
20
30
DISTANCE (KM)

Latite in the East Tintic Mountains for approximately 4 km (2.5 mi), alluvium associated with Goshen Valley for 17 km (10.6 mi), Paleozoic rocks (covered with a thin veneer of alluvium) associateo with the northern margin of Warm Springs Mountain for 3 km (1.9 km), alluvium associated with the southern margin of Utah Valley for 4 km (2.5 km), and Paleozoic rocks in Dry Mountain for 2 km (1.2 mi).

Along profile D-D', the approximate complete Bouguer gravity anomaly values are: -179 mgal over the East Tintic Mountains; -203 mgal over Goshen Valley near Currant Creek; -185 mgal over the northern margin of Warm Springs Mountain; -191 mgal over Utah Valley near Santaquin; and -191 mgal over Dry Mountain. A regional gravity gradient of 0.236 mgal/km, with gravity decreasing eastward, was asssumed between the East Tintic Mountains and the southern margin of West Mountain; and a regional gravity gradient of 0.785 mgal/km, with gravity also decreasing eastward, was assumed between the northern margin of Warm Springs Mountain and Dry Mountain. The geologic cross section (Fig. 7) was modeled using 2 dimensional techniques.

Along most of profile D-D', the geologic model consists of the Goshen Valley graben, which extends across Goshen Valley from the East Tintic Mountains on the west to Warm Springs Mountain on the east. The graben is indicated by the large residual gravity minimum over Currant Creek with a total gravity relief of about 21 mgal. Along the eastern margin of profile D-D', the southern end of the Utah Valley graben is indicated by a narrow residual gravity low of approximately 3 mgal located east of Warm Springs Mountain.

Along profile D-D', the faults associated with the western margin of the Goshen Valley graben (which are in part mapped or inferred from the geology of the East Tintic mining district (Morris and Lovering, 1979) and/or indicated by the gravity data), are (from west to east): 1) a small bounding fault, which is indicated by a small change in the gravity anomaly which coincides with the contact between the Paleozoic rocks and the Packard Quartz Latite as mapped by Morris and Lovering (1979) and which is modeled with a vertical displacement of approximately 0.5 km (1640 ft); 2) the East Tintic thrust, which is inferred by Morris and Lovering (1979) and which coincides with a small positive residual gravity anomaly along the profile; 3) the East Tintic fault zone (which coincides with the projected Inca fault as inferred by Morris and Lovering (1979) and which is designated "F_1" on Fig. 7), which coincides with a significant change in the the slope of the gravity anomaly; and 4) a large steeply dipping fault which was herein designated as the Goshen Valley fault zone (designated "F_2" on Fig. 7) and which is indicated by a large change in the slope of the gravity anomaly in the west central part of Goshen Valley.

The interpreted structural blocks associated with the Goshen Valley graben along profile D-D' are (from west to east): 1) the West Goshen bench; 2) the South Goshen block; and 3) the East Goshen platform. Along profile D-D', the West Goshen bench is bound (1) on the west, by the East Tintic Mountains fault zone (or the projected Inca fault), which is modeled with a vertical displacement of about 0.6 km (1960 ft) and (2) on the east, by the Goshen Valley fault zone. Thus, the bench along profile D-D' is about 4 km (2.5 mi) in width. The depth of the bench, as modeled along profile D-D', is 0.87 km (2650 ft) and compares well with the depth of the bench, as modeled along profile C-C' to the north, which is 0.85 km (2790 ft). It should be noted that along profile D-D', the depth of the West Goshen bench is considered to be deeper than 0.82 km (2700 ft) on the basis of a mineral exploration hole located about 0.5 km (0.3 mi) north of profile D-D' near the mouth of Big Canyon in the East Tintic Mountains, which bottomed in Packard Quartz Latite at a depth of 0.82 km (2700 ft) (Morris and Lovering, 1979). Therefore, the rocks above the West Goshen bench are modeled as Packard Quartz Latite which have an assumed density of 2.47 gm/cc.

Along profile D-D', the South Goshen block is bound on both sides by large steeply dipping faults (or fault zones) which are indicated by steep gravity gradients: (1) on the west, by the Goshen Valley fault zone (designated "F_2" on Fig. 7), with a modeled vertical displacement of about 1.0 km (3280 ft); and (2) on the east, by an unnamed fault (or fault zone), with a modeled vertical displacement of about 1.5 km (4900 ft). Thus, the South Goshen block here has a width of about 6.5 km (4.0 mi). As discussed earlier, the South Goshen block is the deepest of the blocks in the Goshen Valley graben and the depth to bedrock is modeled here to be about 1.9 km (6230 ft). In the deepest part of the Goshen Valley graben along profile D-D', the rocks are modeled to consist of (1) Packard Quartz Latite (or other Tertiary volcanic rocks) with an assumed average thickness of 0.82 km (2,700 ft) and an assumed density of 2.47 gm/cc, overlying (2) the Apex Conglomerate with a modeled thicknesss of about 0.46 km (1500 ft) and an assumed density of 2.40 gm/cc. However, it should be noted that on the complete Bouguer gravity anomaly map, the largest gravity minimum associated with the Goshen Valley graben is 2 km (1.2 mi) north of profile D-D' near Currant Creek; and this fact indicates that the maximum depth of the graben is probably somewhat greater than that modeled along profile D-D'.

Along profile D-D', the East Goshen platform is defined as consisting of a series of blocks in the relatively shallow bedrock of that part of the Goshen Valley graben which extends for a distance of about 8 km (4.9 mi) between the town of Goshen and Warm Springs Mountain. Beneath the town of Goshen, the modeled depth of the platform averages approximately 0.43 km (1410 ft). The East Goshen platform is bounded (1) on the west, by the large steeply dipping unnamed fault about 2 km (1.2 mi) west of the town of Goshen and (2) on the east, by the Long Ridge fault (designated "F_3" on Fig. 9). Within this platform, a small graben is indicated by a gravity low with a closure of 2 mgal, which lies 4 km (2.5 mi) west of the Goshen Warm Springs; and this graben is modeled with a depth of approximately 0.66 km (2170 ft). In addition, the eastern margin of the East Goshen platform is modeled to comprise three bounding faults which are indicated by a steep gravity gradient over the western flank of Warm Springs Mountain. The easternmost fault is coincident with both the Long Ridge fault (which was mapped by Eaton (1929)) and also Goshen Warm Springs and is modeled with a vertical displacement of about 0.1 km (330 ft). The Warm Springs Mountain horst is indicated by a residual gravity high which is bounded on both sides by gravity anomalies which indicate marginal faults -- on the west, the Long Ridge fault just discussed, and on the east, an unnamed fault inferred from the gravity data.

The southern tip of the Utah Valley graben is indicated along profile D-D' by a narrow residual gravity low of approximately 3 mgal located east of the Warm Springs Mountain horst. On the west, the graben is shown as bound by two small faults which are indicated by two small increases in the gravity gradient. On the east, the Utah Valley graben is bounded by a fault which is not only indicated by a gravity gradient, but also coincides with a fault mapped by Metter (1955) which is associated with the Wasatch fault zone.

Profile E-E': Goshen Warm Springs

The Goshen Warm Springs profile E-E' (Fig. 8), totaling 6.5 km (4.0 mi) in length, extends 4.5 km (2.8 mi) west of Goshen Warm Springs across the eastern margin of Goshen Valley and 2 km (1.2 mi) east of Goshen Warm Springs over Warm Springs Mountain. The complete Bouguer gravity anomaly values range from -196 mgal over the alluvium at the western end of the profile to -186 mgal over the Paleozoic rocks of Warm Springs Mountain at the eastern end of the profile. Furthermore, the assumed regional gravity gradient is 0.263 mgal/km (with gravity decreasing toward the east), which is the same as that assumed for the western segment of profile D-D'. The geologic cross section was modeled using 2-1/2 dimensional techniques and assuming a north strike length of 4.5 km (2.8 mi) and a south strike length of 2.5 km (1.5 mi).

The residual gravity anomaly along profile E-E' shows (from west to east) an anomalous small gravity high, a small gravity low, and a pronounced anomalous gravity slope over the eastern margin of Goshen

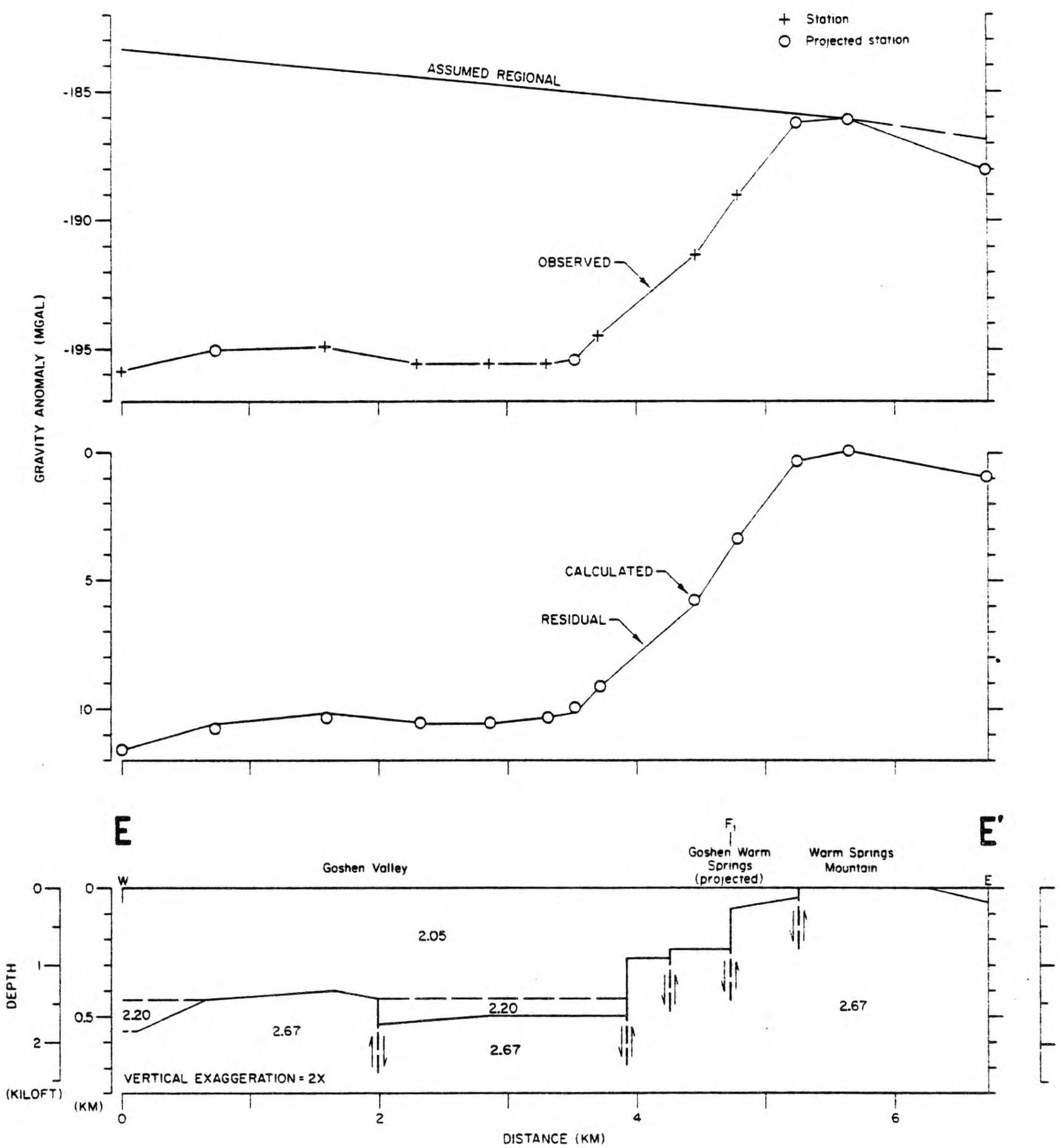

Figure 8. Interpretive geologic cross section along gravity profile E-E'. The number is the density (in gm/cc) of the layer. F_1=Long Ridge fault. This geologic cross section was modeled using 2-1/2 dimensional techniques. All polygons were modeled assuming a north strike length of 4.5 km and a south strike length of 2.5 km.

Valley. The pronounced gravity anomaly, with a total relief of 10 mgal over a horizontal distance of 2 km (1.2 mi), is interpreted to be associated with four faults whose total vertical displacement is approximately 0.60 km (1970 ft). The easternmost fault is interpreted to be coincident with the contact between the alluvium of Goshen Valley and the Paleozoic rocks of Warm Springs Mountain. The next fault to the west is interpreted to be coincident with the Long Ridge fault (mapped by Eaton (1929) and designated "F_1" on Fig. 8) and Goshen Warm Springs (projected); this fault is modeled to have a vertical displacement of approximately 0.2 km (660 ft). The westernmost of the four faults, with a modeled vertical displacement of 0.3 km (980 ft), is interpreted to be the fault which bounds the eastern margin of the small graben located within the East Goshen platform. Over the central part of profile E-E', the small graben within the East Goshen platform is indicated by the small gravity low with a total relief of less than 1 mgal. Along the western part of profile E-E', the small gravity high is interpreted to be associated with the western margin of the East Goshen platform. The East Goshen platform is probably bound on the west by a fault which separates it from the South Goshen block, as seen in profiles C-C' and D-D'; however, this fault apparently lies just west of the west end of profile E-E' and is therefore not shown on profile E-E'.

The fact that Goshen Warm Springs is directly related to the Long Ridge fault, suggests that the Long Ridge fault (and possibly adjacent faults) may act as conduits for the ascension of the thermal water associated with the springs. Further, this relation suggests that the faults may extend to a much greater depth than indicated by their modeled vertical displacements in order to tap the hot water heated by the geothermal gradient within the area. If one assumes that (1) the depth of maximum vertical displacement is 0.6 km (1970 ft), and (2) the temperature of the water may be due to heating by the normal geothermal gradient of approximately 35^{o} C/km (D. S. Chapman, personal commun., 1981), then the resulting temperature of the water is approximately 21^{o}C -- which is identical to the measured surface temperature of the water in the Goshen Warm Springs (see Table 1). Because, the water temperature probably decreases as the water ascends along the faults, then the faults probably extend to a greater depth than 0.6 km (1970 ft) to provide warm water with a temperature of 21^{o}C at the surface. Of course, this reasoning also presumes that the assumed normal geothermal gradient is correct.

DISCUSSION

Interrelationship of Fault Blocks

The interrelationship of the grabens, horsts, and spurs as interpreted from the gravity data within the survey area is complex, but does exhibit differential faulting and tilting which is typical within the Basin and Range province. Within the survey area, the valley blocks (the Utah Valley graben and the Goshen Valley graben) are downdropped relative to the mountain blocks (the Oquirrh-Boulter-Tintic fault block, the Wasatch Range block, the West Mountain horst, and the Warm Springs Mountain horst). In addition, the valley blocks are apparently tilted in different directions; i.e., the Utah Valley graben is probably tilted toward the southeast and the Goshen Valley graben is probably tilted toward the northeast.

It should be noted that this pattern of differential faulting and tilting also pertains to the smaller structural blocks within the large horst and grabens. For example, the small structural blocks within the Goshen Valley graben (i.e., the North Goshen platform, the West Goshen bench, the East Goshen platform, and the South Goshen block) exhibit differential subsidence along faults or fault zones relative to each other. Furthermore, the South Goshen block not only displays the greatest relative subsidence of all the structural blocks within the Goshen Valley graben -- namely, to a depth of 1.9 km (6230 ft) along profile D-D' (Fig. 7) -- but also the block probably tilts toward the northeast, as evident from the gravity patterns over this block. In addition, the horsts within the Oquirrh-Boulter-Tintic fault block in the survey area (i.e., the Lake Mountains horst, the Greeley Hill block, the Mosida Hills block, and the East Tintic Mountains horst), are displaced vertically relative to each other, as evident from the elevations of their crests and the gravity patterns associated with them; and the possibility that the Greeley Hill block and Mosida Hills block are also displaced laterally from each other, as is evident from the offsets of the gravity highs and the few mapped faults associated with the separate horsts, warrants further field investigation.

Furthermore, the Utah Valley graben and the Goshen Valley graben are believed to be part of a north-south trending belt of grabens which define the Wasatch structural trough (Gilbert, 1928). In the study area, the Wasatch structural trough lies between the Oquirrh-Boulter-Tintic fault block and the Wasatch Range block (Gilbert, 1928; Cook and Berg, 1961) where the intervening blocks have been dropped down relative to these two large bounding blocks. The West Mountain horst apparently remained relatively stationary with respect to the Oquirrh-Boulter-Tintic fault block based on the essentially uniform elevations of the crests of West Mountain, the Lake Mountains, and the East Tintic Mountains, according to Cook and Berg (1961). In addition, the bedrock spurs became lodged at an intermediate level relative to the Wasatch Range block and the valley blocks. Furthermore, the Utah Valley graben shows the greatest displacement relative to all the blocks within the survey area, where depth to bedrock is modeled to be 4.2 km (13,780 ft) (along profile B-B', Fig. 5).

Geothermal Significance

The usefulness of gravity surveys in helping to evaluate the geothermal resources of an area was discussed previously (p. 1). In this section, the geothermal significance of the results of the gravity survey in the study area will be discussed.

Within the study area, there is one gravity high located above Saratoga Hot Springs and Crater Hot Springs which may apparently be caused by the increased density of alluvium or host rock as a result of the circulation of hot water. It is unlikely that four small local gravity lows which occur within the survey area (three in or near the Jordan Narrows area and one just west of Goshen Warm Springs) are caused by shallow magma chambers or silicic intrusions, as local heat sources, because no Recent (less than 2 m.y. old) (White and Williams, 1975) volcanic rocks are evident within the study area. The three small gravity lows in or near the Jordan Narrows area are probably the result of a density difference between the alluvium which fills the narrows and the adjacent Paleozoic rocks. The gravity low west of the Goshen Warm Springs is interpreted to be caused by a small graben within the East Goshen platform.

However, within the survey area, many bands of closely spaced gravity contours with large gravity gradients indicate major faults or fault zones which form the boundaries of grabens and horsts. The major faults, which may extend to depths of at least several kilometers, often serve as conduits for the hot water to ascend to the surface, after it has been heated by the normal regional geothermal gradient. The hot springs in the study area appear to be controlled by major faults and tend to be aligned along the faults and are sometimes at the intersection of faults. For example, five thermal springs are located along the Utah Lake fault zone (which is clearly indicated by the band of closely spaced gravity contours with steep gravity gradients on the complete Bouguer gravity anomaly map): 1) Saratoga Hot Springs; 2) Crater Hot Springs; 3) the warm springs near Goose Point; 4) the Bird Island Warm Springs; and 5) the Lincoln Point Warm Springs. In northern Utah Valley, in the Saratoga Hot Springs area, water temperatures of 15.5^{o}C to 46^{o}C were reported from springs and wells (Goode, 1978). Here the Utah Lake fault zone is modeled in this report (profile A-A', Fig. 4) with a vertical displacement of the Paleozoic bedrock surface of approximately 1.5 km (4900 ft) and the Utah Valley graben is modeled (also profile A-A', Fig. 4) with a depth of about 2.5 km (8200 ft). In addition, in the southern part of Utah Valley, on the east side of West Mountain, water temperatures obtained from shallow wells range from 20^{o}C to 34^{o}C (Goode, 1978); in this area, the Utah Lake fault zone comprises a fairly wide band of step faults which trend north-south and which have an indicated total vertical displacement of the Paleozoic bedrock surface of 4.2 km (13,780 ft) along profile B-B' (Fig. 5). This evidence suggests that the faults associated with the Utah Lake fault zone probably extend to several kilometers and provide the conduits for the upward migration of hot water heated by the normal regional geothermal gradient within the area.

In the Goshen Valley area, springs and shallow wells were reported by Goode (1978) to produce water temperatures which range from 18.5^{o} to 22^{o} C. Furthermore, Parry and Cleary (1978) suggest that water as hot as 180^{o}C may exist at depth in Goshen Valley based on Na-K-Ca and SiO_2 geothermometry. The Goshen Warm Springs lie along the Long Ridge fault, and correspond with a band of closely spaced gravity contours. The fault may extend to a greater depth than that [namely 0.1 km (330 ft)] modeled along profile D-D' (Fig. 7) in order to tap the hot water heated by the normal regional geothermal gradient or the geothermal reservoir which may exist at depth. The Goshen Valley graben is shown in this report to comprise several large structural blocks (one containing basin fill to a depth of 1.9 km or 6200 ft) as well as small structural blocks which are complexly faulted and tilted. Thus the many faults associated with these blocks within the Goshen Valley graben may form adequate conduits for the migration of thermal waters which could be heated at depth by the normal regional geothermal gradient.

Gravity data aid in locating increased density areas which are the result of circulation of thermal waters and delineating faults or fault zones which may act as conduits for the circulation of thermal waters and which, in some cases, control the location of thermal springs along the fault or fault zone. The thermal waters may be related to either (1) a convective geothermal system, where circulation occurs in a low-porosity but fracture-permeable environment or (2) a conductive geothermal system, where water in high porosity and/or high permeability sedimentary aquifers is heated in place by a higher than normal geothermal gradient -- as in valley blocks.

SUMMARY AND CONCLUSIONS

The survey area lies within the transition zone between the Basin and Range and the Middle Rocky Mountains physiographic provinces; and within the Sevier orogenic belt and the Wasatch fault zone. Structures related to all of these features affect the gravity patterns within this area.

In the survey area, two dominant trends of gravity contours are evident on the complete Bouguer gravity anomaly map -- northwest-southeast in the northern part of the study area and northeast-southwest in the southern part of the area. These two dominant gravity contour trends roughly parallel the Sevier orogenic belt in this area and suggest that Basin and Range normal faulting patterns may in part be controlled by these older structures.

The survey area lies along the eastern part of the Deep Creek-Tintic belt which is oriented east-west along latitude 40° N.; and within the survey area, two east-west local gravity trends are evident within and parallel to the orientation of this much larger regional feature. Both local gravity trends are defined by bands of gravity contours (which indicate marginal faults) or gravity saddles. The local east-west gravity trends and the Deep Creek-Tintic belt coincide with (1) a large regional east-west gravity lineation (Cook and Montgomery, 1972; Montgomery, 1973), (2) an east-west trending series of aeromagnetic highs (Zeitz and others, 1969; Mabey and others; 1964), and (3) an east-west trending belt of seismicity (Kastrinsky, 1977; McKee, 1982). The broad east-west trend, which manifests itself on several different kinds of geophysical data along latitude 40^{0} N., is believed to be the result of a fracture or fracture zone associated with a transform fault extending into the upper mantle (Zeitz and others, 1969; Cook and Montgomery, 1972; Montgomery, 1973).

The complete Bouguer gravity anomaly map exhibits a pattern of alternating gravity lows and highs over grabens and horsts, respectively, which are separated from each other by bands of closely spaced gravity contours indicative of Basin and Range faults. This pattern is characteristic of gravity patterns over much of the Basin and Range province. The gravity data were interpreted by modeling five east-west profiles, A-A' to E-E', and interpretive geolgic cross sections were modeled. The gravity data define several large fault blocks which exhibit differential displacement and tilting in relation to each other. In particular, the Utah Valley graben and Goshen Valley graben are the major blocks in the survey area which have not only been downdropped relative to the Oquirrh-Boulter-Tintic fault block, the Wasatch Range horst, the West Mountain horst, and the Warm Springs Mountain horst, but also have been tilted in different directions relative to each other. The Utah Valley graben and the Goshen Valley graben are believed to be part of a north-south trending belt of grabens which form part of the Wasatch structural trough (Gilbert, 1928) characterized as follows: 1) within the trough, the intervening blocks have dropped down relative to the the Oquirrh-Boulter-Tintic fault block and the Wasatch Range horst; 2) within the trough, the West Mountain horst has remained stationary relative to the two large bounding blocks (Cook and Berg, 1961); and 3) within the trough, the Traverse and Santaquin spurs have become lodged at intermediates levels relative to the Wasatch Range horst and the valley blocks adjacent to the spurs.

Within the Wasatch structural trough, the Utah Valley graben is bound on the west and east by the Utah Lake fault zone and the Wasatch fault zone, respectively. The Utah Lake fault zone and the Wasatch fault zone produce the steepest gravity gradients within the survey area -- 9 mgal/km over the former at the North end of Utah Lake and 10 mgal/km over the latter just southeast of Provo. Vertical displacements of the bedrock surface associated with faults which bound the deepest part of the graben were modeled to be 3.3 km (10,800 ft) on the west and 3.2 km (10,500 ft) on the east along profile B-B' near Spanish Fork. The Utah Valley graben is bound on the north and south by the Traverse spur and the Santaquin spur, respectively. Depth to Paleozoic bedrock within this graben is interpreted to be somewhat more than 4.2 km (13,780 ft), based on the Gulf Energy and Minerals #1 Bank well and the interpretation of the gravity data along profile B-B'.

Within the Wasatch structural trough, the Goshen Valley graben is shown to be a complexly faulted graben which consists of smaller structural blocks which exhibit differential displacement along faults or fault zones. The minimum vertical displacements along the fault zones within and along the boundaries of the Goshen Valley graben have been modeled to exceed 1.5 km (4920 ft) along profiles C-C', D-D', and

E-E'. The gravity data indicate that the maximum depth to Paleozoic bedrock within this graben is somewhat greater than 1.9 km (6230 ft).

Overall, the gravity data have shown that the structural relationship which exists between the many large and small fault blocks within the study area is primarily related to Basin and Range normal faulting. Furthermore, the gravity data indicate that blocks within the study area were displaced downward relative to the Wasatch Mountains on the east and the Oquirrh-Boulter-Tintic fault block on the west -- with the the greatest vertical displacement of the surface of Paleozoic bedrock occurring in the southern part of the Utah Valley graben. It was also found that the structure underlying the Goshen Valley is far more complex than previously recognized. The results of this study have generally substantiated the findings of the previous investigators, especially those of Gilbert (1928) and Cook and Berg (1961); and the additional gravity data available for this study have permitted a more detailed interpretation of the regional structural patterns.

The association of the Utah Lake fault zone with five thermal springs (Saratoga Hot Springs, Crater Hot Springs, the warm springs at Goose Point, the Bird Island Warm Springs, and the Lincoln Point Warm Springs) substantiates the fact that the thermal springs are fault controlled. In addition, the minimum vertical displacements associated with the Utah Lake fault zone as modeled along profiles A-A' and B-B' [1.66 km (5450 ft) and 3.3 km (10,800 ft), respectively] in conjunction with the thermal springs, indicate that the faults probably extend to depths of at least several kilometers to tap the hot water heated by the normal regional geothermal gradient within the survey area. Along the Long Ridge fault in the Goshen Valley, the gravity data support the conclusion that the Goshen Warm Springs are also fault controlled and aid in delineating the trend of the fault associated with the warm springs. Along profile A-A', a small residual gravity high over the Saratoga Hot Springs and Crater Hot Springs area (as projected onto the profile) is probably caused by either (1) Paleozoic bedrock blocks which are differentially faulted or (2) an increase of the density of the host rocks -- namely, alluvium and/or underlying Paleozoic bedrock -- as a result of cementation caused by ciruculating hot brines associated with the hot springs. The greater definition of the underlying structure within the the Utah Valley graben and Goshen Valley graben will aid in tracing faults through which warm waters are migrating, as evident from warm water temperatures obtained from water wells (Goode, 1978) and the surface manifestations of thermal springs in the study area. It should be noted that although the gravity data do not apparently delineate any deep intrusive bodies which may represent a heat source for the thermal waters in the survey area, this does not preclude the possibility that these features may exist.

APPENDIX A

PRINCIPAL FACTS OF GRAVITY STATIONS

Units are as follows:

	Units
Latitude	degrees, minutes
Longitude	degrees, minutes
Elevation	feet
Observed gravity	milligal
Theoretical gravity[1]	Do
Free-air gravity anomaly value	Do
Simple Bouguer gravity anomaly value[2]	Do
Terrain correction (T.C.)[2]	Do
Complete Bouguer gravity anomaly value[2]	Do

Number designation of gravity stations is as follows:

Designation	Investigator or Project
WO-000	Cook and Berg, 1961 and 1972
P-0000 and PG-000	Applied Geophysics Inc., 1978
MS-000 and 6-0000	Meiiji Resource Consultants, 1980
DD-000	Davis, D. A., 1981

---

[1]Theoretical gravity at mean sea level, using the International Gravity Formula of 1930 (Swick, 1942).

[2]A mean rock density of 2.67 gm/cc was assumed for both the Bouguer and terrain corrections. Terrain corrections were taken out to 166.7 km (100 mi) from each station.

STAT.	LATITUDE	LONGITUDE	ELEV.	OBSERVED GRAVITY	THEOR. GRAVITY	FREE AIR	SIMPLE BOUGUER	T. C.	COMPLETE BOUGUER
MS 1	39. 54.460	112. 1.660	5464.00	979650.65	980172.28	-7.670	-193.830	2.58	-191.250
MS 2	39. 54.430	112. 1.530	5358.00	979656.12	980172.23	-12.180	-194.700	2.63	-192.070
MS 3	39. 54.390	112. 1.210	5263.00	979660.39	980172.18	-16.790	-196.080	2.18	-193.900
MS 4	39. 54.450	112. .930	5159.00	979666.95	980172.26	-20.060	-195.820	1.95	-193.870
MS 5	39. 54.480	112. .720	5104.00	979669.48	980172.31	-22.730	-196.620	1.78	-194.840
MS 7	39. 54.500	112. .270	4973.00	979676.94	980172.34	-27.660	-197.080	1.58	-195.500
MS 8	39. 54.500	111. 59.990	4908.00	979680.44	980172.34	-30.270	-197.470	1.49	-195.980
MS 9	39. 54.500	111. 59.710	4858.00	979682.52	980172.34	-32.860	-198.380	1.38	-197.000
MS 10	39. 54.490	111. 59.380	4814.00	979684.15	980172.32	-35.400	-199.390	1.28	-198.110
MS 11	39. 54.260	111. 59.280	4784.00	979685.02	980171.98	-37.020	-199.990	1.33	-198.660
MS 12	39. 54.420	111. 59.170	4777.00	979685.49	980172.22	-37.370	-200.130	1.27	-198.860
MS 13	39. 54.440	111. 58.700	4722.00	979687.79	980172.25	-40.290	-201.170	1.31	-199.860
MS 14	39. 54.450	111. 58.370	4708.00	979688.05	980172.26	-41.400	-201.790	1.26	-200.530
MS 15	39. 54.460	111. 58.100	4694.00	979688.37	980172.28	-42.410	-202.330	1.24	-201.090
MS 16	39. 54.450	111. 57.800	4682.00	979689.04	980172.26	-42.820	-202.340	1.24	-201.100
MS 17	39. 54.470	111. 57.550	4673.00	979689.54	980172.29	-43.210	-202.410	1.17	-201.240
MS 18	39. 54.470	111. 57.210	4664.00	979690.05	980172.29	-43.570	-202.460	1.16	-201.300
MS 19	39. 54.480	111. 56.980	4654.00	979690.86	980172.31	-43.720	-202.270	1.15	-201.120
MS 20	39. 54.490	111. 56.670	4652.00	979691.35	980172.32	-43.440	-201.920	1.17	-200.750
MS 21	39. 54.480	111. 56.430	4651.00	979692.03	980172.31	-42.800	-201.260	1.19	-200.070
MS 22	39. 54.510	111. 56.140	4655.00	979693.23	980172.35	-41.270	-199.860	1.22	-198.640
MS 23	39. 54.750	111. 55.810	4699.00	979691.79	980172.71	-38.940	-199.020	1.07	-197.950
MS 24	39. 54.940	111. 55.550	4731.00	979691.55	980172.99	-36.430	-197.620	1.02	-196.600
MS 25	39. 54.960	111. 55.250	4754.00	979692.99	980173.02	-32.840	-194.810	1.07	-193.740
MS 26	39. 54.960	111. 54.980	4758.00	979693.71	980173.02	-31.740	-193.850	1.21	-192.640
MS 27	39. 55.170	111. 54.400	4760.00	979693.25	980173.33	-32.390	-194.540	1.13	-193.410
MS 28	39. 55.180	111. 54.060	4680.00	979698.19	980173.34	-34.950	-194.390	1.42	-192.970
MS 29	39. 55.340	111. 53.560	4691.00	979696.92	980173.58	-35.410	-195.230	1.40	-193.830
MS 30	39. 55.280	111. 53.310	4769.00	979692.85	980173.49	-32.050	-194.530	1.32	-193.210
MS 31	39. 55.270	111. 53.060	4785.00	979692.81	980173.48	-30.600	-193.610	1.46	-192.150
MS 32	39. 55.280	111. 52.730	4790.00	979693.54	980173.49	-29.370	-192.570	1.78	-190.790
MS 33	39. 55.310	111. 52.470	4796.00	979693.04	980173.54	-29.380	-192.780	2.16	-190.620
MS 34	39. 55.170	111. 52.370	4850.00	979691.59	980173.33	-25.580	-190.800	2.33	-188.470
MS 35	39. 56.500	111. 54.510	4652.00	979699.40	980175.30	-38.350	-196.830	.87	-195.960
MS 36	39. 56.510	111. 53.920	4609.00	979702.74	980175.31	-39.070	-196.080	.98	-195.100
MS 37	39. 56.490	111. 53.380	4574.00	979704.81	980175.28	-40.270	-196.090	1.15	-194.940
MS 38	39. 56.490	111. 52.790	4545.00	979705.65	980175.28	-42.120	-196.970	1.41	-195.560
MS 39	39. 56.500	111. 52.470	4539.00	979705.91	980175.30	-42.500	-197.120	1.52	-195.600
MS 40	39. 56.490	111. 52.240	4538.00	979705.80	980175.28	-42.660	-197.260	1.65	-195.610
MS 41	39. 56.500	111. 52.000	4541.00	979705.71	980175.30	-42.510	-197.200	1.74	-195.460
MS 42	39. 56.500	111. 51.670	4544.00	979706.24	980175.30	-41.700	-196.490	2.00	-194.490
MS 43	39. 56.490	111. 51.340	4565.00	979707.68	980175.28	-38.190	-193.730	2.36	-191.370
MS 44	39. 56.500	111. 51.090	4618.00	979706.96	980175.30	-34.020	-191.330	2.43	-188.900
MS 45	39. 56.410	111. 50.760	4790.00	979699.38	980175.16	-25.240	-188.430	2.26	-186.170
MS 46	39. 56.370	111. 50.490	4850.00	979695.83	980175.11	-23.130	-188.350	2.32	-186.030
MS 47	39. 58.170	112. 3.430	5988.00	979635.81	980177.77	21.230	-182.760	1.35	-181.410
MS 48	39. 57.940	112. 2.860	5810.00	979645.97	980177.43	15.010	-182.920	1.34	-181.580
MS 49	39. 57.730	112. 2.430	5671.00	979651.94	980177.12	8.200	-184.990	1.22	-183.770
MS 50	39. 57.480	112. 2.130	5587.00	979654.76	980176.75	3.500	-186.830	1.23	-185.600

STAT.	LATITUDE	LONGITUDE	ELEV.	OBSERVED GRAVITY	THEOR. GRAVITY	FREE AIR	SIMPLE BOUGUER	T. C.	COMPLETE BOUGUER
MS 51	39. 57.070	112. 1.380	5319.00	979667.31	980176.14	-8.520	-189.730	1.77	-187.960
MS 52	39. 57.030	112. 1.050	5269.00	979669.98	980176.08	-10.460	-189.990	1.52	-188.470
MS 53	39. 57.030	112. .730	5205.00	979672.82	980176.08	-13.660	-191.000	1.48	-189.520
MS 54	39. 57.050	112. .430	5169.00	979674.06	980176.11	-15.900	-191.980	1.17	-190.810
MS 55	39. 57.070	112. .170	5119.00	979675.33	980176.14	-19.350	-193.740	1.09	-192.650
MS 56	39. 57.090	111. 59.710	5044.00	979678.16	980176.17	-23.610	-195.440	.95	-194.490
MS 57	39. 57.100	111. 59.300	4973.00	979680.44	980176.19	-27.990	-197.410	.89	-196.520
MS 58	39. 57.110	111. 59.050	4933.00	979681.88	980176.20	-30.360	-198.410	.85	-197.560
MS 59	39. 57.120	111. 58.720	4886.00	979683.40	980176.22	-33.280	-199.720	.81	-198.910
MS 60	39. 57.120	111. 58.530	4857.00	979684.19	980176.22	-35.160	-200.640	.79	-199.850
MS 61	39. 57.120	111. 58.250	4824.00	979685.41	980176.22	-37.100	-201.440	.77	-200.670
MS 62	39. 57.120	111. 58.050	4796.00	979686.48	980176.22	-38.580	-201.990	.78	-201.210
MS 63	39. 57.130	111. 57.730	4754.00	979688.24	980176.23	-40.790	-202.770	.76	-202.010
MS 64	39. 57.110	111. 57.300	4697.00	979691.00	980176.20	-43.430	-203.440	.77	-202.670
MS 65	39. 57.130	111. 56.510	4621.00	979694.94	980176.23	-46.630	-204.070	.77	-203.300
MS 66	39. 57.140	111. 56.190	4598.00	979696.52	980176.25	-47.240	-203.890	.77	-203.120
MS 67	39. 57.150	111. 55.580	4579.00	979698.60	980176.26	-46.930	-202.940	.79	-202.150
MS 68	39. 57.160	111. 54.510	4540.00	979705.84	980176.28	-43.380	-198.060	.91	-197.150
MS 69	39. 57.180	111. 53.960	4548.00	979707.00	980176.30	-41.490	-196.450	.94	-195.510
MS 70	39. 57.260	111. 53.320	4526.00	979707.73	980176.42	-42.980	-197.180	1.06	-196.120
MS 71	39. 57.400	111. 52.780	4519.00	979706.94	980176.63	-44.610	-198.580	1.18	-197.400
MS 72	39. 57.520	111. 52.390	4518.00	979706.79	980176.81	-45.050	-198.980	1.26	-197.720
MS 73	39. 57.600	111. 52.090	4517.00	979707.06	980176.93	-44.970	-198.870	1.36	-197.510
MS 74	39. 57.640	111. 51.900	4523.00	979707.51	980176.99	-44.030	-198.130	1.46	-196.670
MS 75	39. 57.800	111. 51.680	4524.00	979709.25	980177.22	-42.450	-196.580	1.62	-194.960
MS 76	39. 57.650	111. 51.500	4517.00	979711.59	980177.00	-40.590	-194.460	2.20	-192.260
MS 77	39. 58.100	111. 51.320	4517.00	979714.01	980177.67	-38.840	-192.710	1.77	-190.940
MS 78	39. 58.160	111. 51.230	4519.00	979715.03	980177.76	-37.710	-191.650	1.78	-189.870
MS 79	39. 58.260	111. 51.100	4533.00	979715.50	980177.90	-36.070	-190.490	1.75	-188.740
MS 80	39. 58.490	111. 50.810	4614.00	979712.75	980178.24	-31.500	-188.700	1.46	-187.240
MS 81	39. 58.610	111. 50.500	4660.00	979710.03	980178.42	-30.100	-188.860	1.39	-187.470
MS 82	39. 58.810	111. 49.990	4699.00	979709.58	980178.72	-27.130	-187.230	1.46	-185.770
MS 83	39. 58.980	111. 49.490	4761.00	979707.39	980178.97	-23.770	-185.970	1.37	-184.600
MS 84	39. 59.100	111. 48.750	4816.00	979703.06	980179.15	-23.090	-187.170	1.50	-185.670
MS 85	39. 58.940	111. 48.120	4870.00	979697.33	980178.91	-23.470	-189.400	1.69	-187.710
MS 86	39. 58.790	111. 47.710	4908.00	979693.86	980178.69	-23.230	-190.430	1.90	-188.530
MS 87	39. 58.840	111. 47.060	4920.00	979690.09	980178.76	-25.860	-193.490	2.34	-191.150
MS 88	39. 59.570	111. 45.240	4808.00	979695.02	980179.84	-32.610	-196.400	4.78	-191.620
MS 89	40. 1.050	112. 1.150	5277.00	979685.50	980182.03	-.160	-179.950	1.48	-178.470
MS 90	40. .950	112. .870	5197.00	979687.36	980181.89	-5.690	-182.740	1.26	-181.480
MS 91	40. .900	112. .700	5154.00	979688.50	980181.81	-8.550	-184.140	1.14	-183.000
MS 92	40. .840	112. .390	5081.00	979691.47	980181.72	-12.380	-185.470	1.02	-184.450
MS 93	40. .830	112. .200	5038.00	979693.62	980181.71	-14.230	-185.860	.94	-184.920
MS 94	40. .880	111. 59.510	4904.00	979701.28	980181.78	-19.200	-186.290	.81	-185.480
MS 95	40. .770	111. 59.130	4838.00	979705.07	980181.62	-21.530	-186.340	.76	-185.580
MS 96	40. .760	111. 58.800	4798.00	979705.36	980181.60	-24.990	-188.440	.71	-187.730
MS 97	40. .780	111. 58.510	4760.00	979706.45	980181.63	-27.450	-189.620	.68	-188.940
MS 98	40. .790	111. 58.230	4728.00	979706.97	980181.65	-29.940	-191.030	.64	-190.390
MS 99	40. .800	111. 57.950	4697.00	979707.31	980181.66	-32.600	-192.600	.63	-191.970

STAT.	LATITUDE		LONGITUDE		ELEV.	OBSERVED GRAVITY	THEOR. GRAVITY	FREE AIR	SIMPLE BOUGUER	T. C.	COMPLETE BOUGUER
MS100	40.	.800	111.	57.710	4669.00	979707.86	980181.66	-34.620	-193.700	.61	-193.090
MS101	40.	.820	111.	57.160	4616.00	979710.20	980181.69	-37.360	-194.610	.59	-194.020
MS102	40.	.800	111.	56.860	4586.00	979711.65	980181.66	-38.700	-194.930	.59	-194.340
MS103	40.	.510	111.	56.580	4560.00	979711.76	980181.23	-40.570	-195.920	.61	-195.310
MS104	40.	.070	111.	55.770	4509.00	979710.35	980180.58	-46.080	-199.710	.64	-199.070
MS105	40.	.080	111.	54.450	4502.00	979720.53	980180.60	-36.620	-189.990	.64	-189.350
MS106	40.	.240	111.	53.950	4505.00	979721.83	980180.83	-35.250	-188.740	.65	-188.090
MS107	40.	.130	111.	52.980	4503.00	979718.24	980180.67	-38.850	-192.270	.74	-191.530
MS108	40.	.130	111.	52.840	4503.00	979718.58	980180.67	-38.520	-191.940	.75	-191.190
MS109	40.	.290	111.	51.670	4503.00	979720.27	980180.91	-37.090	-190.500	.94	-189.560
MS110	40.	.220	111.	51.370	4508.00	979719.61	980180.80	-37.210	-190.770	.99	-189.780
MS111	40.	.230	111.	50.800	4539.00	979716.48	980180.82	-37.410	-192.040	1.03	-191.010
MS112	40.	.220	111.	50.530	4558.00	979715.30	980180.80	-36.810	-192.090	1.05	-191.040
MS113	40.	.230	111.	50.230	4578.00	979714.79	980180.82	-35.450	-191.410	1.08	-190.330
MS114	40.	.240	111.	49.970	4599.00	979714.39	980180.83	-33.900	-190.570	1.13	-189.440
MS115	40.	.250	111.	49.680	4619.00	979714.40	980180.85	-32.000	-189.360	1.18	-188.180
MS116	40.	.260	111.	49.420	4652.00	979712.42	980180.86	-30.900	-189.380	1.21	-188.170
MS117	40.	.250	111.	49.160	4698.00	979710.69	980180.85	-28.290	-188.340	1.18	-187.160
MS118	40.	.260	111.	48.900	4737.00	979709.62	980180.86	-25.700	-187.080	1.17	-185.910
MS119	40.	.320	111.	48.730	4759.00	979709.77	980180.95	-23.550	-185.680	1.16	-184.520
MS120	40.	.290	111.	48.440	4792.00	979707.21	980180.91	-22.950	-186.210	1.17	-185.040
MS121	40.	.270	111.	48.230	4774.00	979707.48	980180.88	-24.330	-186.980	1.25	-185.730
MS122	40.	.240	111.	47.990	4763.00	979706.59	980180.83	-26.270	-188.530	1.34	-187.190
MS123	40.	.220	111.	47.770	4760.00	979706.04	980180.80	-27.040	-189.210	1.42	-187.790
MS124	40.	.260	111.	47.320	4746.00	979705.38	980180.86	-29.110	-190.790	1.57	-189.220
MS125	40.	.260	111.	47.110	4743.00	979704.49	980180.86	-30.250	-191.840	1.65	-190.190
MS126	40.	.260	111.	46.850	4738.00	979703.75	980180.86	-31.500	-192.900	1.76	-191.140
MS127	40.	.280	111.	46.570	4727.00	979702.97	980180.89	-33.290	-194.340	1.90	-192.440
MS128	40.	.280	111.	46.260	4721.00	979701.85	980180.89	-35.010	-195.840	2.08	-193.760
MS129	40.	.260	111.	46.000	4705.00	979701.57	980180.86	-36.780	-197.060	2.32	-194.740
MS130	40.	.270	111.	45.710	4707.00	979700.49	980180.88	-37.700	-198.040	2.54	-195.500
MS131	40.	.280	111.	45.410	4699.00	979699.33	980180.89	-39.570	-199.660	2.86	-196.800
MS132	40.	.280	111.	45.160	4689.00	979698.82	980180.89	-40.990	-200.750	3.25	-197.500
MS133	40.	3.810	112.	1.930	5046.00	979708.65	980186.12	-2.850	-174.760	.74	-174.020
MS134	40.	3.730	112.	1.590	5012.00	979710.08	980186.00	-4.500	-175.250	.70	-174.550
MS135	40.	3.720	112.	1.230	5018.00	979709.00	980185.99	-4.970	-175.940	.58	-175.360
MS136	40.	3.620	112.	1.080	5030.00	979706.69	980185.84	-6.000	-177.380	.56	-176.820
MS137	40.	3.510	112.	.810	5017.00	979706.00	980185.68	-7.810	-178.720	.56	-178.160
MS138	40.	3.440	112.	.610	4987.00	979707.12	980185.57	-9.350	-179.260	.55	-178.710
MS139	40.	3.380	112.	.480	4990.00	979706.69	980185.48	-9.420	-179.430	.55	-178.880
MS140	40.	3.290	111.	59.970	4920.00	979709.50	980185.35	-13.080	-180.700	.53	-180.170
MS141	40.	3.290	111.	59.660	4884.00	979710.69	980185.35	-15.260	-181.650	.50	-181.150
MS142	40.	3.280	111.	59.390	4854.00	979711.53	980185.34	-17.280	-182.640	.50	-182.140
MS143	40.	3.260	111.	59.150	4826.00	979711.95	980185.31	-19.450	-183.860	.49	-183.370
MS144	40.	3.270	111.	58.820	4770.00	979713.86	980185.32	-22.770	-185.290	.47	-184.820
MS145	40.	3.320	111.	58.560	4745.00	979715.13	980185.40	-23.990	-185.640	.46	-185.180
MS146	40.	3.360	111.	58.280	4709.00	979716.90	980185.45	-25.610	-186.040	.45	-185.590
MS147	40.	3.290	111.	58.020	4679.00	979718.02	980185.35	-27.260	-186.650	.45	-186.200
MS148	40.	3.290	111.	57.770	4654.00	979719.52	980185.35	-28.050	-186.620	.44	-186.180

STAT.	LATITUDE	LONGITUDE	ELEV.	OBSERVED GRAVITY	THEOR. GRAVITY	FREE AIR	SIMPLE BOUGUER	T. C.	COMPLETE BOUGUER
MS149	40. 3.210	111. 57.450	4626.00	979721.27	980185.23	-28.840	-186.450	.45	-186.000
MS150	40. 3.250	111. 56.910	4592.00	979724.68	980185.29	-28.660	-185.120	.44	-184.680
MS151	40. 3.250	111. 56.230	4555.00	979725.62	980185.29	-31.200	-186.390	.44	-185.950
MS152	40. 3.360	111. 54.800	4498.00	979728.64	980185.45	-33.770	-187.000	.48	-186.520
MS153	40. 3.320	111. 54.250	4496.00	979730.35	980185.40	-32.130	-185.310	.51	-184.800
MS154	40. 3.250	111. 53.500	4493.00	979726.99	980185.29	-35.680	-188.760	.61	-188.150
MS155	40. 4.170	112. .790	4903.00	979722.12	980186.65	-3.370	-170.410	.79	-169.620
MS156	40. 4.300	112. .620	4883.00	979722.92	980186.85	-4.670	-171.020	.69	-170.330
MS157	40. 4.410	112. .240	4841.00	979722.35	980187.01	-9.300	-174.240	.52	-173.720
MS158	40. 4.380	112. .040	4823.00	979722.66	980186.97	-10.620	-174.950	.48	-174.470
MS159	40. 4.460	111. 59.640	4786.00	979723.61	980187.08	-13.290	-176.350	.43	-175.920
MS160	40. 4.490	111. 59.470	4773.00	979722.97	980187.13	-15.260	-177.850	.42	-177.430
MS161	40. 4.520	111. 59.170	4747.00	979723.75	980187.17	-16.970	-178.680	.40	-178.280
MS162	40. 4.520	111. 58.880	4723.00	979725.79	980187.17	-17.160	-178.060	.40	-177.660
MS163	40. 4.540	111. 58.540	4692.00	979728.72	980187.20	-17.180	-177.020	.39	-176.630
MS164	40. 4.550	111. 58.270	4669.00	979730.62	980187.22	-17.390	-176.470	.39	-176.080
MS165	40. 4.560	111. 58.050	4646.00	979732.14	980187.23	-18.060	-176.360	.39	-175.970
MS166	40. 4.560	111. 57.460	4602.00	979732.57	980187.23	-21.810	-178.590	.39	-178.200
MS167	40. 4.550	111. 56.730	4556.00	979731.95	980187.22	-26.750	-181.960	.39	-181.570
MS168	40. 4.550	111. 55.790	4522.00	979731.44	980187.22	-30.450	-184.510	.40	-184.110
MS169	40. 5.860	111. 59.370	4773.00	979732.23	980189.16	-8.000	-170.600	.33	-170.270
MS170	40. 5.850	111. 59.130	4732.00	979735.92	980189.14	-8.090	-169.320	.35	-168.970
MS171	40. 5.840	111. 58.890	4687.00	979738.09	980189.13	-10.150	-169.840	.39	-169.450
MS172	40. 5.840	111. 58.600	4656.00	979738.00	980189.13	-13.220	-171.830	.39	-171.440
MS173	40. 5.850	111. 58.320	4633.00	979740.18	980189.14	-13.180	-171.020	.38	-170.640
MS174	40. 5.850	111. 58.030	4613.00	979741.16	980189.14	-14.050	-171.220	.37	-170.850
MS175	40. 5.860	111. 57.780	4592.00	979742.50	980189.16	-14.720	-171.170	.36	-170.810
MS176	40. 5.870	111. 57.500	4576.00	979742.24	980189.17	-16.530	-172.420	.36	-172.060
MS177	40. 5.870	111. 56.790	4537.00	979738.84	980189.17	-23.590	-178.160	.36	-177.800
MS178	40. 5.870	111. 55.490	4495.00	979732.93	980189.17	-33.460	-186.590	.38	-186.210
MS179	40. 6.100	111. 55.080	4493.00	979732.02	980189.51	-34.890	-187.960	.38	-187.580
MS183	40. 8.670	111. 59.980	4891.00	979726.53	980193.32	-6.730	-173.370	.25	-173.120
MS184	40. 8.590	111. 59.740	4836.00	979731.33	980193.20	-7.040	-171.790	.38	-171.410
MS185	40. 8.450	111. 59.330	4793.00	979734.57	980193.00	-7.610	-170.900	.33	-170.570
MS186	40. 8.500	111. 59.090	4780.00	979733.27	980193.07	-10.220	-173.060	.35	-172.710
MS187	40. 8.500	111. 58.870	4751.00	979734.57	980193.07	-11.650	-173.500	.36	-173.140
MS188	40. 8.490	111. 58.640	4737.00	979735.96	980193.05	-11.540	-172.920	.37	-172.550
MS189	40. 8.490	111. 58.350	4691.00	979740.06	980193.05	-11.780	-171.590	.39	-171.200
MS190	40. 8.490	111. 58.100	4669.00	979740.67	980193.05	-13.260	-172.310	.40	-171.910
MS191	40. 8.490	111. 57.670	4638.00	979743.85	980193.05	-12.980	-170.980	.38	-170.600
MS192	40. 11.290	111. 57.490	5062.00	979722.05	980197.20	1.020	-171.460	1.07	-170.390
MS193	40. 11.130	111. 57.370	5000.00	979725.87	980196.97	-.810	-171.150	1.16	-169.990
MS194	40. 11.000	111. 57.230	4942.00	979729.00	980196.77	-2.910	-171.290	1.12	-170.170
MS195	40. 10.770	111. 56.960	4871.00	979732.35	980196.43	-5.950	-171.890	.89	-171.000
MS196	40. 10.610	111. 56.800	4821.00	979734.62	980196.20	-8.120	-172.370	.82	-171.550
MS197	40. 10.260	111. 56.390	4705.00	979738.70	980195.68	-14.460	-174.740	.71	-174.030
MS198	40. 10.090	111. 55.860	4615.00	979743.45	980195.43	-17.920	-175.140	.67	-174.470
MS199	40. 9.920	111. 55.590	4569.00	979744.75	980195.17	-20.660	-176.320	.63	-175.690
MS200	40. 9.780	111. 55.500	4545.00	979744.64	980194.97	-22.800	-177.650	.60	-177.050

STAT.	LATITUDE	LONGITUDE	ELEV.	OBSERVED GRAVITY	THEOR. GRAVITY	FREE AIR	SIMPLE BOUGUER	T. C.	COMPLETE BOUGUER
MS201	40. 9.720	111. 55.230	4500.00	979745.94	980194.88	-25.710	-179.010	.59	-178.420
MS202	40. 9.370	111. 55.580	4504.00	979743.09	980194.36	-27.630	-181.070	.52	-180.550
MS203	40. 8.960	111. 55.730	4495.00	979741.87	980193.75	-29.080	-182.220	.47	-181.750
MS204	40. 1.160	111. 50.550	4508.00	979718.53	980182.20	-39.690	-193.250	1.23	-192.020
MS205	40. 1.760	111. 49.970	4765.00	979709.99	980183.09	-24.880	-187.220	1.80	-185.420
MS206	40. 1.800	111. 49.420	5038.00	979693.69	980183.14	-15.620	-187.250	1.50	-185.750
MS207	40. 2.060	111. 48.580	4992.00	979694.81	980183.53	-19.170	-189.240	1.31	-187.930
MS208	40. 2.180	111. 48.430	4969.00	979697.25	980183.71	-19.070	-188.360	1.38	-186.980
MS209	40. 2.270	111. 48.350	4933.00	979698.54	980183.84	-21.270	-189.340	1.38	-187.960
MS210	40. 2.450	111. 47.740	4698.00	979711.65	980184.11	-30.600	-190.650	1.34	-189.310
MS211	40. 2.460	111. 47.500	4641.00	979714.52	980184.12	-33.110	-191.210	1.33	-189.880
MS212	40. 2.890	111. 47.180	4573.00	979716.15	980184.76	-38.470	-194.270	1.33	-192.940
MS213	40. 2.460	111. 46.860	4595.00	979714.35	980184.12	-37.580	-194.120	1.26	-192.860
MS214	40. 2.450	111. 46.590	4584.00	979714.11	980184.11	-38.800	-194.980	1.28	-193.700
MS215	40. 2.450	111. 46.300	4592.00	979713.23	980184.11	-38.940	-195.390	1.26	-194.130
MS216	40. 2.460	111. 46.000	4596.00	979712.53	980184.12	-39.260	-195.850	1.27	-194.580
MS217	40. 2.470	111. 45.640	4608.00	979709.99	980184.14	-40.720	-197.710	1.30	-196.410
MS218	40. 2.610	111. 45.450	4604.00	979710.05	980184.34	-41.280	-198.120	1.29	-196.830
MS219	40. 2.610	111. 45.170	4602.00	979706.57	980184.34	-44.900	-201.690	1.33	-200.360
MS220	40. 2.600	111. 44.660	4611.00	979703.43	980184.33	-47.160	-204.260	1.43	-202.830
MS221	40. 2.590	111. 44.250	4635.00	979701.88	980184.31	-46.480	-204.380	1.49	-202.890
MS222	40. 2.710	111. 43.910	4647.00	979700.30	980184.49	-47.070	-205.400	1.51	-203.890
MS223	40. 2.650	111. 43.660	4647.00	979699.90	980184.40	-47.380	-205.710	1.61	-204.100
MS224	40. 2.660	111. 43.340	4677.00	979696.78	980184.42	-47.690	-207.040	1.66	-205.380
MS225	40. 2.660	111. 42.900	4600.00	979700.08	980184.42	-51.680	-208.390	1.93	-206.460
MS226	40. 2.720	111. 42.500	4583.00	979698.34	980184.51	-55.130	-211.260	2.06	-209.200
MS227	40. 2.770	111. 42.200	4583.00	979697.42	980184.58	-56.100	-212.230	2.11	-210.120
MS228	40. 2.810	111. 41.910	4582.00	979697.06	980184.64	-56.640	-212.730	2.19	-210.540
MS229	40. 2.870	111. 41.620	4581.00	979697.38	980184.73	-56.490	-212.550	2.28	-210.270
MS230	40. 2.950	111. 41.100	4592.00	979696.29	980184.85	-56.650	-213.090	2.46	-210.630
MS231	40. 3.260	111. 40.570	4583.00	979695.32	980185.31	-58.890	-215.040	2.53	-212.510
MS232	40. 3.280	111. 40.120	4617.00	979694.06	980185.34	-56.970	-214.280	2.73	-211.550
MS233	40. 3.210	111. 39.750	4674.00	979691.74	980185.23	-53.850	-213.090	2.96	-210.130
MS234	40. 3.200	111. 39.450	4685.00	979691.96	980185.22	-52.550	-212.180	3.27	-208.910
MS235	40. 3.170	111. 39.200	4704.00	979692.03	980185.17	-50.730	-210.970	3.57	-207.400
MS236	40. 3.170	111. 38.890	4717.00	979692.55	980185.17	-48.950	-209.650	4.04	-205.610
MS237	40. 3.350	111. 38.620	4709.00	979692.86	980185.44	-49.610	-210.060	4.32	-205.740
MS238	40. 3.420	111. 38.330	4709.00	979694.03	980185.54	-48.550	-208.990	5.09	-203.900
MS239	40. 3.420	111. 38.040	4717.00	979694.74	980185.54	-47.140	-207.840	6.49	-201.350
MS240	40. 3.420	111. 37.780	4809.00	979689.89	980185.54	-43.300	-207.150	8.16	-198.990
MS241	40. 3.140	111. 37.610	5027.00	979677.33	980185.13	-35.000	-206.250	9.14	-197.110
MS242	40. 4.640	111. 47.970	4595.00	979716.22	980187.35	-38.950	-195.490	3.13	-192.360
MS243	40. 4.660	111. 47.790	4559.00	979717.81	980187.38	-40.790	-196.090	2.40	-193.690
MS244	40. 4.660	111. 47.520	4529.00	979719.10	980187.38	-42.270	-196.570	1.83	-194.740
MS245	40. 4.660	111. 47.210	4515.00	979719.28	980187.38	-43.380	-197.210	1.46	-195.750
MS246	40. 4.670	111. 46.840	4508.00	979719.17	980187.40	-44.160	-197.760	1.23	-196.530
MS247	40. 4.680	111. 46.560	4504.00	979718.47	980187.41	-45.260	-198.720	1.14	-197.580
MS248	40. 4.680	111. 46.290	4505.00	979717.32	980187.41	-46.390	-199.850	1.09	-198.760
MS249	40. 4.670	111. 46.100	4503.00	979717.07	980187.40	-46.740	-200.170	1.06	-199.110

STAT.	LATITUDE	LONGITUDE	ELEV.	OBSERVED GRAVITY	THEOR. GRAVITY	FREE AIR	SIMPLE BOUGUER	T. C.	COMPLETE BOUGUER
MS250	40. 4.680	111. 45.890	4503.00	979717.04	980187.41	-46.830	-200.240	1.05	-199.190
MS251	40. 4.680	111. 45.670	4501.00	979717.43	980187.41	-46.620	-199.960	1.05	-198.910
MS252	40. 4.690	111. 45.430	4496.00	979717.71	980187.42	-46.800	-199.980	1.07	-198.910
MS253	40. 4.680	111. 45.270	4497.00	979716.67	980187.41	-47.800	-201.000	1.10	-199.900
MS254	40. 5.100	111. 44.680	4511.00	979711.40	980188.03	-52.300	-205.990	.98	-205.010
MS255	40. 5.090	111. 43.800	4522.00	979707.18	980188.02	-55.480	-209.550	1.04	-208.510
MS256	40. 5.110	111. 43.160	4528.00	979701.78	980188.05	-60.410	-214.660	1.09	-213.570
MS257	40. 5.100	111. 42.730	4534.00	979698.35	980188.03	-63.230	-217.700	1.15	-216.550
MS258	40. 5.110	111. 42.180	4542.00	979695.96	980188.05	-64.830	-219.590	1.23	-218.360
MS259	40. 5.110	111. 41.550	4542.00	979695.82	980188.05	-65.020	-219.750	1.36	-218.390
MS260	40. 5.110	111. 40.950	4540.00	979697.06	980188.05	-63.950	-218.630	1.52	-217.110
MS261	40. 5.250	111. 39.950	4581.00	979697.08	980188.25	-60.280	-216.350	1.70	-214.650
MS262	40. 5.190	111. 39.340	4633.00	979695.19	980188.17	-57.220	-215.050	1.88	-213.170
MS263	40. 5.240	111. 38.700	4606.00	979699.35	980188.24	-55.660	-212.580	2.18	-210.400
MS264	40. 5.170	111. 38.100	4626.00	979699.55	980188.14	-53.480	-211.080	2.54	-208.540
MS265	40. 5.050	111. 37.640	4640.00	979699.73	980187.96	-51.830	-209.900	2.99	-206.910
MS266	40. 4.920	111. 37.350	4655.00	979699.43	980187.77	-50.510	-209.090	3.46	-205.630
MS267	40. 4.890	111. 37.070	4660.00	979699.83	980187.72	-49.600	-208.350	3.90	-204.450
MS268	40. 4.880	111. 36.920	4658.00	979700.31	980187.71	-49.240	-207.940	4.22	-203.720
MS269	40. 4.810	111. 36.730	4660.00	979701.05	980187.60	-48.260	-207.010	4.95	-202.060
MS270	40. 4.790	111. 36.620	4662.00	979701.31	980187.57	-47.770	-206.590	5.21	-201.380
MS271	40. 4.780	111. 36.490	4664.00	979701.58	980187.56	-47.240	-206.160	5.62	-200.540
MS272	40. 4.770	111. 36.260	4744.00	979697.46	980187.54	-43.870	-205.490	5.41	-200.080
MS273	40. 4.730	111. 36.150	4888.00	979688.03	980187.48	-39.730	-206.240	4.77	-201.470
MS274	40. 4.670	111. 36.020	4951.00	979683.71	980187.40	-37.960	-206.650	4.97	-201.680
MS275	40. 4.420	111. 35.950	5111.00	979673.56	980187.02	-32.680	-206.820	5.84	-200.980
MS276	40. 6.860	111. 51.030	4503.00	979734.14	980190.64	-32.970	-186.380	1.36	-185.020
MS277	40. 6.850	111. 50.790	4555.00	979731.50	980190.62	-30.730	-185.900	1.70	-184.200
MS278	40. 6.760	111. 50.330	4782.00	979718.59	980190.49	-22.150	-185.050	2.89	-182.160
MS279	40. 6.780	111. 49.940	4992.00	979705.31	980190.52	-15.630	-185.720	3.91	-181.810
MS280	40. 6.760	111. 49.630	5245.00	979690.21	980190.49	-6.940	-185.630	3.20	-182.430
MS281	40. 6.830	111. 48.330	4597.00	979726.90	980190.60	-31.330	-187.930	2.73	-185.200
MS282	40. 6.830	111. 48.010	4517.00	979730.96	980190.60	-34.770	-188.660	1.87	-186.790
MS283	40. 6.840	111. 47.490	4495.00	979728.49	980190.61	-39.340	-192.470	1.11	-191.360
MS284	40. 6.850	111. 47.220	4495.00	979727.07	980190.62	-40.720	-193.870	.95	-192.920
MS285	40. 6.850	111. 46.860	4497.00	979725.09	980190.62	-42.570	-195.770	.84	-194.930
MS286	40. 6.920	111. 46.590	4496.00	979723.30	980190.73	-44.520	-197.700	.78	-196.920
MS287	40. 6.960	111. 46.310	4492.00	979722.40	980190.79	-45.850	-198.900	.76	-198.140
MS288	40. 6.850	111. 46.110	4496.00	979721.20	980190.62	-46.570	-199.730	.76	-198.970
MS289	40. 6.850	111. 45.770	4496.00	979719.82	980190.62	-47.880	-201.070	.76	-200.310
MS290	40. 6.870	111. 45.500	4504.00	979717.73	980190.65	-49.260	-202.710	.75	-201.960
MS291	40. 6.870	111. 45.290	4506.00	979716.56	980190.65	-50.250	-203.770	.75	-203.020
MS292	40. 6.850	111. 44.950	4509.00	979714.38	980190.62	-52.090	-205.720	.76	-204.960
MS293	40. 6.870	111. 44.370	4513.00	979710.88	980190.65	-55.280	-209.030	.79	-208.240
MS294	40. 6.870	111. 43.780	4521.00	979706.86	980190.65	-58.520	-212.550	.83	-211.720
MS295	40. 6.880	111. 43.230	4529.00	979702.47	980190.67	-62.240	-216.520	.87	-215.650
MS296	40. 6.870	111. 42.640	4538.00	979698.99	980190.65	-64.870	-219.460	.94	-218.520
MS297	40. 6.870	111. 41.890	4539.00	979697.20	980190.65	-66.490	-221.140	1.03	-220.110
MS298	40. 6.910	111. 41.140	4552.00	979696.16	980190.71	-66.430	-221.500	1.15	-220.350

STAT.	LATITUDE		LONGITUDE		ELEV.	OBSERVED GRAVITY	THEOR. GRAVITY	FREE AIR	SIMPLE BOUGUER	T. C.	COMPLETE BOUGUER
MS299	40.	6.910	111.	40.740	4556.00	979696.10	980190.71	-66.080	-221.300	1.23	-220.070
MS300	40.	6.900	111.	40.230	4563.00	979696.27	980190.70	-65.250	-220.700	1.33	-219.370
MS301	40.	6.900	111.	39.530	4564.00	979697.24	980190.70	-64.210	-219.690	1.49	-218.200
MS302	40.	6.900	111.	38.910	4584.00	979697.17	980190.70	-62.360	-218.530	1.64	-216.890
MS303	40.	6.910	111.	38.300	4626.00	979695.47	980190.71	-60.090	-217.700	1.80	-215.900
MS304	40.	6.930	111.	37.520	4716.00	979690.94	980190.74	-56.260	-216.910	2.12	-214.790
MS305	40.	6.900	111.	36.650	4719.00	979691.63	980190.70	-55.210	-215.980	2.56	-213.420
MS306	40.	6.930	111.	35.810	4716.00	979692.39	980190.74	-54.780	-215.450	3.14	-212.310
MS307	40.	6.930	111.	35.230	4710.00	979693.74	980190.74	-53.950	-214.420	4.02	-210.400
MS308	40.	6.940	111.	34.930	4732.00	979693.40	980190.76	-52.260	-213.480	4.49	-208.990
MS309	40.	6.940	111.	34.660	4749.00	979693.46	980190.76	-50.600	-212.390	5.14	-207.250
MS310	40.	6.930	111.	34.430	4763.00	979693.41	980190.74	-49.340	-211.610	5.91	-205.700
MS311	40.	6.950	111.	34.240	4770.00	979693.55	980190.77	-48.590	-211.090	6.80	-204.290
MS312	40.	6.950	111.	34.040	4793.00	979692.41	980190.77	-47.590	-210.860	7.90	-202.960
MS313	40.	6.950	111.	33.900	4816.00	979690.57	980190.77	-47.210	-211.280	9.15	-202.130
MS314	40.	6.960	111.	33.740	4857.00	979687.70	980190.79	-46.240	-211.710	10.60	-201.110
MS315	40.	6.960	111.	33.610	4875.00	979686.05	980190.79	-46.230	-212.300	11.98	-200.320
MS316	40.	6.970	111.	33.540	4928.00	979682.58	980190.80	-44.660	-212.560	12.27	-200.290
MS317	40.	6.960	111.	33.420	5110.00	979670.18	980190.79	-40.000	-214.070	12.50	-201.570
MS318	40.	8.270	111.	48.210	4533.00	979733.82	980192.73	-32.570	-186.990	.72	-186.270
MS319	40.	8.250	111.	47.890	4489.00	979733.30	980192.70	-37.160	-190.090	.73	-189.360
MS320	40.	8.150	111.	47.690	4489.00	979731.83	980192.55	-38.490	-191.420	.70	-190.720
MS321	40.	8.160	111.	47.440	4488.00	979730.65	980192.57	-39.790	-192.690	.67	-192.020
MS322	40.	8.240	111.	47.210	4489.00	979729.33	980192.68	-41.080	-194.030	.64	-193.390
MS323	40.	8.280	111.	46.900	4488.00	979727.75	980192.74	-42.890	-195.780	.63	-195.150
MS324	40.	8.160	111.	46.360	4492.00	979725.57	980192.57	-44.460	-197.510	.63	-196.880
MS325	40.	8.160	111.	46.080	4490.00	979724.31	980192.57	-45.960	-198.920	.64	-198.280
MS326	40.	8.210	111.	45.890	4491.00	979722.86	980192.64	-47.380	-200.380	.65	-199.730
MS327	40.	8.180	111.	45.480	4493.00	979720.34	980192.60	-49.630	-202.710	.64	-202.070
MS328	40.	8.180	111.	45.220	4491.00	979718.88	980192.60	-51.300	-204.300	.68	-203.620
MS329	40.	8.190	111.	44.920	4494.00	979716.84	980192.61	-53.020	-206.140	.70	-205.440
MS330	40.	8.190	111.	44.700	4494.00	979715.29	980192.61	-54.620	-207.720	.71	-207.010
MS331	40.	8.190	111.	44.380	4499.00	979712.76	980192.61	-56.660	-209.940	.74	-209.200
MS332	40.	8.190	111.	44.050	4504.00	979710.10	980192.61	-58.880	-212.320	.76	-211.560
MS333	40.	8.170	111.	43.780	4507.00	979707.67	980192.58	-60.990	-214.530	.79	-213.740
MS334	40.	10.000	111.	44.680	4494.00	979713.18	980195.29	-59.410	-212.520	.71	-211.810
MS335	40.	9.830	111.	44.070	4496.00	979708.93	980195.04	-63.250	-216.410	.77	-215.640
MS336	40.	9.460	111.	43.800	4501.00	979706.75	980194.49	-64.410	-217.740	.78	-216.960
MS337	40.	9.520	111.	43.120	4491.00	979703.34	980194.58	-68.790	-221.810	.87	-220.940
MS338	40.	9.510	111.	42.630	4497.00	979701.12	980194.57	-70.460	-223.660	.94	-222.720
MS339	40.	9.510	111.	42.100	4505.00	979699.47	980194.57	-71.350	-224.830	1.02	-223.810
MS340	40.	9.520	111.	41.520	4506.00	979698.42	980194.58	-72.310	-225.830	1.13	-224.700
MS341	40.	9.510	111.	41.030	4506.00	979697.98	980194.57	-72.730	-226.250	1.24	-225.010
MS342	40.	9.520	111.	40.390	4508.00	979697.76	980194.58	-72.850	-226.420	1.40	-225.020
MS343	40.	9.490	111.	39.800	4507.00	979698.35	980194.54	-72.280	-225.820	1.59	-224.230
MS344	40.	9.660	111.	39.330	4503.00	979699.83	980194.79	-71.390	-224.810	1.82	-222.990
MS345	40.	9.660	111.	39.820	4509.00	979700.47	980194.79	-70.200	-223.820	1.62	-222.200
MS346	40.	9.660	111.	38.100	4521.00	979702.33	980194.79	-67.250	-221.260	2.47	-218.790
MS347	40.	9.660	111.	37.620	4534.00	979703.06	980194.79	-65.270	-219.730	2.80	-216.930

STAT.	LATITUDE		LONGITUDE		ELEV.	OBSERVED GRAVITY	THEOR. GRAVITY	FREE AIR	SIMPLE BOUGUER	T. C.	COMPLETE BOUGUER
MS348	40.	9.650	111.	37.190	4559.00	979703.60	980194.77	-62.320	-217.650	3.06	-214.590
MS349	40.	9.650	111.	36.610	4584.00	979704.38	980194.77	-59.210	-215.390	3.55	-211.840
MS350	40.	9.670	111.	36.150	4605.00	979704.53	980194.80	-57.170	-214.040	4.12	-209.920
MS351	40.	9.650	111.	35.820	4615.00	979704.70	980194.77	-56.000	-213.220	4.61	-208.610
MS352	40.	9.080	111.	35.720	4645.00	979700.72	980193.93	-56.300	-214.550	3.69	-210.860
MS353	40.	9.650	111.	35.580	4638.00	979703.72	980194.77	-54.800	-212.810	5.02	-207.790
MS354	40.	9.660	111.	35.380	4673.00	979702.12	980194.79	-53.130	-212.330	5.33	-207.000
MS355	40.	9.660	111.	35.140	4711.00	979700.31	980194.79	-51.360	-211.860	5.72	-206.140
MS356	40.	9.640	111.	34.830	4728.00	979700.58	980194.76	-49.500	-210.570	6.69	-203.880
MS357	40.	9.640	111.	34.610	4755.00	979699.87	980194.76	-47.670	-209.660	7.38	-202.280
MS358	40.	9.650	111.	34.450	4809.00	979697.22	980194.77	-45.180	-209.030	7.84	-201.190
MS359	40.	9.720	111.	34.200	5053.00	979683.38	980194.88	-36.250	-208.390	7.10	-201.290
MS360	40.	9.790	111.	34.030	5155.00	979675.86	980194.98	-34.240	-209.860	7.67	-202.190
MS361	40.	9.820	111.	33.910	5221.00	979671.70	980195.03	-32.220	-210.100	7.65	-202.450
MS362	40.	9.870	111.	33.720	5302.00	979667.01	980195.10	-29.410	-210.030	8.09	-201.940
MS363	40.	9.970	111.	33.580	5457.00	979656.89	980195.25	-25.120	-211.020	8.22	-202.800
MS364	40.	19.290	111.	56.290	5138.00	979721.57	980209.07	-4.190	-179.250	2.36	-176.890
MS365	40.	19.550	111.	56.050	4989.00	979731.53	980209.45	-8.620	-178.600	1.79	-176.810
MS366	40.	19.870	111.	55.720	4835.00	979740.81	980209.93	-14.320	-179.050	1.39	-177.660
MS367	40.	19.990	111.	55.550	4752.00	979745.36	980210.11	-17.820	-179.700	1.34	-178.360
MS368	40.	20.120	111.	55.390	4677.00	979749.48	980210.30	-20.940	-180.270	1.28	-178.990
MS369	40.	20.160	111.	55.230	4632.00	979751.95	980210.36	-22.720	-180.530	1.25	-179.280
MS370	40.	20.260	111.	55.080	4591.00	979754.15	980210.51	-24.560	-180.960	1.21	-179.750
MS371	40.	20.570	111.	54.840	4539.00	979755.93	980210.97	-28.080	-182.730	1.07	-181.660
MS372	40.	20.730	111.	54.580	4522.00	979755.84	980211.20	-30.000	-184.070	.99	-183.080
MS373	40.	20.800	111.	54.460	4516.00	979755.68	980211.31	-30.900	-184.740	.97	-183.770
MS374	40.	20.840	111.	54.390	4514.00	979755.56	980211.37	-31.250	-185.020	.95	-184.070
MS375	40.	21.010	111.	54.340	4511.00	979756.06	980211.62	-31.300	-184.970	.92	-184.050
MS376	40.	21.120	111.	54.140	4498.00	979756.86	980211.78	-31.820	-185.070	.90	-184.170
MS377	40.	21.190	111.	54.110	4499.00	979756.73	980211.89	-31.970	-185.250	.89	-184.360
MS378	40.	21.430	111.	54.000	4498.00	979755.29	980212.24	-33.840	-187.090	.87	-186.220
MS379	40.	21.740	111.	53.650	4493.00	979753.09	980212.70	-36.970	-190.050	.86	-189.190
MS380	40.	22.360	111.	52.580	4507.00	979739.60	980213.62	-50.090	-203.640	.90	-202.740
MS381	39.	57.760	111.	41.390	5887.00	979623.43	980177.16	-.040	-200.590	9.37	-191.220
MS382	39.	59.030	111.	41.820	5334.00	979657.24	980179.04	-20.090	-201.810	8.48	-193.330
MS383	39.	59.450	111.	41.930	5218.00	979665.70	980179.66	-23.180	-200.950	8.13	-192.820
MS384	40.	.310	111.	42.280	5066.00	979678.01	980180.94	-26.400	-199.000	7.31	-191.690
MS385	40.	.790	111.	42.540	4978.00	979684.62	980181.65	-28.820	-198.410	5.36	-193.050
MS386	40.	1.180	111.	43.160	4899.00	979691.05	980182.23	-30.340	-197.260	3.51	-193.750
MS387	40.	1.180	111.	43.240	4843.00	979694.23	980182.23	-32.500	-197.480	4.11	-193.370
MS388	40.	1.530	111.	43.520	4814.00	979695.31	980182.74	-34.600	-198.620	2.41	-196.210
MS389	40.	1.720	111.	43.680	4789.00	979695.98	980183.03	-36.560	-199.730	2.08	-197.650
MS390	40.	1.950	111.	43.730	4768.00	979696.59	980183.37	-38.350	-200.770	1.88	-198.890
MS391	40.	2.190	111.	43.880	4741.00	979697.04	980183.72	-40.710	-202.240	1.70	-200.540
MS392	40.	2.470	111.	43.890	4676.00	979700.07	980184.14	-44.220	-203.540	1.61	-201.930
MS394	40.	3.020	111.	43.870	4612.00	979700.98	980184.95	-50.170	-207.290	1.43	-205.860
MS395	40.	3.870	111.	43.890	4552.00	979703.69	980186.21	-54.350	-209.440	1.24	-208.200
MS396	40.	4.310	111.	43.880	4537.00	979705.54	980186.86	-54.620	-209.170	1.16	-208.010
MS398	40.	5.870	111.	43.820	4530.00	979706.22	980189.17	-56.890	-211.220	.90	-210.320

STAT.	LATITUDE	LONGITUDE	ELEV.	OBSERVED GRAVITY	THEOR. GRAVITY	FREE AIR	SIMPLE BOUGUER	T. C.	COMPLETE BOUGUER
MS399	40. 6.430	111. 43.780	4527.00	979706.34	980190.00	-57.860	-212.090	.85	-211.240
MS401	40. 7.250	111. 43.770	4519.00	979707.13	980191.22	-59.000	-212.970	.81	-212.160
MS402	40. 7.740	111. 43.790	4513.00	979707.73	980191.94	-59.720	-213.480	.79	-212.690
MS404	40. 8.600	111. 43.790	4503.00	979707.63	980193.22	-62.070	-215.470	.78	-214.690
MS406	40. 9.820	111. 43.790	4495.00	979706.85	980195.03	-65.360	-218.510	.80	-217.710
MS407	40. 3.330	111. 44.810	4563.00	979707.47	980185.41	-48.730	-204.190	1.23	-202.960
MS408	40. 3.790	111. 44.390	4545.00	979706.86	980186.09	-51.770	-206.600	1.21	-205.390
MS411	40. 5.890	111. 42.440	4543.00	979697.74	980189.20	-64.160	-218.930	1.06	-217.870
MS412	40. 6.430	111. 41.910	4555.00	979696.44	980190.00	-65.130	-220.310	1.06	-219.250
MS414	40. 7.320	111. 40.400	4556.00	979696.05	980191.32	-66.780	-221.980	1.28	-220.700
MS415	40. 7.560	111. 40.010	4553.00	979696.36	980191.68	-67.060	-222.180	1.36	-220.820
MS416	40. 7.820	111. 39.550	4549.00	979696.59	980192.06	-67.580	-222.560	1.47	-221.090
MS417	40. 8.010	111. 39.240	4537.00	979697.43	980192.34	-68.150	-222.730	1.57	-221.160
MS418	40. 8.310	111. 38.730	4556.00	979696.42	980192.79	-67.870	-223.080	1.72	-221.360
MS419	40. 8.560	111. 38.390	4524.00	979699.20	980193.16	-68.440	-222.570	1.95	-220.620
MS420	40. 8.920	111. 38.200	4522.00	979700.06	980193.69	-68.320	-222.370	2.13	-220.240
MS421	40. 9.230	111. 38.200	4517.00	979700.88	980194.15	-68.380	-222.280	2.25	-220.030
MS423	40. 10.000	111. 38.160	4511.00	979703.70	980195.29	-67.270	-220.970	2.65	-218.320
MS424	40. 10.450	111. 38.160	4507.00	979705.93	980195.96	-66.090	-219.640	2.99	-216.650
MS425	40. 10.880	111. 38.180	4503.00	979708.31	980196.60	-64.750	-218.150	3.40	-214.750
MS427	39. 59.330	111. 47.130	4848.00	979696.86	980179.49	-26.660	-191.810	2.02	-189.790
MS429	40. 1.200	111. 47.160	4674.00	979709.39	980182.26	-33.220	-192.460	1.45	-191.010
MS430	40. 1.590	111. 47.170	4647.00	979711.77	980182.83	-33.940	-192.270	1.40	-190.870
MS431	40. 2.020	111. 47.180	4623.00	979714.02	980183.47	-34.580	-192.090	1.34	-190.750
MS433	40. 3.800	111. 47.220	4537.00	979718.22	980186.11	-41.150	-195.720	1.45	-194.270
MS434	40. 4.230	111. 47.210	4523.00	979719.14	980186.74	-42.140	-196.240	1.47	-194.770
MS436	40. 5.550	111. 47.230	4508.00	979721.16	980188.70	-43.520	-197.100	1.34	-195.760
MS437	40. 5.840	111. 47.240	4501.00	979722.62	980189.13	-43.140	-196.490	1.29	-195.200
MS438	40. 5.970	111. 47.790	4539.00	979725.22	980189.32	-37.200	-191.830	2.00	-189.830
MS439	40. 6.430	111. 47.800	4499.00	979729.63	980190.00	-37.170	-190.450	1.82	-188.630
MS441	40. 7.290	111. 48.230	4529.00	979731.34	980191.28	-33.980	-188.270	1.72	-186.550
MS442	40. 7.700	111. 48.320	4519.00	979733.48	980191.88	-33.320	-187.290	1.24	-186.050
MS443	40. 8.000	111. 48.440	4645.00	979727.12	980192.33	-28.310	-186.560	.76	-185.800
MS446	39. 59.370	111. 50.550	4603.00	979711.96	980179.55	-34.600	-191.430	1.13	-190.300
MS447	39. 59.780	111. 50.550	4595.00	979712.91	980180.15	-35.060	-191.600	1.04	-190.560
MS450	40. 3.120	111. 51.850	4609.00	979718.40	980185.10	-33.190	-190.210	1.51	-188.700
MS451	40. 3.360	111. 51.520	4620.00	979719.53	980185.45	-31.340	-188.750	3.17	-185.580
MS452	40. 3.910	111. 51.570	4541.00	979724.73	980186.27	-34.450	-189.150	3.21	-185.940
MS453	40. 4.720	111. 51.390	4543.00	979725.71	980187.47	-34.420	-189.200	2.80	-186.400
MS454	40. 5.220	111. 51.590	4498.00	979728.11	980188.21	-37.020	-190.260	1.77	-188.490
MS455	40. 5.580	111. 51.490	4502.00	979729.46	980188.74	-35.860	-189.230	1.66	-187.570
MS456	40. 6.000	111. 51.220	4508.00	979730.88	980189.37	-34.440	-188.030	1.90	-186.130
MS457	40. 6.420	111. 51.200	4499.00	979733.32	980189.99	-33.530	-186.800	1.52	-185.280
MS459	40. 7.220	111. 50.260	4726.00	979722.56	980191.17	-24.130	-185.120	1.66	-183.460
MS460	40. 7.290	111. 50.670	4500.00	979735.47	980191.28	-32.560	-185.860	1.53	-184.330
MS461	40. 7.700	111. 50.440	4504.00	979736.10	980191.88	-32.120	-185.570	1.11	-184.460
MS462	40. 7.910	111. 50.160	4514.00	979734.94	980192.20	-32.690	-186.470	1.04	-185.430
MS463	40. 8.020	111. 49.930	4512.00	979735.31	980192.36	-32.660	-186.380	1.03	-185.350
MS464	40. 8.180	111. 49.700	4511.00	979735.97	980192.60	-32.300	-186.000	.88	-185.120

STAT.	LATITUDE	LONGITUDE	ELEV.	OBSERVED GRAVITY	THEOR. GRAVITY	FREE AIR	SIMPLE BOUGUER	T.C.	COMPLETE BOUGUER
MS465	40. 8.420	111. 49.200	4506.00	979736.20	980192.95	-32.870	-186.400	.86	-185.540
MS466	40. 8.540	111. 48.910	4510.00	979735.87	980193.13	-33.050	-186.700	.72	-185.980
MS467	40. 8.620	111. 48.600	4517.00	979735.74	980193.25	-32.610	-186.510	.65	-185.860
MS468	40. 1.190	111. 56.250	4530.00	979716.60	980182.24	-39.560	-193.890	.57	-193.320
MS469	40. 1.580	111. 56.010	4516.00	979718.57	980182.82	-39.500	-193.340	.54	-192.800
MS470	40. 2.370	111. 55.730	4501.00	979722.80	980183.99	-37.830	-191.170	.51	-190.660
MS471	40. 2.730	111. 55.470	4497.00	979724.82	980184.52	-36.680	-189.900	.50	-189.400
MS472	40. 3.690	111. 55.480	4511.00	979728.98	980185.94	-32.670	-186.350	.44	-185.910
MS474	40. 5.150	111. 56.340	4527.00	979733.20	980188.11	-29.080	-183.320	.38	-182.940
MS475	39. 52.570	111. 56.560	5088.00	979674.45	980169.48	-16.450	-189.800	1.79	-188.010
MS476	39. 52.730	111. 56.950	4948.00	979681.03	980169.72	-23.260	-191.840	1.65	-190.190
MS477	39. 53.230	111. 57.200	4783.00	979689.19	980170.46	-31.430	-194.360	1.38	-192.980
MS478	39. 53.610	111. 57.220	4719.00	979690.77	980171.02	-36.430	-197.180	1.31	-195.870
MS479	39. 54.040	111. 57.230	4681.00	979690.34	980171.66	-41.000	-200.490	1.24	-199.250
MS481	39. 54.850	111. 57.260	4654.00	979690.40	980172.86	-44.660	-203.230	1.11	-202.120
MS482	39. 55.770	111. 57.280	4638.00	979692.77	980174.22	-45.220	-203.230	1.02	-202.210
MS483	39. 56.200	111. 57.290	4670.00	979691.12	980174.85	-44.450	-203.560	.86	-202.700
MS484	39. 56.660	111. 57.300	4693.00	979689.94	980175.54	-44.140	-204.040	.79	-203.250
MS486	39. 57.540	111. 57.320	4681.00	979692.80	980176.84	-43.770	-203.240	.76	-202.480
MS487	39. 58.000	111. 57.370	4669.00	979694.96	980177.52	-43.430	-202.490	.74	-201.750
MS488	39. 58.480	111. 57.370	4670.00	979696.22	980178.23	-42.770	-201.860	.71	-201.150
MS489	39. 59.260	111. 57.390	4659.00	979699.40	980179.38	-41.740	-200.470	.68	-199.790
MS490	39. 59.730	111. 57.430	4641.00	979702.97	980180.08	-40.540	-198.670	.67	-198.000
MS491	40. .130	111. 57.440	4649.00	979705.16	980180.67	-38.260	-196.630	.65	-195.980
MS492	40. 1.430	111. 57.460	4615.00	979712.89	980182.60	-35.640	-192.860	.58	-192.280
MS493	40. 2.020	111. 57.470	4626.00	979714.32	980183.47	-34.040	-191.640	.53	-191.110
MS494	40. 2.390	111. 57.470	4628.00	979715.56	980184.02	-33.180	-190.840	.50	-190.340
MS495	40. 2.850	111. 57.450	4617.00	979719.32	980184.70	-31.070	-188.380	.48	-187.900
MS497	40. 3.700	111. 57.450	4625.00	979725.03	980185.96	-25.870	-183.450	.42	-183.030
MS498	40. 4.120	111. 57.450	4608.00	979728.61	980186.58	-24.510	-181.510	.40	-181.110
MS500	40. 4.990	111. 57.490	4597.00	979735.41	980187.87	-20.080	-176.690	.37	-176.320
MS502	40. 6.270	111. 57.510	4566.00	979743.92	980189.77	-16.350	-171.910	.37	-171.540
MS503	40. 7.170	111. 57.490	4550.00	979747.07	980191.10	-16.060	-171.070	.43	-170.640
MS504	40. 8.060	111. 56.920	4551.00	979746.18	980192.42	-18.200	-173.240	.39	-172.850
MS505	40. 8.430	111. 56.940	4561.00	979744.88	980192.97	-19.080	-174.470	.40	-174.070
MS506	40. 9.350	111. 56.940	4604.00	979739.87	980194.33	-21.410	-178.260	.50	-177.760
MS507	40. 10.030	111. 56.360	4662.00	979740.11	980195.34	-16.680	-175.530	.63	-174.900
W0628	40. .220	111. 51.130	4518.00	979718.27	980180.79	-37.556	-191.480	1.01	-190.470
W0834	39. 57.530	112. 4.200	6295.00	979614.78	980176.83	30.064	-184.400	1.83	-182.570
W0835	39. 56.420	112. 4.740	6172.00	979617.93	980175.18	23.284	-186.990	3.29	-183.700
W0836	39. 56.090	112. 3.880	5949.00	979630.47	980174.70	15.336	-187.340	2.28	-185.060
W0857	39. 55.420	111. 32.780	5399.00	979635.64	980173.70	-30.231	-214.170	5.10	-209.070
W0858	39. 56.580	111. 32.470	5329.00	979643.45	980175.41	-30.716	-212.270	5.17	-207.100
W0859	39. 58.200	111. 30.510	5170.00	979655.97	980177.81	-35.553	-211.690	5.81	-205.880
W0860	39. 57.300	111. 40.630	6205.00	979601.84	980176.49	8.988	-202.410	10.00	-192.410
W0861	39. 56.520	111. 40.430	6872.00	979565.44	980175.32	36.502	-197.620	4.48	-193.140
W0862	39. 56.420	111. 39.230	7522.00	979525.06	980175.18	57.397	-198.870	4.45	-194.420
W0633	39. 59.160	111. 45.550	4824.00	979693.22	980179.24	-32.281	-196.630	5.52	-191.110
W0634	39. 58.860	111. 46.070	4899.00	979689.62	980178.79	-28.366	-195.270	4.06	-191.210

STAT.	LATITUDE	LONGITUDE	ELEV.	OBSERVED GRAVITY	THEOR. GRAVITY	FREE AIR	SIMPLE BOUGUER	T.C.	COMPLETE BOUGUER
W0637	39. 57.160	111. 55.000	4549.00	979702.65	980176.27	-45.740	-200.720	.86	-199.860
W0638	39. 57.120	111. 56.990	4658.00	979692.71	980176.21	-45.367	-204.060	.77	-203.290
W0640	39. 57.040	112. 1.850	5399.00	979663.59	980176.09	-4.671	-188.610	1.68	-186.930
W0641	39. 56.860	112. 2.820	5601.00	979654.26	980175.84	5.250	-185.570	1.75	-183.820
W0642	39. 56.530	112. 3.360	5746.00	979644.77	980175.34	9.900	-185.860	2.07	-183.790
W0643	39. 58.510	112. 3.680	5863.00	979644.49	980178.28	17.687	-182.060	1.99	-180.070
W0644	39. 59.310	112. 2.170	5474.00	979667.85	980179.46	3.274	-183.220	2.76	-180.460
W0645	39. 58.780	112. .040	5069.00	979684.72	980178.67	-17.164	-189.860	1.02	-188.840
W0646	39. 58.980	111. 59.330	4925.00	979686.67	980178.97	-29.050	-196.840	.85	-195.990
W0647	39. 58.860	111. 57.400	4672.00	979697.22	980178.79	-42.120	-201.290	.69	-200.600
W0648	39. 58.900	111. 55.380	4517.00	979702.09	980178.85	-51.890	-205.780	.70	-205.080
W0649	39. 58.460	111. 54.050	4526.00	979711.42	980178.21	-41.074	-195.270	.77	-194.500
W0742	39. 56.380	111. 58.090	4767.00	979686.31	980175.12	-40.423	-202.830	.83	-202.000
W0743	39. 56.300	112. .500	5104.00	979676.50	980175.00	-18.422	-192.310	1.42	-190.890
W0744	39. 56.310	112. 1.740	5452.00	979658.75	980175.02	-3.446	-189.190	1.67	-187.520
W0745	39. 55.740	111. 58.990	4797.00	979685.43	980174.17	-37.541	-200.970	1.06	-199.910
W0752	39. 55.340	111. 57.240	4638.00	979691.52	980173.58	-45.808	-203.820	1.08	-202.740
W0775	39. 55.400	111. 54.950	4755.00	979692.46	980173.68	-33.962	-195.960	.99	-194.970
W0778	39. 58.060	111. 47.700	5005.00	979685.11	980177.61	-21.725	-192.240	2.26	-189.980
W0779	39. 57.460	111. 46.720	5175.00	979670.91	980176.72	-19.053	-195.360	4.25	-191.110
W0780	39. 55.660	111. 48.710	4973.00	979682.62	980174.05	-23.675	-193.100	3.85	-189.250
W0781	39. 55.000	111. 49.110	4960.00	979680.39	980173.08	-26.148	-195.130	3.73	-191.400
W0789	39. 58.360	111. 41.500	5604.00	979640.63	980178.05	-10.307	-201.230	10.33	-190.900
W0579	40. 5.900	111. 40.800	4592.00	979694.35	980189.21	-62.935	-219.380	1.31	-218.070
W0580	40. 6.030	111. 39.280	4585.00	979698.57	980189.40	-59.564	-215.770	1.67	-214.100
W0582	40. 6.050	111. 35.810	4745.00	979693.16	980189.43	-49.953	-211.610	3.57	-208.040
W0583	40. 5.620	111. 35.230	4766.00	979692.54	980188.80	-47.977	-210.350	5.24	-205.110
W0584	40. 4.830	111. 35.070	4837.00	979689.33	980187.62	-43.328	-208.120	6.90	-201.220
W0585	40. 3.380	111. 33.670	4860.00	979676.90	980185.48	-51.455	-217.030	18.77	-198.260
W0586	40. 2.030	111. 31.160	4932.00	979672.27	980183.48	-47.312	-215.340	8.40	-206.940
W0587	40. 1.630	111. 30.220	4960.00	979675.65	980182.89	-40.708	-209.690	5.52	-204.170
W0588	40. 4.420	111. 36.940	4713.00	979696.88	980187.02	-46.843	-207.410	7.26	-200.150
W0589	40. 4.270	111. 38.080	4675.00	979695.39	980186.79	-51.667	-210.940	3.63	-207.310
W0590	40. 4.270	111. 39.720	4612.00	979694.26	980186.79	-58.724	-215.850	2.22	-213.630
W0591	40. 3.430	111. 40.340	4586.00	979694.88	980185.55	-59.320	-215.560	2.53	-213.030
W0593	40. .710	111. 44.670	4739.00	979694.73	980181.52	-41.037	-202.490	2.82	-199.670
W0594	40. 1.870	111. 44.680	4648.00	979703.21	980183.23	-42.837	-201.190	1.78	-199.410
W0595	40. 2.570	111. 44.360	4631.00	979702.17	980184.27	-46.516	-204.290	1.48	-202.810
W0596	40. 3.910	111. 42.380	4528.00	979696.18	980186.27	-64.186	-218.450	1.59	-216.860
W0597	40. 1.180	111. 42.230	4952.00	979685.24	980182.22	-31.190	-199.900	3.23	-196.670
W0598	40. 2.030	111. 42.300	4693.00	979696.91	980183.48	-45.154	-205.040	2.60	-202.440
W0599	40. 2.240	111. 41.480	4694.00	979695.79	980183.79	-46.480	-206.400	2.72	-203.680
W0600	40. 1.630	111. 40.310	4952.00	979681.92	980182.89	-35.190	-203.900	3.91	-199.990
W0602	40. 2.430	111. 39.480	4824.00	979688.20	980184.07	-42.121	-206.470	4.00	-202.470
W0603	40. 2.870	111. 38.340	4829.00	979688.61	980184.73	-41.901	-206.420	6.18	-200.240
W0601	40. 1.640	111. 39.460	5093.00	979672.42	980182.90	-31.427	-204.940	4.84	-200.100
W0605	40. .840	111. 45.730	4655.00	979702.37	980181.72	-41.499	-200.090	2.11	-197.980
W0606	40. 4.220	111. 46.120	4514.00	979716.93	980186.72	-45.203	-198.990	1.11	-197.880
W0607	40. 5.870	111. 46.180	4498.00	979718.78	980189.17	-47.308	-200.550	.90	-199.650

STAT.	LATITUDE	LONGITUDE	ELEV.	OBSERVED GRAVITY	THEOR. GRAVITY	FREE AIR	SIMPLE BOUGUER	T.C.	COMPLETE BOUGUER
W0612	40. 3.330	111. 47.190	4555.00	979716.79	980185.41	-40.176	-195.360	1.38	-193.980
W0613	40. 2.450	111. 47.180	4599.00	979715.25	980184.09	-36.267	-192.950	1.32	-191.630
W0614	40. 2.450	111. 48.000	4757.00	979708.67	980184.09	-27.984	-190.050	1.41	-188.640
W0615	40. 4.650	111. 48.220	4734.00	979710.40	980187.36	-31.677	-192.960	3.80	-189.160
W0621	40. 4.440	111. 51.320	4498.00	979726.91	980187.05	-37.068	-190.310	4.85	-185.460
W0623	40. 2.790	111. 51.690	4598.00	979720.39	980184.61	-31.731	-188.380	1.54	-186.840
W0624	40. 2.400	111. 51.410	4590.00	979720.59	980184.02	-31.693	-188.070	1.55	-186.520
W0625	40. 1.980	111. 50.870	4581.00	979720.51	980183.40	-32.000	-188.070	1.73	-186.340
W0626	40. 1.530	111. 50.570	4511.00	979721.49	980182.74	-36.945	-190.630	1.55	-189.080
W0627	40. .770	111. 50.560	4518.00	979717.71	980181.60	-38.926	-192.850	1.13	-191.720
W0629	40. .680	111. 49.420	4618.00	979714.08	980181.48	-33.029	-190.360	1.33	-189.030
W0630	40. 1.960	111. 48.870	5122.00	979687.92	980183.37	-13.669	-188.170	1.32	-186.850
W0631	40. 1.140	111. 47.630	4761.00	979706.33	980182.16	-28.007	-190.210	1.30	-188.910
W0632	40. .700	111. 47.140	4703.00	979706.96	980181.50	-32.173	-192.400	1.57	-190.830
W0682	40. 5.510	112. 2.840	5038.00	979718.57	980188.63	3.810	-167.830	.48	-167.350
W0683	40. 5.370	112. 2.030	4989.00	979720.43	980188.42	1.270	-168.700	.63	-168.070
W0685	40. 5.860	112. .070	4799.00	979727.32	980189.16	-10.443	-173.940	.43	-173.510
W0686	40. 5.350	112. .650	4847.00	979726.42	980188.40	-6.068	-171.200	.61	-170.590
W0687	40. 4.670	112. .600	4881.00	979723.81	980187.39	-4.469	-170.760	.63	-170.130
W0688	40. 3.810	112. 2.270	5092.00	979704.85	980186.12	-2.321	-175.800	.71	-175.090
W0689	40. 3.330	112. 3.830	5175.00	979697.25	980185.41	-1.393	-177.700	1.13	-176.570
W0691	40. 2.470	112. 4.230	5322.00	979688.87	980184.12	5.335	-175.980	1.57	-174.410
W0692	40. 1.030	112. 3.920	5772.00	979657.36	980182.00	18.276	-178.370	1.87	-176.500
W0693	40. .680	112. 4.190	5725.00	979658.32	980181.48	15.335	-179.710	2.01	-177.700
W0699	40. 4.920	112. 3.380	5038.00	979713.39	980187.76	-.490	-172.130	.50	-171.630
W0700	40. 4.260	112. 3.440	5077.00	979706.94	980186.78	-2.302	-175.270	.64	-174.630
W0701	40. 3.270	112. .310	4975.00	979706.43	980185.32	-10.947	-180.440	.56	-179.880
W0702	40. 1.030	111. 59.910	4993.00	979697.36	980182.00	-14.993	-185.100	.87	-184.230
W0776	39. 59.680	111. 47.130	4804.00	979700.02	980180.02	-28.133	-191.800	1.84	-189.960
W0788	39. 59.880	111. 42.060	5166.00	979671.01	980180.30	-23.380	-199.380	6.95	-192.430
W0425	40. 6.010	111. 58.200	4618.00	979741.82	980189.37	-13.189	-170.520	.38	-170.140
W0426	40. 5.450	111. 57.480	4583.00	979738.64	980188.54	-18.822	-174.960	.36	-174.600
W0427	40. 4.880	111. 57.460	4597.00	979734.43	980187.70	-20.875	-177.490	.37	-177.120
W0430	40. 5.110	111. 58.930	4693.00	979729.83	980188.05	-16.794	-176.680	.40	-176.280
W0431	40. 4.570	111. 55.240	4494.00	979731.84	980187.24	-32.694	-185.800	.42	-185.380
W0432	40. 5.650	111. 56.350	4519.00	979735.14	980188.85	-28.652	-182.610	.37	-182.240
W0435	40. 4.580	111. 56.330	4535.00	979731.65	980187.26	-29.047	-183.550	.39	-183.160
W0436	40. 4.040	111. 55.180	4496.00	979731.53	980186.46	-32.036	-185.210	.44	-184.770
W0437	40. 3.400	111. 54.970	4505.00	979727.30	980185.51	-34.469	-187.950	.46	-187.490
W0438	40. 3.270	111. 55.470	4503.00	979726.76	980185.32	-35.007	-188.420	.47	-187.950
W0439	40. 2.030	111. 55.730	4498.00	979720.48	980183.48	-39.918	-193.160	.54	-192.620
W0440	40. 1.710	111. 57.450	4614.00	979713.81	980183.00	-35.196	-192.390	.57	-191.820
W0441	40. .830	111. 57.450	4645.00	979708.52	980181.70	-36.269	-194.520	.60	-193.920
W0539	40. 10.460	111. 38.190	4505.00	979705.99	980195.98	-66.249	-219.730	2.99	-216.740
W0540	40. 11.290	111. 38.220	4495.00	979710.53	980197.21	-63.880	-217.020	3.86	-213.160
W0541	40. 12.380	111. 38.470	4496.00	979718.10	980198.83	-57.836	-211.010	4.60	-206.410
W0542	40. 12.900	111. 38.080	4536.00	979724.40	980199.59	-48.533	-203.070	6.67	-196.400
W0543	40. 13.050	111. 39.470	4491.00	979717.38	980199.80	-60.006	-213.010	3.33	-209.680
W0544	40. 13.210	111. 40.610	4508.00	979711.50	980200.04	-64.517	-218.100	2.19	-215.910

STAT.	LATITUDE	LONGITUDE	ELEV.	OBSERVED GRAVITY	THEOR. GRAVITY	FREE AIR	SIMPLE BOUGUER	T.C.	COMPLETE BOUGUER
W0554	40. 12.170	111. 37.360	4554.00	979720.15	980198.51	-50.010	-205.160	9.34	-195.820
W0555	40. 10.330	111. 36.160	4564.00	979709.80	980195.78	-56.689	-212.180	6.32	-205.860
W0556	40. 10.000	111. 35.140	4672.00	979703.51	980195.29	-52.330	-211.500	8.60	-202.900
W0558	40. 9.210	111. 34.400	4763.00	979697.92	980194.12	-48.199	-210.470	5.45	-205.020
W0559	40. 9.070	111. 33.130	4860.00	979692.82	980193.92	-43.975	-209.550	7.97	-201.580
W0560	40. 9.320	111. 32.310	4935.00	979681.58	980194.28	-48.519	-216.650	13.52	-203.130
W0561	40. 9.830	111. 30.000	5101.00	979672.56	980195.04	-42.674	-216.460	9.51	-206.950
W0563	40. 7.810	111. 34.890	4717.00	979695.30	980192.04	-53.057	-213.760	3.95	-209.810
W0566	40. 7.820	111. 38.980	4539.00	979697.88	980192.05	-67.241	-221.880	1.64	-220.240
W0567	40. 7.820	111. 41.310	4538.00	979696.28	980192.05	-68.935	-223.540	1.08	-222.460
W0575	40. 10.480	111. 39.760	4492.00	979701.96	980196.00	-71.522	-224.560	1.87	-222.690
W0576	40. 8.010	111. 37.130	4618.00	979695.76	980192.34	-62.219	-219.550	2.27	-217.280
W0581	40. 6.490	111. 36.680	4729.00	979692.50	980190.09	-52.778	-213.890	2.63	-211.260
W0609	40. 8.150	111. 46.660	4492.00	979726.48	980192.55	-43.552	-196.590	.63	-195.960
W0610	40. 6.840	111. 47.780	4497.00	979730.45	980190.61	-37.172	-190.380	1.43	-188.950
W0616	40. 7.930	111. 48.750	4877.00	979712.52	980192.23	-20.975	-187.130	1.42	-185.710
W0617	40. 8.690	111. 48.390	4526.00	979735.33	980193.35	-32.304	-186.500	.59	-185.910
W0619	40. 6.840	111. 50.610	4624.00	979727.22	980190.61	-28.455	-185.990	2.10	-183.890
W0655	40. 12.850	112. .050	4860.00	979726.70	980199.52	-15.685	-181.260	.77	-180.490
W0684	40. 6.610	112. 1.460	4958.00	979722.70	980190.26	-1.206	-170.120	.32	-169.800
W0402	40. 12.880	111. 53.200	4728.00	979742.50	980199.56	-12.352	-173.430	1.56	-171.870
W0404	40. 11.450	111. 53.920	4560.00	979749.65	980197.45	-18.885	-174.240	1.13	-173.110
W0405	40. 11.080	111. 54.560	4629.00	979744.26	980196.89	-17.225	-174.930	1.07	-173.860
W0407	40. 10.440	111. 56.690	4765.00	979735.66	980195.95	-12.091	-174.430	.79	-173.640
W0408	40. 9.700	111. 56.920	4648.00	979737.53	980194.85	-20.127	-178.480	.55	-177.930
W0410	40. 8.510	111. 57.500	4643.00	979743.77	980193.09	-12.598	-170.780	.38	-170.400
W0412	40. 7.630	111. 57.500	4561.00	979747.84	980191.77	-14.921	-170.310	.43	-169.880
W0413	40. 8.150	111. 56.240	4493.00	979746.50	980192.55	-23.438	-176.510	.41	-176.100
W0414	40. 8.760	111. 56.930	4574.00	979743.53	980193.45	-19.688	-175.520	.42	-175.100
W0415	40. 9.030	111. 56.360	4543.00	979740.96	980193.86	-25.585	-180.360	.47	-179.890
W0416	40. 9.370	111. 56.370	4575.00	979740.26	980194.36	-23.774	-179.640	.51	-179.130
W0424	40. 6.750	111. 57.500	4558.00	979744.56	980190.48	-17.193	-172.480	.40	-172.080
W0433	40. 6.320	111. 56.360	4512.00	979738.51	980189.84	-26.931	-180.650	.36	-180.290
W0434	40. 6.750	111. 56.360	4501.00	979741.40	980190.48	-25.715	-179.060	.37	-178.690
W0916	40. 19.770	111. 31.620	5858.00	979646.71	980209.77	-12.064	-211.640	9.01	-202.630
W0917	40. 19.850	111. 37.130	4997.00	979703.53	980209.89	-36.347	-206.590	18.04	-188.550
W0545	40. 14.040	111. 42.730	4496.00	979710.75	980201.28	-67.636	-220.810	1.38	-219.430
W0546	40. 13.600	111. 42.740	4493.00	979709.58	980200.62	-68.438	-221.510	1.32	-220.190
W0547	40. 14.280	111. 44.080	4490.00	979712.21	980201.63	-67.090	-220.060	1.07	-218.990
W0548	40. 14.560	111. 41.670	4528.00	979712.89	980202.04	-63.246	-217.510	1.87	-215.640
W0549	40. 15.350	111. 42.540	4530.00	979715.05	980203.22	-62.077	-216.410	1.62	-214.790
W0550	40. 15.630	111. 42.940	4524.00	979716.40	980203.62	-61.702	-215.830	1.54	-214.290
W0551	40. 15.620	111. 40.800	4704.00	979711.19	980203.61	-49.959	-210.220	2.56	-207.660
W0552	40. 15.160	111. 38.540	4706.00	979718.71	980202.94	-41.581	-201.910	6.65	-195.260
W0553	40. 14.020	111. 38.590	4545.00	979723.32	980201.25	-50.426	-205.270	6.06	-199.210
W0656	40. 14.240	111. 59.720	4867.00	979726.95	980201.57	-16.826	-182.640	1.32	-181.320
W0734	40. 19.930	111. 59.670	5006.00	979728.70	980210.01	-10.441	-180.990	.86	-180.130
W0735	40. 18.980	111. 59.570	4935.00	979730.69	980208.61	-13.729	-181.860	1.10	-180.760
W0736	40. 18.110	111. 59.540	4892.00	979734.27	980207.31	-12.904	-179.570	1.49	-178.080

STAT.	LATITUDE	LONGITUDE	ELEV.	OBSERVED GRAVITY	THEOR. GRAVITY	FREE AIR	SIMPLE BOUGUER	T.C.	COMPLETE BOUGUER
W0737	40. 17.390	111. 59.510	4899.00	979735.04	980206.25	-10.406	-177.310	1.59	-175.720
W0738	40. 16.380	111. 59.590	4868.00	979734.51	980204.75	-12.352	-178.200	1.68	-176.520
W0739	40. 15.680	111. 59.600	4845.00	979733.11	980203.71	-14.876	-179.940	1.78	-178.160
W0358	40. 19.640	111. 45.550	4506.00	979720.77	980209.59	-64.985	-218.500	1.69	-216.810
W0359	40. 20.010	111. 44.280	4541.00	979725.20	980210.14	-57.813	-212.520	2.44	-210.080
W0360	40. 20.020	111. 43.440	4640.00	979723.15	980210.16	-50.570	-208.650	2.84	-205.810
W0361	40. 20.020	111. 42.760	4739.00	979720.73	980210.16	-43.677	-205.130	3.25	-201.880
W0362	40. 20.020	111. 41.630	4854.00	979719.72	980210.16	-33.869	-199.240	4.46	-194.780
W0363	40. 20.100	111. 40.870	5097.00	979707.82	980210.27	-23.030	-196.680	5.62	-191.060
W0364	40. 18.260	111. 42.270	4749.00	979716.79	980207.53	-44.046	-205.840	2.34	-203.500
W0365	40. 18.260	111. 43.410	4624.00	979720.99	980207.53	-51.605	-209.140	1.89	-207.250
W0366	40. 17.390	111. 43.400	4584.00	979721.05	980206.25	-54.028	-210.200	1.66	-208.540
W0367	40. 17.170	111. 44.330	4527.00	979721.72	980205.91	-58.380	-212.610	1.38	-211.230
W0368	40. 17.380	111. 45.130	4506.00	979720.97	980206.23	-61.425	-214.940	1.23	-213.710
W0369	40. 17.830	111. 44.750	4522.00	979722.50	980206.89	-59.050	-213.110	1.41	-211.700
W0370	40. 17.820	111. 45.510	4508.00	979720.86	980206.87	-61.997	-215.580	1.23	-214.350
W0371	40. 18.230	111. 45.640	4506.00	979720.72	980207.48	-62.925	-216.440	1.29	-215.150
W0372	40. 19.000	111. 45.810	4506.00	979720.36	980208.64	-64.445	-217.960	1.41	-216.550
W0373	40. 16.850	111. 43.820	4531.00	979720.82	980205.45	-58.443	-212.810	1.45	-211.360
W0374	40. 16.520	111. 43.600	4534.00	979719.68	980204.95	-58.801	-213.270	1.45	-211.820
W0375	40. 16.520	111. 42.810	4585.00	979718.36	980204.95	-55.324	-211.530	1.68	-209.850
W0376	40. 16.510	111. 42.230	4712.00	979711.59	980204.94	-50.137	-210.670	1.98	-208.690
W0377	40. 17.400	111. 42.250	4747.00	979713.87	980206.27	-45.894	-207.620	2.22	-205.400
W0378	40. 18.270	111. 40.540	4826.00	979718.66	980207.55	-34.953	-199.370	3.36	-196.010
W0380	40. 19.270	111. 38.910	4850.00	979722.72	980209.03	-30.115	-195.350	8.73	-186.620
W0381	40. 17.870	111. 39.180	4838.00	979720.00	980206.96	-31.894	-196.720	5.52	-191.200
W0382	40. 17.020	111. 39.070	4783.00	979718.69	980205.70	-37.118	-200.070	5.51	-194.560
W0383	40. 16.100	111. 38.510	4840.00	979713.61	980204.33	-35.466	-200.360	6.76	-193.600
W0384	40. 16.970	111. 39.510	4691.00	979723.12	980205.62	-41.272	-201.090	4.63	-196.460
W0385	40. 17.340	111. 39.470	4721.00	979723.84	980206.18	-38.280	-199.120	4.84	-194.280
W0386	40. 18.050	111. 39.770	4760.00	979724.19	980207.23	-35.312	-197.480	4.48	-193.000
W0387	40. 16.960	111. 40.070	4699.00	979721.28	980205.61	-42.340	-202.430	3.58	-198.850
W0388	40. 17.380	111. 40.520	4787.00	979716.49	980206.23	-39.482	-202.570	3.02	-199.550
W0389	40. 17.380	111. 41.460	4761.00	979715.48	980206.23	-42.937	-205.140	2.37	-202.770
W0390	40. 16.940	111. 41.260	4756.00	979714.56	980205.58	-43.668	-205.700	2.40	-203.300
W0392	40. 17.470	111. 52.690	4594.00	979750.61	980206.37	-23.647	-180.160	1.62	-178.540
W0393	40. 15.720	111. 52.720	4807.00	979739.25	980203.77	-12.380	-176.150	2.43	-173.720
W0394	40. 15.100	111. 52.680	5085.00	979722.20	980202.84	-2.339	-175.580	2.16	-173.420
W0395	40. 14.910	111. 52.770	5150.00	979717.81	980202.56	-.345	-175.800	2.54	-173.260
W0396	40. 16.050	111. 53.980	5445.00	979699.83	980204.25	7.736	-177.770	3.69	-174.080
W0397	40. 16.510	111. 53.120	4884.00	979734.13	980204.94	-11.417	-177.810	2.16	-175.650
W0398	40. 15.930	111. 51.220	4502.00	979750.03	980204.08	-30.591	-183.970	1.12	-182.850
W0399	40. 15.780	111. 51.980	4620.00	979747.65	980203.86	-21.651	-179.050	1.66	-177.390
W0400	40. 14.780	111. 52.000	4628.00	979746.39	980202.37	-20.679	-178.350	2.65	-175.700
W0401	40. 13.440	111. 52.570	4647.00	979747.21	980200.37	-16.071	-174.390	1.65	-172.740
W0403	40. 13.290	111. 53.630	4944.00	979728.96	980200.16	-6.163	-174.600	2.18	-172.420
W0419	40. 19.970	111. 54.670	4555.00	979755.33	980210.07	-26.296	-181.480	1.40	-180.080
W0420	40. 19.780	111. 54.450	4593.00	979752.55	980209.79	-25.221	-181.700	1.30	-180.400
W0421	40. 19.130	111. 55.930	5124.00	979722.36	980208.83	-4.500	-179.070	2.32	-176.750

STAT.	LATITUDE	LONGITUDE	ELEV.	OBSERVED GRAVITY	THEOR. GRAVITY	FREE AIR	SIMPLE BOUGUER	T.C.	COMPLETE BOUGUER
W0423	40. 17.280	111. 53.420	4882.00	979733.96	980206.08	-12.915	-179.240	2.20	-177.040
W0904	40. 21.880	111. 33.340	5218.00	979689.37	980212.91	-32.728	-210.500	17.92	-192.580
W0913	40. 21.380	111. 34.380	5196.00	979690.87	980212.16	-32.557	-209.580	16.20	-193.380
W0914	40. 20.890	111. 32.690	5465.00	979670.90	980211.44	-26.503	-212.690	14.86	-197.830
W0915	40. 20.140	111. 31.350	5675.00	979655.97	980210.33	-20.568	-213.910	11.38	-202.530
W0324	40. 21.670	111. 43.100	4780.00	979724.56	980212.60	-38.430	-201.280	5.50	-195.780
W0323	40. 21.840	111. 44.280	4623.00	979731.09	980212.85	-46.919	-204.420	3.95	-200.470
W0325	40. 21.670	111. 42.310	5062.00	979709.86	980212.60	-26.613	-199.070	7.22	-191.850
W0333	40. 22.160	111. 54.930	4522.00	979755.60	980213.34	-32.400	-186.460	.94	-185.520
W0334	40. 22.150	111. 56.080	4609.00	979752.79	980213.32	-27.006	-184.030	.95	-183.080
W0335	40. 21.810	111. 56.900	4774.00	979743.66	980212.80	-20.105	-182.750	.79	-181.960
W0336	40. 21.740	111. 59.020	4885.00	979738.90	980212.70	-14.323	-180.750	.84	-179.910
W0337	40. 21.290	111. 54.930	4543.00	979755.24	980212.04	-29.485	-184.260	.90	-183.360
W0338	40. 21.290	111. 54.060	4499.00	979756.07	980212.04	-32.794	-186.070	.88	-185.190
W0339	40. 21.600	111. 53.750	4493.00	979753.28	980212.50	-36.608	-189.680	.87	-188.810
W0340	40. 21.740	111. 53.220	4493.00	979747.88	980212.70	-42.208	-195.280	.86	-194.420
W0341	40. 21.900	111. 53.150	4494.00	979746.59	980212.94	-43.644	-196.750	.87	-195.880
W0342	40. 22.200	111. 48.030	4567.00	979723.21	980213.39	-60.607	-216.200	1.54	-214.660
W0343	40. 21.150	111. 48.770	4492.00	979721.92	980211.83	-67.392	-220.430	1.20	-219.230
W0344	40. 21.910	111. 49.820	4498.00	979726.19	980212.95	-63.678	-216.920	1.14	-215.780
W0345	40. 22.110	111. 50.620	4496.00	979729.39	980213.24	-60.956	-214.130	1.05	-213.080
W0346	40. 21.880	111. 50.910	4493.00	979730.25	980212.91	-60.048	-213.120	.99	-212.130
W0347	40. 21.900	111. 51.400	4497.00	979732.40	980212.94	-57.552	-210.760	.95	-209.810
W0348	40. 21.620	111. 51.740	4490.00	979734.90	980212.53	-55.300	-208.270	.91	-207.360
W0349	40. 21.900	111. 51.980	4498.00	979735.74	980212.94	-54.118	-207.360	.91	-206.450
W0350	40. 20.760	111. 48.230	4491.00	979719.53	980211.25	-69.296	-222.300	1.23	-221.070
W0351	40. 20.600	111. 48.050	4490.00	979718.75	980211.02	-69.940	-222.910	1.24	-221.670
W0352	40. 20.860	111. 47.660	4498.00	979719.27	980211.39	-69.038	-222.280	1.38	-220.900
W0353	40. 20.860	111. 47.080	4501.00	979719.56	980211.39	-68.465	-221.810	1.56	-220.250
W0354	40. 21.320	111. 46.390	4523.00	979722.06	980212.08	-64.586	-218.680	1.95	-216.730
W0355	40. 21.320	111. 47.090	4523.00	979720.76	980212.08	-65.886	-219.980	1.67	-218.310
W0356	40. 20.870	111. 46.410	4505.00	979720.10	980211.41	-67.569	-221.050	1.79	-219.260
W0357	40. 20.650	111. 45.530	4501.00	979721.66	980211.09	-66.065	-219.410	2.13	-217.280
W0417	40. 20.850	111. 54.930	4549.00	979755.16	980211.38	-28.340	-183.320	.98	-182.340
W0418	40. 20.220	111. 54.900	4559.00	979755.15	980210.45	-26.479	-181.800	1.23	-180.570
W0885	40. 27.000	111. 40.270	6032.00	979640.52	980220.51	-12.620	-218.070	22.71	-195.360
W0887	40. 26.990	111. 38.910	6332.00	979629.19	980220.50	4.280	-211.390	17.68	-193.710
W0888	40. 25.980	111. 38.140	7260.00	979581.80	980219.00	45.680	-201.600	9.80	-191.800
W0889	40. 26.130	111. 37.700	7479.00	979569.10	980219.22	53.350	-201.380	6.31	-195.070
W0266	40. 26.570	111. 55.310	4491.00	979751.47	980219.87	-45.980	-198.940	2.00	-196.940
W0267	40. 25.210	111. 55.530	4705.00	979737.52	980217.85	-37.780	-198.030	1.40	-196.630
W0268	40. 25.220	111. 54.370	4546.00	979745.12	980217.87	-45.150	-199.990	1.24	-198.750
W0269	40. 24.350	111. 54.360	4521.00	979745.63	980216.58	-45.700	-199.690	1.11	-198.580
W0270	40. 24.350	111. 53.150	4522.00	979742.35	980216.58	-48.890	-202.910	1.10	-201.810
W0271	40. 24.370	111. 51.590	4578.00	979731.92	980216.61	-54.080	-210.010	1.22	-208.790
W0272	40. 25.140	111. 52.610	4570.00	979739.47	980217.75	-48.430	-204.080	1.33	-202.750
W0273	40. 25.890	111. 53.430	4627.00	979741.54	980218.86	-42.100	-199.700	1.43	-198.270
W0288	40. 25.240	111. 50.940	4769.00	979720.89	980217.90	-48.440	-210.870	1.49	-209.380
W0289	40. 25.240	111. 50.370	4783.00	979720.13	980217.90	-47.880	-210.790	1.59	-209.200

STAT.	LATITUDE	LONGITUDE	ELEV.	OBSERVED GRAVITY	THEOR. GRAVITY	FREE AIR	SIMPLE BOUGUER	T.C.	COMPLETE BOUGUER
W0290	40. 25.250	111. 49.230	4801.00	979719.40	980217.91	-46.930	-210.450	1.82	-208.630
W0291	40. 25.250	111. 48.080	4836.00	979718.52	980217.91	-44.520	-209.230	2.22	-207.010
W0292	40. 25.250	111. 47.500	4866.00	979717.52	980217.91	-42.690	-208.430	2.53	-205.900
W0293	40. 25.250	111. 46.350	4898.00	979719.06	980217.91	-38.140	-204.970	3.66	-201.310
W0295	40. 26.050	111. 44.140	5180.00	979691.05	980219.10	-40.820	-217.250	21.82	-195.430
W0296	40. 26.170	111. 43.640	5283.00	979681.71	980219.28	-40.650	-220.590	27.55	-193.040
W0297	40. 26.400	111. 43.130	5425.00	979673.07	980219.62	-36.270	-221.050	28.60	-192.450
W0298	40. 26.690	111. 41.860	5755.00	979654.49	980220.05	-24.240	-220.260	26.28	-193.980
W0299	40. 26.820	111. 41.100	5923.00	979645.10	980220.24	-18.020	-219.760	24.57	-195.190
W0300	40. 26.630	111. 42.130	5659.00	979659.13	980219.96	-28.540	-221.290	27.49	-193.800
W0301	40. 26.820	111. 46.650	4941.00	979712.26	980220.24	-43.230	-211.520	4.36	-207.160
W0312	40. 26.990	111. 50.700	5362.00	979688.84	980220.50	-27.310	-209.940	3.00	-206.940
W0313	40. 23.430	111. 49.790	4558.00	979728.42	980215.21	-58.060	-213.310	1.37	-211.940
W0314	40. 23.210	111. 49.260	4549.00	979728.79	980214.89	-58.220	-213.160	1.47	-211.690
W0315	40. 23.430	111. 48.180	4622.00	979728.06	980215.21	-52.400	-209.830	1.79	-208.040
W0316	40. 23.450	111. 47.390	4674.00	979726.94	980215.24	-48.660	-207.860	2.12	-205.740
W0317	40. 23.510	111. 46.350	4754.00	979724.23	980215.33	-43.940	-205.860	2.89	-202.970
W0318	40. 23.520	111. 45.190	4733.00	979727.36	980215.35	-42.800	-204.010	4.68	-199.330
W0319	40. 23.530	111. 44.670	4756.00	979727.00	980215.36	-41.010	-203.000	6.42	-196.580
W0320	40. 24.380	111. 44.950	4940.00	979717.89	980216.62	-34.070	-202.330	6.77	-195.560
W0322	40. 22.970	111. 44.340	4666.00	979731.10	980214.53	-44.550	-203.470	6.29	-197.180
W0326	40. 23.400	111. 50.920	4558.00	979728.68	980215.17	-57.760	-213.010	1.14	-211.870
W0327	40. 23.460	111. 51.970	4536.00	979733.99	980215.26	-54.610	-209.110	1.04	-208.070
W0328	40. 23.230	111. 52.570	4521.00	979737.49	980214.92	-52.180	-206.170	.97	-205.200
W0329	40. 23.230	111. 53.550	4500.00	979743.98	980214.92	-47.670	-200.940	.95	-199.990
W0330	40. 23.240	111. 54.920	4546.00	979750.10	980214.93	-37.230	-192.070	.97	-191.100
W0331	40. 23.210	111. 56.080	4679.00	979746.32	980214.89	-28.460	-187.830	1.01	-186.820
W0332	40. 23.080	111. 56.930	4807.00	979741.77	980214.69	-20.770	-184.500	1.00	-183.500
W0921	40. 25.900	111. 50.940	4809.00	979720.53	980218.88	-46.020	-209.810	1.74	-208.070
W0922	40. 25.890	111. 49.270	4825.00	979718.31	980218.86	-46.710	-211.050	2.04	-209.010
W0923	40. 25.900	111. 48.650	4838.00	979717.76	980218.88	-46.060	-210.840	2.26	-208.580
W0924	40. 25.900	111. 48.080	4858.00	979716.79	980218.88	-45.150	-210.610	2.49	-208.120
W0925	40. 26.130	111. 47.040	4909.00	979715.32	980219.22	-42.160	-209.360	3.34	-206.020
W0926	40. 26.130	111. 46.360	4946.00	979715.04	980219.22	-38.960	-207.420	4.15	-203.270
W0927	40. 24.600	111. 46.340	4840.00	979721.67	980216.95	-40.030	-204.880	3.40	-201.480
W0928	40. 24.820	111. 45.210	4979.00	979714.86	980217.27	-34.090	-203.670	6.07	-197.600
W0929	40. 24.390	111. 45.210	4861.00	979722.15	980216.64	-37.260	-202.830	5.82	-197.010
W0930	40. 22.980	111. 45.500	4632.00	979731.54	980214.54	-47.310	-205.080	3.62	-201.460
W0931	40. 22.540	111. 45.500	4578.00	979732.71	980213.89	-50.570	-206.500	3.30	-203.200
W0932	40. 22.980	111. 46.350	4629.00	979729.83	980214.54	-49.310	-206.970	2.70	-204.270
W0933	40. 24.390	111. 47.360	4798.00	979721.73	980216.64	-43.610	-207.030	2.38	-204.650
W0934	40. 24.380	111. 48.120	4777.00	979721.23	980216.62	-46.070	-208.770	2.02	-206.750
W0935	40. 24.370	111. 49.210	4767.00	979719.91	980216.61	-48.320	-210.680	1.80	-208.880
W0936	40. 24.030	111. 50.560	4596.00	979727.95	980216.10	-55.850	-212.390	1.29	-211.100
W0256	40. 29.240	111. 55.200	4451.00	979749.01	980223.84	-56.17	-207.770	1.51	-206.260
W0257	40. 29.360	111. 56.360	4439.00	979746.52	980224.01	-59.960	-211.150	1.37	-209.780
W0258	40. 29.370	111. 56.870	4488.00	979743.50	980224.03	-58.390	-211.250	1.31	-209.940
W0259	40. 28.720	111. 56.860	4579.00	979739.24	980223.06	-53.120	-209.080	1.36	-207.720
W0261	40. 29.370	111. 58.550	4662.00	979732.73	980224.03	-52.790	-211.580	1.32	-210.260

STAT.	LATITUDE	LONGITUDE	ELEV.	OBSERVED GRAVITY	THEOR. GRAVITY	FREE AIR	SIMPLE BOUGUER	T.C.	COMPLETE BOUGUER
W0262	40. 29.800	111. 59.130	4664.00	979732.20	980224.67	-53.770	-212.630	1.32	-211.310
W0302	40. 27.340	111. 46.640	4956.00	979711.99	980221.02	-42.870	-211.670	5.02	-206.650
W0303	40. 27.470	111. 45.520	5052.00	979706.84	980221.21	-39.180	-211.250	8.20	-203.050
W0304	40. 27.910	111. 45.730	5121.00	979702.18	980221.86	-38.000	-212.420	7.66	-204.760
W0305	40. 27.930	111. 46.710	5055.00	979705.29	980221.89	-41.130	-213.300	5.80	-207.500
W0306	40. 27.320	111. 47.090	4963.00	979710.66	980220.99	-43.510	-212.550	4.37	-208.180
W0307	40. 27.650	111. 48.010	5156.00	979698.92	980221.48	-37.590	-213.200	3.55	-209.650
W0308	40. 29.760	111. 50.080	5004.00	979716.96	980224.61	-36.970	-207.410	7.77	-199.640
W0310	40. 27.600	111. 48.450	5134.00	979700.04	980221.40	-38.460	-213.320	3.34	-209.980
P0411	40. 29.930	111. 51.866	4591.76	979738.20	980224.86	-54.758	-211.195	3.61	-207.585
P0412	40. 29.775	111. 51.768	4689.84	979733.05	980224.62	-50.449	-210.227	3.47	-206.757
P0413	40. 29.639	111. 51.649	4772.21	979729.09	980224.42	-46.458	-209.042	3.63	-205.412
P0414	40. 29.475	111. 51.579	4901.24	979721.88	980224.17	-41.281	-208.262	3.88	-204.382
P0415	40. 29.346	111. 51.468	5081.90	979709.88	980223.98	-36.101	-209.236	3.55	-205.686
P0416	40. 29.190	111. 51.369	5306.10	979695.26	980223.75	-29.398	-210.172	3.42	-206.752
P0417	40. 29.064	111. 51.307	5397.96	979689.81	980223.56	-26.020	-209.923	3.72	-206.203
P0501	40. 28.791	111. 51.774	5583.96	979678.41	980223.16	-19.519	-209.759	3.28	-206.479
P0502	40. 28.907	111. 51.815	5227.31	979701.15	980223.33	-30.497	-208.587	4.98	-203.607
P0503	40. 29.185	111. 52.055	5123.05	979707.67	980223.75	-34.206	-208.743	3.29	-205.453
P0504	40. 29.052	111. 51.954	4977.07	979716.94	980223.55	-38.464	-208.027	4.53	-203.497
P0505	40. 29.335	111. 52.170	4885.11	979722.50	980223.97	-41.975	-208.406	3.19	-205.216
P0506	40. 29.471	111. 52.251	4759.81	979729.35	980224.17	-47.114	-209.276	3.53	-205.746
P0507	40. 29.608	111. 52.382	4654.23	979734.60	980224.38	-52.006	-210.571	3.04	-207.531
P0508	40. 29.752	111. 52.484	4560.18	979740.09	980224.59	-55.565	-210.926	3.05	-207.876
P0509	40. 29.902	111. 52.615	4494.03	979743.73	980224.82	-58.382	-211.489	2.98	-208.509
P0610	40. 29.847	111. 53.376	4442.44	979746.94	980224.73	-59.931	-211.280	2.42	-208.860
P0611	40. 29.706	111. 53.278	4461.01	979746.50	980224.52	-58.421	-210.403	2.60	-207.803
P0612	40. 29.545	111. 53.150	4504.75	979744.39	980224.28	-56.174	-209.647	2.76	-206.887
P0613	40. 29.404	111. 53.036	4599.18	979739.14	980224.07	-52.331	-209.021	2.85	-206.171
P0614	40. 29.285	111. 52.935	4735.56	979732.48	980223.90	-45.992	-207.327	2.70	-204.627
P0615	40. 29.135	111. 52.842	4833.93	979727.07	980223.66	-41.915	-206.602	3.02	-203.582
P0616	40. 29.006	111. 52.717	4993.83	979717.16	980223.48	-36.597	-206.732	3.67	-203.062
P0617	40. 28.849	111. 52.609	5118.40	979709.37	980223.24	-32.435	-206.814	3.87	-202.944
P0618	40. 28.530	111. 52.375	5987.15	979652.25	980222.77	-7.372	-211.348	6.89	-204.458
P0619	40. 28.453	111. 52.300	5908.84	979659.32	980222.66	-7.551	-208.859	4.68	-204.179
P0707	40. 29.040	111. 53.496	4688.98	979738.15	980223.53	-44.336	-204.085	2.47	-201.615
P0708	40. 28.895	111. 53.379	4756.28	979734.97	980223.31	-40.967	-203.009	3.21	-199.799
P0709	40. 28.757	111. 53.269	4826.68	979729.95	980223.11	-39.162	-203.602	3.58	-200.022
P0710	40. 28.617	111. 53.151	5119.28	979711.38	980222.91	-30.007	-204.416	2.79	-201.626
P0711	40. 28.371	111. 52.913	6115.53	979642.00	980222.55	-5.320	-213.670	10.86	-202.810
P0712	40. 28.272	111. 52.800	5926.58	979764.73	980222.40	99.786	-102.127	6.35	-95.777
P0812	40. 27.980	111. 53.419	5782.64	979669.69	980221.96	-8.356	-205.365	6.68	-198.685
P0811	40. 28.159	111. 53.543	5622.24	979680.50	980222.22	-12.891	-204.435	5.83	-198.605
P0810	40. 28.339	111. 53.636	5125.43	979713.06	980222.48	-27.326	-201.945	2.40	-199.545
P0809	40. 28.554	111. 53.776	4782.07	979735.48	980222.80	-37.523	-200.444	2.55	-197.894
P0808	40. 28.682	111. 53.893	4737.99	979738.36	980222.99	-38.977	-200.395	2.18	-198.215
P0807	40. 28.814	111. 54.013	4650.68	979743.58	980223.20	-42.172	-200.616	2.14	-198.476
P0806	40. 29.816	111. 54.759	4430.43	979749.97	980224.69	-57.991	-208.932	1.57	-207.362
P0805	40. 29.954	111. 54.871	4425.54	979750.12	980224.89	-58.504	-209.278	1.52	-207.758

STAT.	LATITUDE	LONGITUDE	ELEV.	OBSERVED GRAVITY	THEOR. GRAVITY	FREE AIR	SIMPLE BOUGUER	T.C.	COMPLETE BOUGUER
P0912	40. 27.800	111. 53.941	5327.90	979701.00	980221.68	-19.537	-201.054	3.49	-197.564
P0911	40. 28.070	111. 54.179	5065.52	979717.18	980222.09	-28.451	-201.028	2.61	-198.418
P0910	40. 28.211	111. 54.185	4836.45	979732.42	980222.30	-34.960	-199.733	1.91	-197.823
P0909	40. 28.365	111. 54.327	4702.45	979743.01	980222.53	-37.209	-197.417	2.04	-195.377
P0908	40. 28.512	111. 54.446	4615.83	979746.61	980222.75	-41.975	-199.232	1.91	-197.322
P0907	40. 28.637	111. 54.565	4546.88	979749.79	980222.94	-45.468	-200.376	1.86	-198.516
P0906	40. 29.594	111. 55.308	4361.54	979753.97	980224.35	-60.135	-208.728	1.65	-207.078
P0905	40. 29.709	111. 55.394	4364.79	979753.46	980224.52	-60.511	-209.215	1.58	-207.635
P0904	40. 29.854	111. 55.496	4368.04	979753.06	980224.74	-60.824	-209.639	1.53	-208.109
P1003	40. 29.876	111. 56.021	4433.66	979747.53	980224.77	-60.213	-211.264	1.31	-209.954
P1004	40. 29.729	111. 55.922	4392.43	979750.45	980224.55	-60.953	-210.598	1.42	-209.178
P1005	40. 29.586	111. 55.823	4384.29	979751.07	980224.34	-60.880	-210.248	1.47	-208.778
P1006	40. 29.436	111. 55.724	4374.14	979752.12	980224.12	-60.566	-209.588	1.55	-208.038
P1007	40. 29.293	111. 55.625	4378.59	979752.20	980223.91	-59.864	-209.038	1.58	-207.458
P1008	40. 29.146	111. 55.526	4462.54	979746.64	980223.70	-57.309	-209.343	1.45	-207.893
P1009	40. 28.860	111. 55.302	4494.48	979747.02	980223.26	-53.487	-206.609	1.49	-205.119
P1010	40. 28.720	111. 55.191	4493.80	979747.96	980223.05	-52.408	-205.507	1.55	-203.957
P1011	40. 28.575	111. 55.077	4498.70	979748.55	980222.84	-51.138	-204.404	1.62	-202.784
P1012	40. 28.431	111. 54.964	4521.29	979748.29	980222.63	-49.070	-203.106	1.72	-201.386
P1013	40. 28.296	111. 54.864	4593.82	979744.18	980222.43	-46.155	-202.662	1.65	-201.012
P1014	40. 28.213	111. 54.788	4617.26	979744.77	980222.30	-43.227	-200.533	1.67	-198.863
P1015	40. 28.010	111. 54.613	4758.16	979735.28	980222.00	-39.167	-201.273	1.66	-199.613
P1016	40. 27.897	111. 54.615	4856.70	979729.17	980221.83	-35.837	-201.300	1.72	-199.580
P1017	40. 27.730	111. 54.396	5077.41	979714.64	980221.58	-29.357	-202.339	2.47	-199.869
P1018	40. 27.608	111. 54.295	5126.83	979711.55	980221.41	-27.627	-202.293	2.62	-199.673
P1019	40. 27.466	111. 54.179	5143.23	979710.10	980221.19	-27.315	-202.540	2.96	-199.580
P1020	40. 27.309	111. 54.075	4849.49	979730.86	980220.95	-33.950	-199.167	1.58	-197.587
P1021	40. 27.274	111. 54.021	4828.20	979732.42	980220.91	-34.354	-198.846	1.67	-197.176
P1022	40. 27.168	111. 53.938	4813.72	979733.52	980220.75	-34.452	-198.450	1.70	-196.750
P1023	40. 27.035	111. 53.835	4803.02	979734.02	980220.55	-34.755	-198.389	1.76	-196.629
P1024	40. 26.889	111. 53.708	4822.95	979732.56	980220.34	-34.137	-198.450	1.70	-196.750
P1025	40. 26.755	111. 53.601	4868.89	979728.95	980220.14	-33.223	-199.101	1.71	-197.391
P1026	40. 26.608	111. 53.487	4859.37	979729.49	980219.92	-33.360	-198.913	1.63	-197.283
P1027	40. 26.467	111. 53.373	4830.95	979731.12	980219.72	-34.200	-198.785	1.61	-197.175
P1028	40. 26.310	111. 53.259	4788.74	979733.08	980219.48	-35.975	-199.123	1.55	-197.573
P1029	40. 26.181	111. 53.149	4765.53	979733.91	980219.30	-37.141	-199.498	1.51	-197.988
P1030	40. 26.042	111. 53.028	4741.94	979734.35	980219.09	-38.709	-200.262	1.51	-198.752
P1031	40. 25.784	111. 52.803	4678.95	979736.64	980218.71	-41.969	-201.376	1.46	-199.916
P1032	40. 25.628	111. 52.698	4663.63	979736.54	980218.48	-43.276	-202.161	1.41	-200.751
P1101	40. 29.505	111. 56.306	4441.02	979746.78	980224.22	-59.716	-211.018	1.34	-209.678
P1102	40. 29.341	111. 56.395	4446.61	979746.46	980223.97	-59.261	-210.752	1.36	-209.392
P1103	40. 29.205	111. 56.449	4473.75	979745.11	980223.78	-57.870	-210.287	1.34	-208.947
P1104	40. 29.030	111. 56.535	4496.96	979744.10	980223.52	-56.439	-209.646	1.36	-208.286
P1105	40. 28.863	111. 56.608	4519.87	979743.06	980223.27	-55.074	-209.062	1.37	-207.692
P1106	40. 28.714	111. 56.678	4558.50	979740.95	980223.05	-53.332	-208.636	1.37	-207.266
P1107	40. 28.547	111. 56.748	4589.90	979739.44	980222.80	-51.639	-208.012	1.41	-206.602
P1108	40. 28.401	111. 56.805	4620.92	979738.19	980222.59	-49.752	-207.182	1.42	-205.762
P1109	40. 28.212	111. 56.754	4632.23	979738.25	980222.30	-48.339	-206.155	1.48	-204.675
P1110	40. 28.051	111. 56.685	4631.53	979738.99	980222.06	-47.431	-205.222	1.60	-203.622

STAT.	LATITUDE	LONGITUDE	ELEV.	OBSERVED GRAVITY	THEOR. GRAVITY	FREE AIR	SIMPLE BOUGUER	T.C.	COMPLETE BOUGUER
P1111	40. 27.917	111. 56.609	4632.70	979740.21	980221.86	-45.898	-203.729	1.78	-201.949
P1112	40. 27.755	111. 56.543	4634.96	979741.35	980221.62	-44.311	-202.219	1.90	-200.319
P1113	40. 27.616	111. 56.478	4638.01	979742.41	980221.42	-42.761	-200.773	1.96	-198.813
P1114	40. 27.451	111. 56.396	4660.60	979741.82	980221.17	-40.976	-199.758	2.10	-197.658
P1115	40. 27.311	111. 56.337	4684.46	979741.06	980220.97	-39.288	-198.883	2.15	-196.733
P1116	40. 27.142	111. 56.255	4702.86	979740.25	980220.70	-38.102	-198.324	2.03	-196.294
P1117	40. 27.002	111. 56.184	4721.60	979739.41	980220.50	-36.976	-197.836	1.96	-195.876
P1118	40. 26.832	111. 56.104	4741.42	979738.78	980220.26	-35.500	-197.035	1.98	-195.055
P1119	40. 26.690	111. 56.037	4758.79	979737.74	980220.04	-34.687	-196.814	1.86	-194.954
P1120	40. 26.529	111. 55.968	4768.96	979736.40	980219.80	-34.836	-197.310	1.65	-195.660
P1121	40. 26.360	111. 55.893	4772.55	979735.48	980219.57	-35.184	-197.780	1.58	-196.200
P1122	40. 26.211	111. 55.812	4786.15	979733.76	980219.34	-35.391	-198.450	1.45	-197.000
P1123	40. 25.908	111. 55.680	4837.15	979729.23	980218.90	-34.686	-199.483	1.30	-198.183
P1124	40. 25.743	111. 55.632	4829.26	979729.16	980218.65	-35.248	-199.776	1.30	-198.476
P1125	40. 25.575	111. 55.581	4751.26	979734.61	980218.41	-36.893	-198.763	1.37	-197.393
P1201	40. 29.003	111. 55.424	4453.19	979749.10	980223.48	-55.510	-207.225	1.50	-205.725
P1202	40. 28.852	111. 55.515	4451.89	979748.80	980223.26	-55.713	-207.384	1.51	-205.874
P1203	40. 28.704	111. 55.611	4448.29	979748.85	980223.04	-55.783	-207.332	1.54	-205.792
P1204	40. 28.555	111. 55.700	4445.59	979749.65	980222.80	-55.002	-206.459	1.57	-204.889
P1205	40. 28.404	111. 55.789	4434.15	979750.29	980222.59	-55.220	-206.287	1.65	-204.637
P1206	40. 28.250	111. 55.877	4446.55	979750.65	980222.35	-53.459	-204.949	1.68	-203.269
P1207	40. 28.084	111. 55.899	4445.58	979750.91	980222.11	-53.048	-204.505	1.77	-202.735
P1208	40. 27.919	111. 55.931	4444.86	979751.37	980221.87	-52.421	-203.853	1.92	-201.933
P1209	40. 27.756	111. 55.952	4447.59	979752.42	980221.62	-50.865	-202.390	2.14	-200.250
P1210	40. 27.596	111. 55.908	4451.10	979753.57	980221.39	-49.150	-200.795	2.16	-198.635
P1211	40. 27.446	111. 55.822	4455.16	979754.71	980221.16	-47.394	-199.177	2.29	-196.887
P1212	40. 27.333	111. 55.666	4461.24	979754.72	980221.00	-46.656	-198.646	2.19	-196.456
P1213	40. 27.211	111. 55.516	4468.37	979754.28	980220.81	-46.238	-198.471	2.05	-196.421
P1214	40. 27.098	111. 55.388	4473.45	979753.52	980220.65	-46.356	-198.762	1.96	-196.802
P1215	40. 26.934	111. 55.291	4480.07	979752.81	980220.40	-46.193	-198.825	1.95	-196.875
P1216	40. 26.781	111. 55.290	4482.09	979752.49	980220.18	-46.104	-198.805	1.99	-196.815
P1217	40. 26.602	111. 55.302	4492.41	979751.31	980219.91	-46.040	-199.092	1.97	-197.122
P1218	40. 26.494	111. 55.159	4499.42	979750.79	980219.74	-45.737	-199.027	1.94	-197.087
P1219	40. 26.477	111. 54.948	4501.76	979750.17	980219.73	-46.121	-199.491	1.71	-197.781
P1220	40. 26.439	111. 54.745	4506.58	979749.76	980219.69	-46.039	-199.573	1.65	-197.923
P1221	40. 26.320	111. 54.590	4512.53	979748.85	980219.51	-46.209	-199.947	1.57	-198.377
P1222	40. 26.186	111. 54.455	4518.44	979748.44	980219.30	-45.860	-199.799	1.52	-198.279
P1223	40. 26.062	111. 54.326	4528.31	979748.31	980219.12	-44.874	-199.149	1.46	-197.689
P1224	40. 25.933	111. 54.165	4534.05	979748.10	980218.93	-44.357	-198.827	1.44	-197.387
P1225	40. 25.801	111. 54.032	4539.34	979747.69	980218.74	-44.082	-198.733	1.39	-197.343
P1226	40. 25.681	111. 53.909	4546.25	979746.83	980218.55	-44.097	-198.983	1.36	-197.623
P1227	40. 25.554	111. 53.776	4549.54	979745.98	980218.36	-44.450	-199.448	1.32	-198.128
P1228	40. 25.422	111. 53.643	4551.26	979745.37	980218.17	-44.710	-199.767	1.32	-198.447
P1229	40. 25.302	111. 53.494	4549.45	979744.69	980217.99	-45.381	-200.376	1.30	-199.076
P1230	40. 25.178	111. 53.349	4549.58	979743.98	980217.80	-45.891	-200.891	1.26	-199.631
P1231	40. 25.031	111. 53.212	4548.51	979743.37	980217.59	-46.383	-201.346	1.22	-200.126
P1301	40. 25.634	111. 56.453	5060.00	979719.17	980218.49	-23.379	-195.768	1.49	-194.278
P1302	40. 25.737	111. 56.275	4943.39	979727.08	980218.64	-26.585	-195.002	1.60	-193.402
P1303	40. 25.813	111. 56.139	4842.75	979731.78	980218.75	-31.461	-196.449	1.84	-194.609

STAT.	LATITUDE	LONGITUDE	ELEV.	OBSERVED GRAVITY	THEOR. GRAVITY	FREE AIR	SIMPLE BOUGUER	T.C.	COMPLETE BOUGUER
P1304	40. 25.951	111. 55.942	4810.27	979732.96	980218.96	-33.547	-197.428	1.52	-195.908
P1305	40. 26.051	111. 55.788	4780.47	979733.59	980219.10	-35.861	-198.726	1.44	-197.286
P1306	40. 26.149	111. 55.623	4693.61	979738.38	980219.25	-39.389	-199.296	1.58	-197.716
P1307	40. 26.263	111. 55.448	4685.96	979738.75	980219.42	-39.910	-199.556	1.47	-198.086
P1308	40. 26.382	111. 55.253	4634.65	979742.27	980219.60	-41.396	-199.294	1.42	-197.874
P1309	40. 26.613	111. 54.906	4650.98	979741.10	980219.92	-41.351	-199.805	1.39	-198.415
P1310	40. 26.730	111. 54.751	4742.09	979735.34	980220.09	-38.713	-200.271	1.82	-198.451
P1311	40. 26.864	111. 54.613	4766.66	979733.65	980220.30	-38.295	-200.690	1.69	-199.000
P1312	40. 26.968	111. 54.451	4791.72	979732.97	980220.46	-36.782	-200.031	1.53	-198.501
P1313	40. 27.072	111. 54.281	4844.24	979730.00	980220.60	-34.952	-199.991	1.51	-198.481
P1314	40. 27.181	111. 54.154	4896.04	979726.29	980220.77	-33.954	-200.757	1.53	-199.227
P1315	40. 27.238	111. 54.053	4990.44	979720.81	980220.85	-30.641	-200.660	1.80	-198.860
P1316	40. 27.406	111. 53.835	5064.18	979716.24	980221.10	-28.525	-201.056	1.97	-199.086
P1317	40. 27.473	111. 53.654	5132.63	979711.92	980221.20	-26.508	-201.372	2.18	-199.192
PG002	40. 29.51	111. 55.24	4371.28	979753.52	980224.23	-59.55	-208.48	1.66	-206.82
PG006	40. 29.75	111. 54.72	4431.01	979749.88	980224.59	-57.93	-208.89	1.59	-207.30
PG060	40. 29.309	111. 55.079	4443.71	979749.79	980223.93	-56.164	-207.557	1.55	-206.007
PG064	40. 29.428	111. 54.812	4446.42	979748.94	980224.10	-56.931	-208.416	1.62	-206.796
PG068	40. 29.550	111. 54.563	4438.45	979749.20	980224.29	-57.608	-208.822	1.70	-207.122
PG072	40. 29.670	111. 54.304	4434.60	979749.39	980224.47	-57.960	-209.043	1.81	-207.233
PG077	40. 29.814	111. 53.981	4425.98	979749.31	980224.69	-59.070	-209.859	1.99	-207.869
PG148	40. 29.111	111. 54.912	4463.31	979750.10	980223.63	-53.714	-205.774	1.63	-204.144
PG152	40. 29.231	111. 54.656	4457.16	979750.87	980223.81	-53.702	-205.553	1.74	-203.813
PG156	40. 29.348	111. 54.401	4463.45	979749.44	980223.98	-54.712	-206.778	1.83	-204.948
PG160	40. 29.441	111. 54.119	4462.74	979748.34	980224.13	-56.027	-208.069	1.99	-206.079
PG164	40. 29.584	111. 53.872	4449.18	979748.81	980224.34	-57.036	-208.615	2.13	-206.485
PG236	40. 28.911	111. 54.767	4484.01	979750.93	980223.34	-50.648	-203.414	1.77	-201.644
PG240	40. 29.031	111. 54.497	4481.08	979751.85	980223.52	-50.183	-202.849	1.88	-200.969
PG244	40. 29.149	111. 54.245	4497.72	979749.39	980223.70	-51.250	-204.483	1.96	-202.523
PG248	40. 29.266	111. 53.980	4488.43	979747.93	980223.87	-53.755	-206.672	2.19	-204.482
PG252	40. 29.386	111. 53.719	4498.04	979746.43	980224.05	-54.531	-207.775	2.35	-205.425
PG277	40. 29.459	111. 53.431	4513.22	979744.67	980224.16	-54.981	-208.741	2.55	-206.191
PG280	40. 28.754	111. 54.645	4504.99	979751.51	980223.11	-47.860	-201.341	1.88	-199.461
PG284	40. 29.003	111. 54.132	4574.60	979747.30	980223.48	-45.890	-201.742	1.96	-199.782
PG288	40. 29.243	111. 53.614	4582.49	979742.73	980223.83	-50.069	-206.190	2.28	-203.910
66008	40. 29.720	111. 59.800	4784.00	979727.90	980224.50	-46.600	-209.000	1.00	-208.300
66009	40. 29.740	111. 59.650	4759.00	979728.42	980224.58	-48.530	-210.660	1.26	-209.400
66010	40. 29.790	111. 59.410	4700.00	979730.39	980224.65	-52.180	-212.300	1.30	-211.000
67001	40. 22.830	111. 58.560	4928.00	979736.09	980214.32	-14.700	-182.590	.86	-181.730
67002	40. 23.090	111. 58.610	4986.00	979732.91	980214.70	-12.810	-182.680	.93	-181.750
67003	40. 23.500	111. 58.530	5164.00	979723.85	980215.31	-5.740	-181.670	.98	-180.690
67004	40. 23.920	111. 58.450	5112.00	979726.09	980215.94	-9.020	-183.180	1.39	-181.790
67005	40. 24.040	111. 58.970	5250.00	979717.42	980216.12	-4.880	-183.740	1.45	-182.290
67006	40. 24.270	111. 59.380	5463.00	979704.12	980216.45	1.510	-184.610	1.29	-183.320
67007	40. 24.810	111. 59.360	5858.00	979677.58	980217.26	11.330	-188.250	2.25	-186.000
67008	40. 24.840	111. 58.890	6445.00	979634.23	980217.30	23.140	-196.4[illegible]0	10.29	-186.140
67009	40. 25.110	111. 59.220	6200.00	979654.59	980217.70	20.060	-191.170	3.89	-187.280
67010	40. 25.530	111. 59.640	6328.00	979645.96	980218.33	22.850	-192.740	3.82	-188.920
67011	40. 25.930	111. 59.650	5961.00	979669.26	980218.92	11.020	-192.060	2.73	-189.330

STAT.	LATITUDE	LONGITUDE	ELEV.	OBSERVED GRAVITY	THEOR. GRAVITY	FREE AIR	SIMPLE BOUGUER	T.C.	COMPLETE BOUGUER
67012	40. 26.080	111. 59.130	5786.00	979679.37	980219.14	4.460	-192.660	2.15	-190.510
67013	40. 26.580	111. 58.960	5755.00	979678.41	980219.88	-.160	-196.230	1.66	-194.570
67014	40. 26.970	111. 59.340	5400.00	979701.55	980220.46	-11.000	-194.970	3.44	-191.530
67015	40. 27.270	111. 59.320	5300.00	979708.37	980220.91	-14.020	-194.590	3.13	-191.460
67016	40. 27.580	111. 59.280	5477.00	979696.74	980221.37	-9.460	-196.060	1.64	-194.420
67017	40. 27.730	111. 59.030	5320.00	979705.43	980221.59	-15.760	-197.010	1.58	-195.430
67018	40. 27.920	111. 58.990	5107.00	979717.10	980221.87	-24.410	-198.400	1.96	-196.440
67019	40. 27.980	111. 58.630	5037.00	979719.31	980221.96	-28.870	-200.480	1.82	-198.660
67020	40. 28.130	111. 58.690	5050.00	979717.45	980222.19	-29.730	-201.780	1.51	-200.270
67021	40. 28.380	111. 58.640	4923.00	979723.21	980222.55	-36.290	-204.010	1.73	-202.280
67022	40. 28.350	111. 58.360	4858.00	979727.09	980222.52	-38.470	-203.980	1.67	-202.310
67023	40. 28.490	111. 58.010	4734.00	979731.91	980222.72	-45.530	-206.810	1.61	-205.200
67024	40. 28.710	111. 58.010	4691.00	979733.63	980223.05	-48.180	-208.000	1.50	-206.500
67025	40. 28.920	111. 58.010	4647.00	979735.28	980223.36	-50.980	-209.300	1.45	-207.850
67026	40. 29.130	111. 58.010	4614.00	979736.07	980223.67	-53.610	-210.800	1.39	-209.410
67027	40. 29.360	111. 58.000	4587.00	979736.91	980224.02	-55.660	-211.930	1.34	-210.590
67028	40. 29.360	111. 58.270	4621.00	979735.17	980224.02	-54.190	-211.620	1.34	-210.280
67030	40. 29.570	111. 58.550	4643.00	979733.64	980224.33	-53.970	-212.150	1.26	-210.890
67031	40. 29.800	111. 58.550	4617.00	979734.78	980224.66	-55.610	-212.910	1.22	-211.690
DD001	40. 19.020	111. 53.740	4591.00	979751.77	980208.66	-25.060	-181.430	1.47	-179.960
DD002	40. 18.510	111. 55.050	5135.00	979719.97	980207.91	-4.950	-179.850	2.78	-177.070
DD003	40. 16.960	111. 56.160	7641.00	979550.78	980205.61	63.880	-196.370	17.42	-178.950
DD004	40. 16.390	111. 55.450	7550.00	979556.99	980204.76	62.390	-194.770	18.41	-176.360
DD005	40. 16.000	111. 55.760	7598.00	979559.05	980204.18	69.540	-189.250	14.32	-174.930
DD006	40. 15.670	111. 55.750	7590.00	979560.27	980203.69	70.500	-188.010	14.62	-173.390
DD007	40. 15.090	111. 56.290	6735.00	979619.07	980202.82	49.740	-179.650	6.88	-172.770
DD008	40. 14.470	111. 56.310	6378.00	979641.33	980201.91	39.340	-177.900	4.89	-173.010
DD009	40. 13.600	111. 56.710	5936.00	979669.38	980200.62	27.100	-175.080	3.84	-171.240
DD010	40. 12.970	111. 57.740	5460.00	979700.92	980199.69	14.800	-171.170	1.68	-169.490
DD011	40. 12.270	111. 58.720	5122.00	979714.77	980198.66	-2.110	-176.560	.76	-175.800
DD012	40. 12.680	111. 59.770	4905.00	979726.52	980199.27	-11.390	-178.450	.73	-177.720
DD013	40. 12.200	111. 57.470	5397.00	979702.63	980198.55	11.720	-172.100	1.59	-170.510
DD014	40. 10.250	111. 56.050	4649.00	979742.18	980195.66	-16.200	-174.540	.73	-173.810
DD015	40. 26.770	111. 48.090	4909.00	979712.60	980220.15	-45.810	-213.010	3.02	-209.990
DD016	40. 29.130	111. 49.360	5855.00	979662.59	980223.66	-10.350	-209.770	3.61	-206.160
DD017	40. 29.590	111. 48.740	5780.00	979668.96	980224.35	-11.720	-208.590	7.49	-201.100
DD018	40. 18.920	111. 39.220	4828.00	979725.05	980208.51	-29.340	-193.780	6.74	-187.040
DD019	40. 19.650	111. 37.870	4950.00	979714.01	980209.60	-30.000	-198.590	11.90	-186.690
DD020	40. 18.550	111. 37.930	6233.00	979636.92	980207.97	15.230	-197.070	9.47	-187.600
DD021	40. 18.280	111. 37.100	6710.00	979605.79	980207.56	29.370	-199.170	9.86	-189.310
DD022	40. 17.510	111. 36.220	7530.00	979550.31	980206.42	52.160	-204.310	12.34	-191.970
DD023	40. 16.690	111. 35.820	7290.00	979565.84	980205.20	46.350	-201.950	10.16	-191.790
DD025	40. 15.600	111. 34.590	7420.00	979553.22	980203.58	47.570	-205.160	11.22	-193.940
DD026	40. 15.020	111. 34.660	7950.00	979522.17	980202.73	67.220	-203.550	10.72	-192.830
DD027	40. 14.540	111. 34.620	8340.00	979495.80	980202.01	78.250	-205.810	11.43	-194.380
DD028	40. 13.580	111. 33.960	8280.00	979488.05	980200.59	66.280	-215.740	14.56	-201.180
DD029	40. 12.740	111. 34.260	8540.00	979476.31	980199.35	80.230	-210.640	13.18	-197.460
DD030	40. 11.130	111. 33.980	7800.00	979515.50	980196.96	52.210	-213.460	15.43	-198.030
DD031	40. 11.500	111. 32.760	7118.00	979561.31	980197.52	33.310	-209.130	7.08	-202.050

STAT.	LATITUDE	LONGITUDE	ELEV.	OBSERVED GRAVITY	THEOR. GRAVITY	FREE AIR	SIMPLE BOUGUER	T.C.	COMPLETE BOUGUER
DD032	40. 11.740	111. 30.150	5500.00	979650.79	980197.87	-29.760	-217.090	7.61	-209.480
DD033	40. 7.870	111. 32.370	5200.00	979663.34	980192.12	-39.680	-216.790	15.54	-201.250
DD034	40. 8.210	111. 31.130	5612.00	979639.18	980192.64	-25.600	-216.740	12.34	-204.400
DD035	40. 8.050	111. 33.530	4848.00	979691.02	980192.40	-45.370	-210.500	6.30	-204.200
DD036	40. 1.840	111. 33.360	5295.00	979655.49	980183.20	-29.660	-210.000	9.81	-200.190
DD037	40. 2.570	111. 32.760	4897.00	979677.84	980184.27	-45.810	-212.600	10.12	-202.480
DD038	39. 58.920	111. 50.410	4628.00	979711.27	980178.88	-32.300	-189.930	1.35	-188.580
DD039	39. 52.740	111. 54.160	5048.00	979675.50	980169.73	-19.410	-191.350	1.61	-189.740
DD040	39. 53.430	111. 51.500	4923.00	979685.66	980170.75	-22.030	-189.710	2.54	-187.170
DD041	39. 53.690	111. 49.660	5021.00	979673.57	980171.14	-25.300	-196.310	3.69	-192.620
DD042	39. 54.380	111. 50.510	5078.00	979676.99	980172.16	-17.540	-190.490	2.62	-187.870
DD043	39. 55.560	111. 49.940	5220.00	979672.48	980173.91	-10.430	-188.220	2.12	-186.100
DD044	39. 56.640	111. 49.780	5180.00	979674.99	980175.49	-13.270	-189.700	1.71	-187.990
DD045	39. 56.640	111. 48.310	5111.00	979678.30	980175.49	-16.450	-190.540	2.86	-187.680
DD046	39. 56.230	111. 46.960	5680.00	979641.67	980174.90	1.030	-192.430	4.29	-188.140
DD047	39. 54.900	111. 44.790	6280.00	979586.38	980172.93	4.150	-209.750	21.00	-188.750
DD048	39. 54.120	111. 43.620	7035.00	979551.91	980171.77	41.860	-197.750	9.92	-187.830
DD049	39. 55.040	111. 43.080	7768.00	979510.09	980173.14	67.600	-196.970	5.88	-191.090
DD050	39. 54.550	111. 42.040	8330.00	979473.00	980172.41	84.110	-199.610	6.30	-193.310
DD051	39. 54.060	111. 40.840	8450.00	979464.95	980171.68	88.080	-199.730	5.80	-193.930
DD052	39. 53.890	111. 39.350	8444.00	979463.04	980171.43	85.850	-201.750	6.12	-195.630
DD053	39. 55.500	111. 37.940	8042.00	979486.93	980173.83	69.530	-204.380	4.98	-199.400
DD054	39. 54.680	111. 38.340	8355.00	979466.91	980172.59	80.180	-204.390	6.41	-197.980
DD055	39. 58.110	111. 45.990	5178.00	979672.10	980177.69	-18.540	-194.910	5.01	-189.90
DD056	40. 10.590	111. 48.040	4499.00	979734.52	980196.16	-38.460	-191.700	.50	-191.200
DD057	40. 8.310	111. 49.520	4511.00	979735.22	980192.78	-33.260	-186.900	.83	-186.070
DD059	40. 5.350	111. 49.380	6813.00	979575.67	980188.40	28.100	-203.950	18.70	-185.250
DD060	40. 7.480	111. 48.850	5132.00	979695.73	980191.55	-13.110	-187.910	2.68	-185.230
W0772	39. 52.920	111. 52.670	4871.00	979688.35	980169.98	-23.48	-189.430	1.75	-187.680
W0773	39. 53.540	111. 53.380	4840.00	979692.31	980170.91	-23.350	-188.240	1.79	-186.450
W0890	40. 26.330	111. 37.290	7687.00	979557.51	980219.51	61.040	-200.850	5.22	-195.630
W0891	40. 25.870	111. 36.780	8060.00	979531.98	980218.84	71.260	-203.340	5.45	-197.890
W0892	40. 25.670	111. 36.590	7911.00	979540.98	980218.54	66.550	-202.970	5.46	-197.510
W0893	40. 25.450	111. 36.280	7799.00	979548.00	980218.21	63.370	-202.340	5.56	-196.780
W0894	40. 25.170	111. 36.000	7454.00	979569.98	980217.79	53.310	-200.640	6.89	-193.750
W0896	40. 24.240	111. 36.170	6850.00	979601.42	980216.41	29.320	-204.050	14.03	-190.020
W0897	40. 23.940	111. 35.440	6608.00	979618.23	980215.97	23.810	-201.320	7.83	-193.490
W0898	40. 27.010	111. 35.670	7042.00	979593.35	980220.52	35.210	-204.710	6.47	-198.240
W0899	40. 27.180	111. 34.690	7364.00	979573.53	980220.77	45.430	-205.460	4.49	-200.970
W0900	40. 26.490	111. 33.580	6210.00	979639.45	980219.74	3.820	-207.750	5.00	-202.750
W0901	40. 27.600	111. 32.950	6264.24	979635.03	980221.39	1.970	-211.430	6.00	-205.430
W0902	40. 28.860	111. 31.820	7119.00	979582.24	980223.26	28.600	-213.940	6.07	-207.870
W0903	40. 29.400	111. 31.590	7501.00	979555.81	980224.05	37.290	-218.260	8.91	-209.350
W0774	39. 54.880	111. 54.500	4678.00	979700.67	980172.90	-32.230	-191.610	2.48	-189.130
W0782	39. 54.340	111. 50.000	4947.00	979683.27	980172.10	-23.530	-192.070	3.12	-188.950
W0783	39. 53.420	111. 50.040	4952.00	979673.78	980170.73	-31.180	-199.890	3.40	-196.490
W0837	39. 54.710	112. 4.630	6654.00	979583.10	980172.64	36.340	-190.360	2.03	-188.330
W0918	40. 22.820	111. 34.160	5713.00	979663.45	980214.30	-13.500	-208.140	11.86	-196.280
W0919	40. 23.480	111. 34.580	6087.00	979645.59	980215.28	2.850	-204.530	9.03	-195.500

STAT.	LATITUDE	LONGITUDE	ELEV.	OBSERVED GRAVITY	THEOR. GRAVITY	FREE AIR	SIMPLE BOUGUER	T.C.	COMPLETE BOUGUER
W0746	39. 52.660	112. .570	4998.00	979669.82	980169.61	-29.680	-199.960	2.56	-197.400
W0747	39. 53.640	111. 59.500	4801.00	979682.67	980171.07	-36.820	-200.390	1.53	-198.860
W0749	39. 52.940	111. 58.100	4777.00	979685.56	980170.03	-35.150	-197.900	1.58	-196.320
W0905	40. 23.430	111. 32.550	5303.00	979690.02	980215.21	-26.390	-207.060	9.59	-197.470
W0907	40. 24.680	111. 30.610	5537.00	979674.93	980217.06	-21.330	-209.970	4.49	-205.480
W0909	40. 25.470	111. 32.890	5664.00	979670.06	980218.24	-15.430	-208.400	7.46	-200.940
W0910	40. 26.380	111. 33.290	5959.00	979652.02	980219.60	-7.090	-210.110	6.06	-204.050
W0111	40. 24.090	111. 31.960	5332.00	979688.17	980216.19	-26.490	-208.150	8.21	-199.940
W0912	40. 22.580	111. 33.290	5234.00	979690.71	980213.95	-30.940	-209.260	14.32	-194.940
W0838	39. 54.130	112. 5.770	6372.00	979599.31	980171.78	26.880	-190.210	1.80	-188.410
W0839	39. 52.880	112. 6.800	6079.00	979613.52	980169.93	15.390	-191.720	1.25	-190.470
W0833	39. 57.560	112. 6.110	6583.00	979595.84	980176.87	38.166	-186.110	1.89	-184.220
W0694	40. .920	112. 5.340	5675.00	979664.13	980181.84	16.082	-177.260	2.18	-175.080
W0695	40. 2.150	112. 6.240	5662.00	979667.16	980183.66	16.069	-176.830	2.33	-174.500
W0690	40. 2.550	112. 4.880	5292.00	979687.69	980184.24	1.213	-179.080	1.25	-177.830
W0696	40. 3.280	112. 5.560	5176.00	979693.05	980185.34	-5.429	-181.770	1.23	-180.540
W0697	40. 4.520	112. 5.860	5036.00	979705.17	980187.17	-8.319	-179.890	.89	-179.000
W0698	40. 5.340	112. 6.470	5016.00	979714.76	980188.38	-1.820	-172.710	.75	-171.960
W0679	40. 6.100	112. 5.690	4940.00	979720.01	980189.50	-4.829	-173.130	.48	-172.650
W0680	40. 6.340	112. 4.620	4929.00	979719.02	980189.87	-7.224	-175.150	.39	-174.760
W0681	40. 6.700	112. 3.270	4944.00	979721.54	980190.41	-3.833	-172.270	.36	-171.910
W0678	40. 6.37	112. 6.520	4981.00	979722.09	980189.90	.708	-168.990	.48	-168.510

APPENDIX B

FIELD AND DATA REDUCTION TECHNIQUES

Standard looping field techniques were employed in all surveys; namely, loops were closed at least twice a day in order to check for instrument tares and determine instrument and tidal drift. In the reduction of the data, all surveys utilized the International Gravity Formula of 1930 (Swick, 1942) to obtain theoretical gravity values at mean sea level. Also, all surveys utilized a mean rock density of 2.67 gm/cc for the Bouguer and terrain corrections. The free-air correction used for the surveys varied slightly -- though not significantly -- from survey to survey, as will be noted below.

The gravity survey by Cook and Berg (1961), which was a reconnaissance survey, included the entire area of this report, and consisted of 357 stations in the present study area. The survey utilized a Frost gravimeter. Essentially all the gravity stations were taken at bench marks or spot elevations on U. S. Geological Survey topographic quadrangle maps. Although the Liberty Park (in Salt Lake City) gravity base station was used originally for the reference of absolute gravity, this base station was later tied to the University of Utah base station and the values of all gravity stations for this survey were recomputed by L. F. Serpa (K. L. Cook, oral commun., 1982) using the published absolute gravity value of 979,786.13 mgal (Cook and others, 1971) for the University of Utah base station. All data were drift-corrected for instrument drift. The simple Bouguer gravity anomaly values were originally obtained by using a combined elevation correction (free-air and Bouguer effects) of 0.06000 mgal/ft (0.19685 mgal/m). Terrain corrections for these gravity data were made by L. F. Serpa in 1980 (K. L. Cook, oral commun., 1982), using U. S. Geological Survey digitized topography provided by R. H. Godson of the U. S. Geological Survey and a computer program provided also by R. H. Godson and modified for use on the University of Utah UNIVAC 1108 digital computer by Serpa (1980).

The Applied Geophysics Inc. gravity survey consisted of 173 stations in the Crystal Hot Springs area and utilized a LaCoste and Romberg Model G gravimeter. Elevations were surveyed to the nearest 0.1 ft (0.03 m) and gravity values were determined to the nearest 0.01 mgal.

The gravity survey by Meiiji Resource Consultants consisted of 511 stations and used a LaCoste and Romberg Model G gravimeter. This survey was made principally in the Goshen Valley area and the southern part of Utah Valley. One profile was taken in the Saratoga Hot Springs area. The Eureka, Utah gravity base station, which was used as the main base station for the survey, has a published absolute gravity value of 979,606.34 mgal (Cook and others, 1971). The survey included 5 other minor base stations which were tied to this main base station. Tidal corrections were computed and applied to the original gravity data. Elevations were surveyed to the nearest 1 ft (0.3 m) and bench marks were used as reference points when possible. The listed free-air anomaly was computed using 0.09406 mgal/ft (0.30860 mgal/m), and the value used for the combined free-air and Bouguer correction was 0.059991 mgal/ft (0.19682 mgal/m).

The Davis gravity survey consisted of 58 stations which were taken generally along roads in mountainous areas selected judiciously to facilitate the contouring of the Complete Bouguer gravity anomaly map (Plate 1). The survey utilized LaCoste and Romberg gravimeter model G No. 461 with a sensitivity of 1.06354 mgal/dial division. Readings were obtained with an accuracy of 0.001 mgal. Horizontal control was established by using U. S. Geological Survey 7 1/2 minute topographic quadrangle maps with a scale of 1:24,000. The latitude and longitude of each station were determined within 0.01 minute of arc giving a location accuracy of approximately 15 m (49.2 ft). Vertical control was obtained from bench marks, spot elevations, two Wallace and Tiernan altimeters, and by interpolation between topographic contours. Altimeters were read to the nearest foot; however, because of the large changes in elevation from station to station, it was found that elevations determined from the altimeters were generally not sufficiently reliable. Consequently, topographic maps were used for elevation determinations when bench marks or spot elevations were not available. About 33 percent of the station elevations were controlled by bench marks and spot elevations. The accuracy for elevations of the stations are as follows: 1) bench marks -- 1 ft (0.3 m); 2) spot elevations -- 4 ft (1.2 m); and 3) interpolation between contours on topographic maps -- 0-10 ft (0-3 m) (Pe, 1980).

The University of Utah gravity base station, which was used as the main base for the Davis survey, has a published absolute gravity value of 979,786.13 mgal (Cook and others, 1971). All Davis stations were tied directly to this base station.

The original instrument readings for the Davis stations were corrected for drift, which included instrument drift and the effects of the earth tides. Separate tidal corrections were not made. The data were reduced to simple Bouguer gravity anomaly values by using the University of Utah UNIVAC 1108 digital computer. For the reduction of the gravity data, the total elevation correction factor was taken as 0.05999 mgal/ft (0.19682 mgal/m), which includes a free-air correction of 0.09406 mgal/ft (0.30860 mgal/m) and a Bouguer correction of 0.03407 mgal/ft (0.11178 mgal/m). Terrain corrections were carried out to a radial distance of 166.7 km (100 mi) from each station by using a computer program provided by R. H. Godson of the U.S. Geological Survey and modified for use on the University of Utah UNIVAC 1108 digital computer by Serpa (1980). The computer program uses digitized topography data, which was also provided by R. H. Godson of the U. S. Geological Survey. It should be emphasized that terrain corrections were <u>not</u> done by hand for the inner zones (out to a radial distance of 0.895 km from each station) of the Hammer (1939) zone chart because the error associated with doing it by hand would be about 0.05 mgal (Gabbert, 1980) as compared to the computer-computed inner-zone corrections; and the time associated with performing this task would be unreasonable.

APPENDIX C

DISCUSSION OF ERRORS

Errors associated with the compilation and reduction of gravity data are as follows: 1) instrument error; 2) instrument drift and tidal variation; 3) elevation determination; 4) horizontal control; 5) assumed mean rock density; and 6) errors inherent in using the terrain correction program. Instrument error involves instrument tare, which was checked in all surveys by looping techniques. It was found that in all surveys no gravimeter sustained instrument tare. Errors due to instrument drift and tidal variation for the survey are hard to quantify as four different data sources were involved. However, in most gravity reduction programs, the correction for instrument and tidal drift is assumed to be linear[1]. Gabbert (1980) estimates a maximum error of 0.15 mgal for instrument and tidal drift during new and full moon phases. The maximum error associated with elevation determination would be one obtained from interpolation between contours on a 7 1/2 minute topographic quadrangle which utilizes a contour interval of 40 ft (12 m). Elevations obtained in this way are estimated to be accurate within 10 percent of the contour interval; thus an error of 4 ft (1.3 m) or 0.24 mgal could result. Errors

---

[1]It should be noted that tidal corrections were made for the Meiiji Resource Consultants survey only.

associated with horizontal control would involve odometer readings which may have an accuracy of 0.05 mi (260 ft or 80 m). This would correspond to an error of about 0.06 mgal.

The error involved in assuming a mean rock density of 2.67 gm/cc for all data reductions is difficult to estimate quantitatively, but is assumed to be negligible. The accuracy of the terrain corrections for stations which lie in valley areas is believed to be within 0.05 mgal (Gabbert, 1980). This would constitute about 85 percent of the stations involved in this study. For stations in rugged relief, the maximum error in terrain corrections is postulated to be as large as 0.2 mgal (Gabbert, 1980).

In summary, then the estimated maximum error if all the above sources of error were to accumulate would be about 0.65 mgal to 1.0 mgal. However, it should be noted that the accumulation of these errors at one station is unlikely.

APPENDIX D

DENSITY MEASUREMENTS

Density was determined by first weighing the dry rock sample in air using a Welch Scientific Company balance and recording this measurement. The sample was then immersed in water and weighed again. The weight of the sample in air over the difference between the weight of the sample in air and the weight in water yielded the density of the rock. Table 4 gives the results of the density measurements of the rocks in the study area.

Table 4. -- Density measurements of rocks in study area.[1]

Sample No.	Type	Latitude (North) Degrees	Latitude (North) Minutes	Longitude (West) Degrees	Longitude (West) Minutes	Density (gm/cc)
1	Quartzite	40	17.12	111	56.39	2.70
2	Sandstone	40	16.31	111	56.26	2.31
3	Limestone	40	14.82	111	56.46	2.65
4	Limestone	40	13.30	111	56.87	2.67
5	Limestone	40	16.52	111	35.90	2.64
6	Limestone	40	14.53	111	34.49	2.53
7	Limestone	40	11.52	111	34.12	2.59
8	Sandstone	40	05.35	111	49.27	2.53
9	Limestone	40	07.48	111	48.85	2.64
10	Limestone	40	05.98	111	49.40	2.60
11	Limestone	30	56.27	111	49.86	2.58
12	Packard Quartz Latite[2]	39	57.49	112	02.12	2.47
13	Do[2]	Do		Do		2.47
14	Do[2]	Do		Do		2.49
15	Do[2]	Do		Do		2.47

[1]Except for the Packard Quartz Latite (Tertiary in age), all rock samples are Paleozoic or older.

[2]All Packard Quartz Latite samples were taken within a few meters of each other.

APPENDIX E

WELL LOGS

Table 5. -- Log of well 1. Location: sec. 25, T. 4 S., R. 1 E. (D-4-1--25ddd)

Depth (ft)	Lithology
0-5	Soil
6-22	Gravel, cobbles, and boulders
22-58	Clay, sand, and gravel
58-181	Gravel and cobbles
181-244	Sandy clay
244-265	Cemented gravel
265-355	Clay and gravel
355-385	Cemented gravel
385-398	Conglomerate
398-624	Alternating layers of clay ano gravel
624-664	Clay, with traces of gravel
664-715	Clay and gravel
715-1077	Limestone layers with clay zones

Table 6. -- Log of well 2. Location: sec. 14, T. 5 S., R. 1 E. (D-5-1--14bdc)

Depth (ft)	Lithology
0-3	Soil
3-12	Clay and gravel
12-29	Sandy clay
29-182	Clay and gravel
182-190	Blue clay
190-230	Clay and gravel
230-232	Brown clay
232-241	Clay and gravel
241-254	Clay
254-265	Clay and gravel
265-271	Clay
271-409	Clay and gravel, with trace of sand
409-423	Blue clay and gravel
423-461	Brown clay and gravel, with trace of sand
461-467	Conglomerate
467-724	Brown clay and gravel
724-736	Blue clay
736-910	Clay and gravel

Table 7. -- Log of well 3. Location: sec. 8, T. 6 S., R. 2 E. (D-6-2--8acb-1)

Depth (ft)	Lithology
0-40	Clay and gravel fill
40-80	Sandy blue clay
80-116	Blue clay
116-226	Sand and gravel
226-298	Blue clay
298-475	Sand and gravel, with traces of clay
475-492	Clay with traces of gravel
492-682	Alternating layers of sand, gravel, and blue clay
682-758	Tight gravel and sand
758-784	Brown clay
784-904	Sand and gravel
904-936	Brown sandy clay
936-964	Blue clay
964-1018	Sand and gravel, with traces of clay
1018-1028	Blue clay
1028-1054	Sand and gravel, with clay streaks
1054-1085	Blue clay
1085-1160	Tight gravel, with traces of clay
1160-1172	Brown clay
1172-1192	Sand and gravel

Table 8. -- Log of well 4. Location: sec. 8, T. 6 S., R. 2 E. (D-6-2--8bca-6)

Depth (ft)	Lithology
0-3	Soil
3-9	Clay
9-112	Alternating layers of sand and clay
112-430	Alternating layers of clay, gravel, and sand
430-436	Brown clay
436-452	Coarse gravel
452-532	Alternating layers of blue clay, sand, and gravel
532-556	Green clay
556-564	Gravel
564-570	Sand and gravel
570-576	Sandy clay
576-590	Gravel and silt
590-603	Clay
603-644	Alternating layers of gravel, sand, and clay
644-676	Blue and white clay, with some gravel
676-732	Gravel and sand, with traces of clay
732-744	Clay
744-806	Gravel, with traces of clay and sand
806-856	Blue clay
856-952	Alternating layers of clay and sand
952-1066	Alternating layers of sand, gravel, and clay

Table 9. -- Log of well 5. Location: sec. 8, T. 6 S., R. 2 E. (D-6-2--8cac-5)

Depth (ft)	Lithology
0-18	Alternating layers of clay and gravel
18-60	Blue clay and silt
60-296	Alternating layers of sand, clay, and gravel
296-346	Sand grading to gravel
346-380	Alternating layers of gravel, sand, and clay
380-426	Silt, sand, and gravel
426-524	Clay, with layers of sand and gravel
524-531	Silt, sand, and gravel
531-576	Clay, with traces of gravel
576-596	Silt, sand, and gravel
596-638	Blue clay, with traces of gravel
638-658	Silt, with sand and gravel
658-710	Clay, with traces of gravel
710-805	Alternating layers of clay, silt, sand, and gravel
805-880	Clay, with traces of gravel
880-906	Tight gravel
906-952	Clay
952-958	Silt, with sand and gravel
958-1054	Alternating layers of sand, gravel, and clay

Table 9. -- (cont.)

Depth ft	Lithology
1054-1060	Silt, with sand and gravel
1060-1082	Clay, with a layer of sand
1082-1093	Silt, with sand and gravel
1093-1190	Alternating layers of clay, gravel, and sand

Table 10. -- Log of well 6. Location: sec. 8, T. 6 S., R. 2 E. (D-6-2--8cda-1)

Depth (ft)	Lithology
0-4	Soil
4-8	Clay
8-15	Sand
15-39	Sand and gravel
39-110	Blue clay and silt
110-228	Sand and gravel
228-264	Blue clay
264-286	Fine sand
286-300	Blue clay
300-504	Sand and gravel
504-542	Blue clay
542-582	Sand and gravel, with some clay
582-610	Gray clay
610-624	Gravel
624-665	Blue clay, with some gravel
665-700	Sand and gravel
700-704	Blue clay
704-736	Alternating layers of brown clay, sand, and gravel
736-942	Alternating layers of blue clay, sand, and gravel

Table 10. -- (cont.)

Depth (ft)	Lithology
942-954	Clay, with gravel streaks
954-1090	Alternating layers of gravel, sand, and blue clay

Table 11. -- Log of well 7. Location: sec. 19, T. 8 S., R. 3 E. (D-8-3--19bbb)

Depth (ft)	Lithology
0-15	Sand, gravel, and boulders
15-157	Gray clay and blue clay
157-220	Clay, with traces of sand
220-225	Gravel and water
225-281	Clay and gravel
281-331	Clay
331-359	Conglomerate
359-630	Alternating layers of sand and gravel
630-720	Alternating layers of sand, gravel, and clay
720-771	Clay
771-811	Sand and gravel
811-820	Brown clay
820-911	Sand and gravel, with traces of clay
911-920	Gravel
920-955	Clay, with traces of gravel and sand
955-1000	Brown and blue clay

Table 12. -- Log of well 8. Location: sec. 32, T. 8 S., R. 2 E. (D-8-2--32dda)

Depth (ft)	Lithology
0-73	Clay and sand, with trace of gravel
73-83	Gravel and water
83-92	Brown clay, with trace of gravel
92-160	Clay and conglomerate
160-183	Clay and gravel
183-261	Clay, sand, and gravel
261-266	Clay
266-273	Clay and sand
273-448	Clay and gravel
448-450	Sand and gravel
450-474	Alternating layers of clay and sand
474-830	Clay, with trace of sand

Table 13. -- Log of well 9. Location: sec. 23, T. 9 S., R. 2 E. (D-9-2--23abb)

Depth (ft)	Lithology
0-2	Soil
2-38	Clay and sand
38-50	Gravel, cobbles, and boulders
50-74	Clay
74-81	Gravel and cobbles
81-142	Clay and gravel
142-212	Sand, gravel, cobbles, and boulders
212-330	Clay, gravel, and boulders
330-345	Clay
345-518	Clay, gravel, and boulders
518-552	Sandstone, with clay streaks
552-611	Hard-packed gravel and boulders
611-782	Clay, with gravel and cobbles
782-797	Hard-packed gravel and boulders
797-812	?
812-972	Alternating layers of clay, gravel, and boulders
972-982	Clay

Table 14. -- Log of well 10. Location: sec. 5, T. 9 S., R. 1 W. (C-9-1--5ddb)

Depth (ft)	Lithology
0-1	Soil
1-37	Clay and gravel
37-71	Sand and gravel
71-83	Clay and gravel
83-170	Clay, sand, and gravel
170-289	Clay, sand, gravel, and silt
289-307	Sand and gravel
307-394	Clay, sand, and gravel
394-520	Clay and sand
520-544	Clay and gravel
544-547	Sand and gravel
547-662	Alternating layers of clay, sand, and gravel
662-668	Sand and gravel
668-744	Alternating layers of clay, sand, and gravel
744-772	Clay, silt, and gravel
772-823	Clay

Table 15. -- Log of well 11 . Location: sec. 4, T. 9 S., R. 1 W. (C-9-1--4ccc)

Depth (ft)	Lithology
0-14	Soil and clay
14-108	Clay, sand, and gravel
108-186	Sand and gravel
186-330	Clay and sand
330-407	Sand and gravel
407-563	Clay and hardpan
563-597	Clay, sand, and gravel
597-698	Sand and gravel
698-776	Alternating layers of clay, sand, and gravel
776-800	Clay

Table 16. -- Log of well 12. Location: sec. 28, T. 10 S., R. 1 W. (C-10-1--28dad)

Depth (ft)	Lithology
0-68	Clay, silt, and sand
68-112	Blue clay
112-168	Sand and clay
168-186	Red and tan clay
186-218	Sand, with some clay
218-221	Coarse sand
221-230	Clay and gravel
230-283	Gravel, with some sand and clay
283-344	Coarse sand, with some clay
344-377	Alternating layers of hard lava and brown clay
377-398	Conglomerate
398-416	Clay
416-417	Hard lava
417-709	Alternating layers of brown clay and sand
709-785	Alternating layers of hard lava and clay
785-805	Brown clay and sand

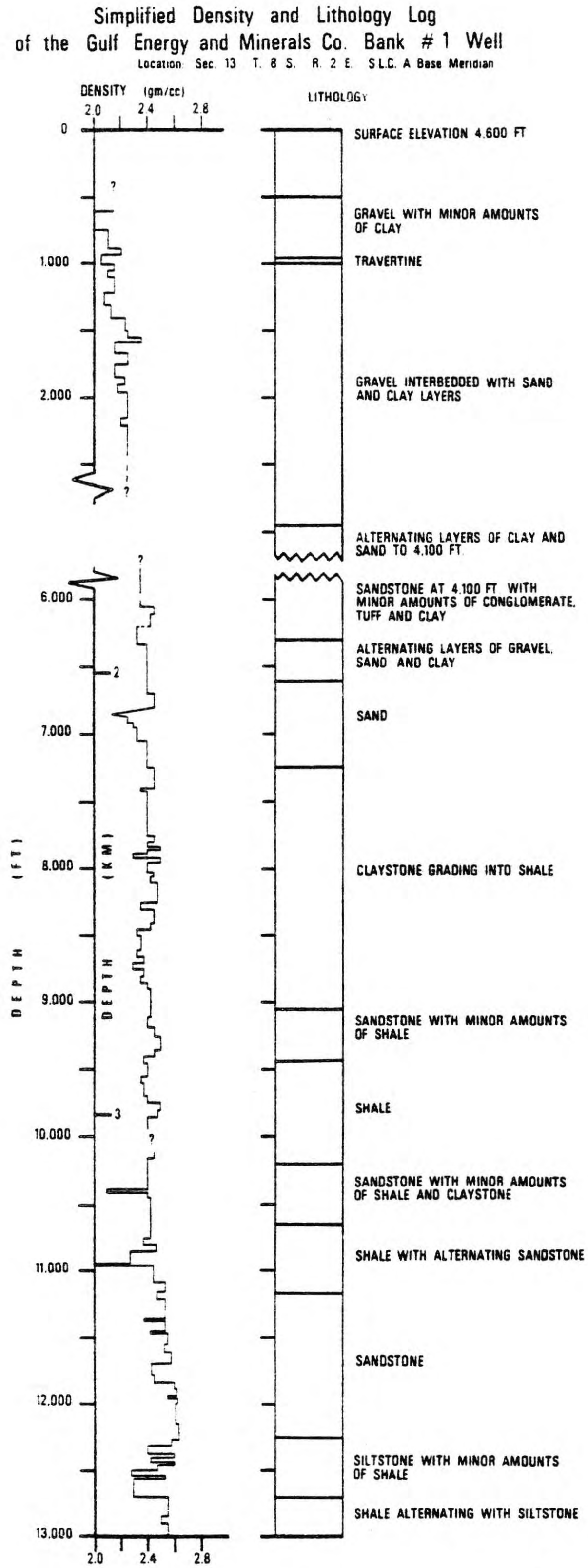

Figure 11. Simplified density and lithology log of Gulf Energy and Minerals Company #1 Bank well. Well drilled during July 1977. (Data furnished by Gulf Energy and Minerals Company.

REFERENCES

Anderson, P. N., and Axtell, L. H., 1972, Geothermal resources in California: geothermal overviews of the western United States: published by Geothermal Resources Council, Davis, California.

Armstrong, R. L., 1968, Sevier orogenic belt in Nevada and Utah: Geol. Soc. America Bull., v. 79, p. 429-458.

Baker, A. A., 1947, Stratigraphy of the Wasatch Mountains, in the vicinity of Provo, Utah: U. S. Geol. Survey Oil and Gas Investigations Preliminary Chart 30.

Baker, A. A., 1959, Faults in the Wasatch Range near Provo, Utah, in Guidebook to the geology of the Wasatch and Uinta Mountains transition area: Intermountain Assoc. Petroleum Geologists, 10th Ann. Field Conf., Guidebook, p. 153-158.

Biehler, S., and Coombs, J., 1972, Correlations of gravity and geothermal anomalies in the Imperial Valley, Southern California (abs.): Geol. Soc. America Abstracts with Programs, v. 4, no. 3, p. 128.

Bissell, H. J., 1963, Lake Bonneville: Geology of southern Utah Valley Utah: U. S. Geol. Survey Prof. Paper 257-B, p. 101-130.

Bullock, K. C., 1951, Geology of Lake Mountain, Utah: Utah Geol. and Mineralog. Survey Bull. 41, 46 p.

Bullock, R. L., 1958, The geology of Lehi quadrangle: unpublished M. S. Thesis, Brigham Young University.

Cady, J. W., 1977, Calculation of gravity and magnetic anomalies along profiles with end corrections and inverse solutions for density and magnetization: U. S. Geol. Survey Open-file Report no. 77-463.

Cady, J. W., 1980, Calculation of gravity and magnetic anomalies of finite-length right polygonal prisms: Geophysics, v. 45, p. 1507-1512.

Cook, K. L., and Berg, J. W., Jr., 1961, Regional gravity survey along the central and southern Wasatch Front, Utah: U. S. Geol. Survey Prof. Paper 316-E, p. 75-89.

Cook, K. L., and Berg, J. W., Jr., 1972, Principal facts for gravity stations along the central and southern Wasatch front, Utah: U. S. Geolog. Survey Rept. USGS-72-018, 32 p.; available only from U. S. Dept. Commerce Natl. Tech. Inf. Service, Springfield, Va. 22151, as Rept. PB-206-675.

Cook, K. L., and Montgomery, J. R., 1972, East-west transverse trends in eastern Basin and Range province as indicated by gravity data (abstract): in Symposium, Gravity fields and earth structure, Abstracts with Programs, North-Central Section 6th annual meeting, Geol. Soc. America, Dekalb, Illinois, May 11-12, 1972, v. 4, no. 5, March 1972, Boulder, Colo., p. 315.

Cook, K. L., Nilsen, T. H., and Lambert, J. F., 1971, Gravity base station network in Utah -- 1967: Utah Geol. and Mineralog. Survey Bull. 92, 57 p.

Coombs, J. and Muffler, L. J. P., 1973, Exploration for geothermal resources: in Kruger, P., and Otte, C. eds., Geothermal Energy, Resources, Production, Stimulation: Stanford University Press, Stanford, Calif., 1972, p. 107.

Crittenden, M. D., Jr., Stuckless, J. S., Kistler, R. W., and Stern, T. W., 1973, Radiometric dating of intrusive rocks in the Cottowood area, Utah: Jour. Research, U. S. Geol. Survey, v. 1, no. 2, p. 173-178.

Currey, D. R., 1980, Events associated with the last cycle of Lake Bonneville-Idaho, Nevada, Utah, in Abstracts and Programs 6th Biennial Meeting American Quat. Assoc., p. 59-60.

Davis, F. D., 1983, Geologic map of the southern Wasatch Front, Utah: Utah Geol. and Mineral Survey Map 55-A.

Eardley, A. J., 1933, Structure and physiography of the Southern Wasatch Mountains, Utah: Michigan Acad. Sci. Papers, v. 19, p. 377-400.

Eardley, A. J., 1939, Stucture of the Wasatch-Great Basin region: Geol. Soc. of America Bull., v. 50, p. 1277-1310.

Eaton, G. P., 1979, Regional geophysics, Cenozoic tectonics, and geologic resources of the Basin and Range province and adjoining regions, in Newman G. W. and Goode H. D., eds., Basin and Range Symposium and Great Basin Field Conference: Rocky Mtn. Assoc. of Geologists, Denver, and Utah Geol. Assoc., Salt Lake City, p. 11-39.

Eaton, H. J., 1929, Structural features of Long Ridge and West Mountain, Central Utah: Am. Jour. Sci., v. 18, p. 71-79.

Fenneman, N. M., 1928, Physiographic divisions of the United States: Annals of the Assoc. of Am. Geographers, v. 18, no. 4, 3rd ed., p. 263-353.

Fenneman, N. M., 1946, Physical divisions of the United States: U. S. Geol. Survey Map, Washington, D. C.

Gabbert, S. C., 1980, Gravity survey of parts of Millard, Beaver, and Iron Counties, Utah: unpublished M. S. Thesis, University of Utah, 107 p.

Gilbert, G. K., 1928, Studies of Basin-Range structure: U. S. Geol. Survey Prof. Paper 153, 89 p.

Goode, H. D., 1978, Thermal waters of Utah topical report: D. O. E. report no. et/28393-7, Utah Geol. and Mineral Survey, p. 58-64.

Grose, L. T., 1971, Geothermal energy, geology, exploration, and developments: Colorado School of Mines and Mineral Industries Bull., pt, 1, v. 14, no. 6, p. 1-14.

Hammer, Sigmund, 1939, Terrain corrections for gravimeter stations: Geophysics, v. 4, p. 184-194.

Hilpert, L. S., and Roberts, R. J., 1964, Economic geology, in Mineral and water resources of Utah: Utah Geol. and Minerlog. Survey Bull. 73, p. 28-37.

Hintze, L. F., 1973, Geologic history of Utah: Brigham Young University Geol. Studies, v. 20, pt. 3, 181 p.

Hochstein, M. P. and Hunt, T. M., 1970, Seismic, gravity and magnetic studies, Broadlands geothermal field, New Zealand: Geothermics, special issue 2, v. 2, pt. 1, p. 333-346.

Hunt, C. B., Varnes, H. D., and Thomas, H. E., 1953, Lake Bonneville: Geology of northern Utah Valley, Utah: U. S. Geol. Survey Prof. Paper 257-A, 99 p.

Isherwood. W. F., 1975, Gravity and magnetic studies of the Geyser-Clear Lake geothermal region, California: U. S. Geol. Survey Open-file Report 75-368.

Kastrinsky, A. J., 1977, Seismicity of the Wasatch front, Utah: Detailed epicentral patterns and anomalous activity: unpublished M. S. Thesis, University of Utah, 139 p.

Lovering, T. S., and Goode, H. D., 1963, Measuring geothermal gradients in drill holes less than 60 feet deep, East Tintic District, Utah: U. S. Geol. Survey Bull. 1172, 48 p.

Lovering, T. S., and Morris, H. T., 1965, Underground temperatures and heat flow in the East Tintic district, Utah: U. S. Geol. Survey Prof. Paper 504-F, 28 p.

Mabey, D. R., Crittenden, M. D., Jr., Morris, H. T., Roberts, R. J., and Tooker, E. W., 1964, Aeromagnetic and generalized geologic map of part of North-Central Utah: U. S. Geol. Survey Geophysical Investigations map GP-422.

Mabey, D. R., Zietz, I., Eaton, G. P., and Kleinkopf, M. D., 1978, Regional magnetic patterns in part of the Cordillera, in the western United States: Geol. Soc. America Mem. 152, p. 93-106.

Madsen, R. A., 1952, Geology of the Beverly Hills area, Utah: unpublished M. S. Thesis, Brigham Young University.

Marsell, R. E., 1932, Geology of the Jordan Narrows region, Traverse Mountains, Utah: unpublished M. S. Thesis, University of Utah.

McKee, M. E., 1982, Microearthquake studies across the Basin and Range-Colorado Plateau transition zone in Central Utah: unpublished M. S. Thesis, University of Utah, 117 p.

McNitt, J. T., 1965, Review of geothermal resources: in W. H. K. Lee, ed., Terrestial heat flow, Amer. Geophys. Union Mon., sec. 8, p. 240-266.

Metter, R. E., 1955, Geology of the northern part of the Southern Wasatch Mountains, Utah: unpublished Ohio State University Ph. D. Thesis.

Milligan, J. H., Marsell, R. E., and Bagley, J. M., 1966, Mineralized springs in Utah -- their effect on manageable water supplies: Utah Water Research Laboratory, Utah State University, and Utah Water and Power Board cooperating, Logan, Utah, Report WG 23-6, 50 p.

Moore, W. J., 1973, Igneous rocks in the Bingham mining district, Utah: U. S. Geol. Survey Prof. Paper 679-B, 42 p.

Montgomery, J. R., 1973, A regional gravity survey of western Utah: unpublished Ph. D. Thesis, University of Utah, 143 p.

Morris, H. T., and Lovering, T. S., 1961, Stratigraphy of the East Tintic Mountains, Utah: U. S. Geol. Survey Prof. Paper 361, 145 p.

Morris, H. T., and Lovering, T. S., 1979, General geology and mines of the East Tintic mining district, Utah and Juab Counties, Utah: U. S. Geol. Survey Prof. Paper 1024, 203 p.

Morris, H. T., and Mogensen, A. P., 1978, Tintic mining district, Utah: Brigham Young University Geol. Studies, v. 25, pt. 1, p. 33-46.

Morris, H. T., and Shepard, W. M., 1964, Evidence for a concealed tear fault of large displacement in the central East Tintic Mountains, Utah: Geological Survey Research 1964; U. S. Geol. Survey Prof. Paper 501-C, p. C19-C21.

Mundorff, J. C., 1970, Major thermal springs of Utah: Utah Geol. and Mineralog. Water-Resouces Bull. 13, 60 p.

Murphy, P. J., and Gwynn, J. W., 1979, Geothermal investigations at Crystal Hot Springs Salt Lake County, Utah: in Utah Geol. and Mineral Survey Report of Investigation, no. 139, 86 p.

Parry, W. T., and Cleary, M., 1978, Na-K-Ca and SiO_2 temperature estimates for Utah spring and well waters: U. S. Geol. Survey, Geothermal Research Program, v. 78-1. 51 p.

Pe, W., 1980, Gravity survey of the Escalante Desert and vicinity, in Iron and Washington counties, Utah: unpublished M. S. Thesis, University of Utah, 151 p.

Peters, S., 1974, Civil engineering features of a geothermal power plant, presented at A. S. C. E. National Meeting on Water Resources Engineering at Los Angeles, California.

Rawson, R. R., 1957, Geology of the southern part of the Spanish Fork quadrangle, Utah: Brigham Young University Research Studies, Geol. Ser., v. 4, no. 2.

Rybach, L., 1981, Geothermal systems, conductive heat flow, geothermal anomalies: in Rybach, L., and Muffler, L. J. P., eds., <u>Geothermal Systems: Principles, and Case Histories</u>: John Wiley and Sons Ltd., p. 3-34.

Scott, W. E., 1980, New interpretations of the Lake Quaternary history of Lake Bonneville, western United States, in Abstracts and Programs 6th Biennial Meeting American Quat. Assoc., p. 168-169.

Serpa, L. F., 1980, Detailed gravity and aeromagnetic surveys in the Black Rock Desert area, Utah: unpublished M. S. Thesis, University of Utah, 211 p.

Sill, W. R., Wilson, W. R., Bodell, J., Ward, S. H., and Chapman, D. S., 1977, Heat flow measurements in southern Utah and northern Basin and Range - Colorado Plateau transition (abstract): EOS, Amer. Geophy. Union Trans., v. 58, p. 1237-1238.

Snow, J. H., 1978, Study of structural and tectonic patterns in south-central Utah as interpreted from gravity and aeromagnetic data: unpublished M. S. Thesis, University of Utah, 245 p.

Stewart, J. H., 1971, Basin and Range structures: a system of horsts and grabens produced by deep-seated extension: Geol. Soc. America Bull., v. 82, p. 1019-1044.

Stewart, J. H., Moore, W. J., and Zietz, I., 1977, East-west patterns of Cenozoic igneous rocks, aeromagnetic anomalies, and mineral deposits, Nevada and Utah: Geol. Soc. America Bull., v. 88, no. IX, p. 67-77.

Stokes, W. L., 1968, Relation of fault trends and mineralization, eastern Great Basin, Utah: Econ. Geology, v. 63, p. 751-759.

Stokes, W. L., 1976, What is the Wasatch Line?, in Hill J. G., editor, Symposium on geology of the Cordilleran Hingeline: Rocky Mtn. Assoc. of Geologists, Denver, Colo., p. 11-25.

Stokes, W. L., 1977, Subdivisions of the major physiographic provinces in Utah: Utah Geology, v. 4, no. 1, p. 1-17.

Stokes, W. L., 1979, Stratigraphy of the Great Basin region, in Neuman G. W. and Goode H. D., eds., Basin and Range Symposium and Great Basin Field Conference: Rocky Mtn. Assoc. of Geologists, p. 195-219.

Swick, C. H., 1942, Pendulum gravity measurements and isostatic reductions: U. S. Coast and Geodetic Survey, Special Pub. No. 232, 82 p.

Talwani, M., Worzel, J. L., and Landisman, M., 1959, Rapid gravity computations for two-dimensional bodies with application to the Mendocino submarine fracture zone: Jour. Geophy. Research, v. 64, p. 49-59.

Thangsupanich, I., 1976, Regional gravity survey of the southern Mineral Mountains, Beaver County, Utah: unpublished M. S. Thesis, Univ. of Utah, 38 p.

Utah Energy Office, 1981, Resource assessment report, Crystal Hot Springs geothermal area: Department of Energy/ET27027-4, 108 p.

White, D. F., and Williams, D. L., editors, 1975, Assessment of geothermal resources of the United States -- 1975: U. S. Geol. Survey Circular 726, compilation of 8 papers, 155 p.

Zietz, I., Bateman, J. F., Case, J. F., Crittenden, M. D., Jr., Griscom, A., King, E. R., Roberts, R. S., and Lorentzen, G. R., 1969, Aeromagnetic investigation of crustal structure for a strip across the western United States: Geol. Soc. America Bull., v. 80, p. 1703-1714.

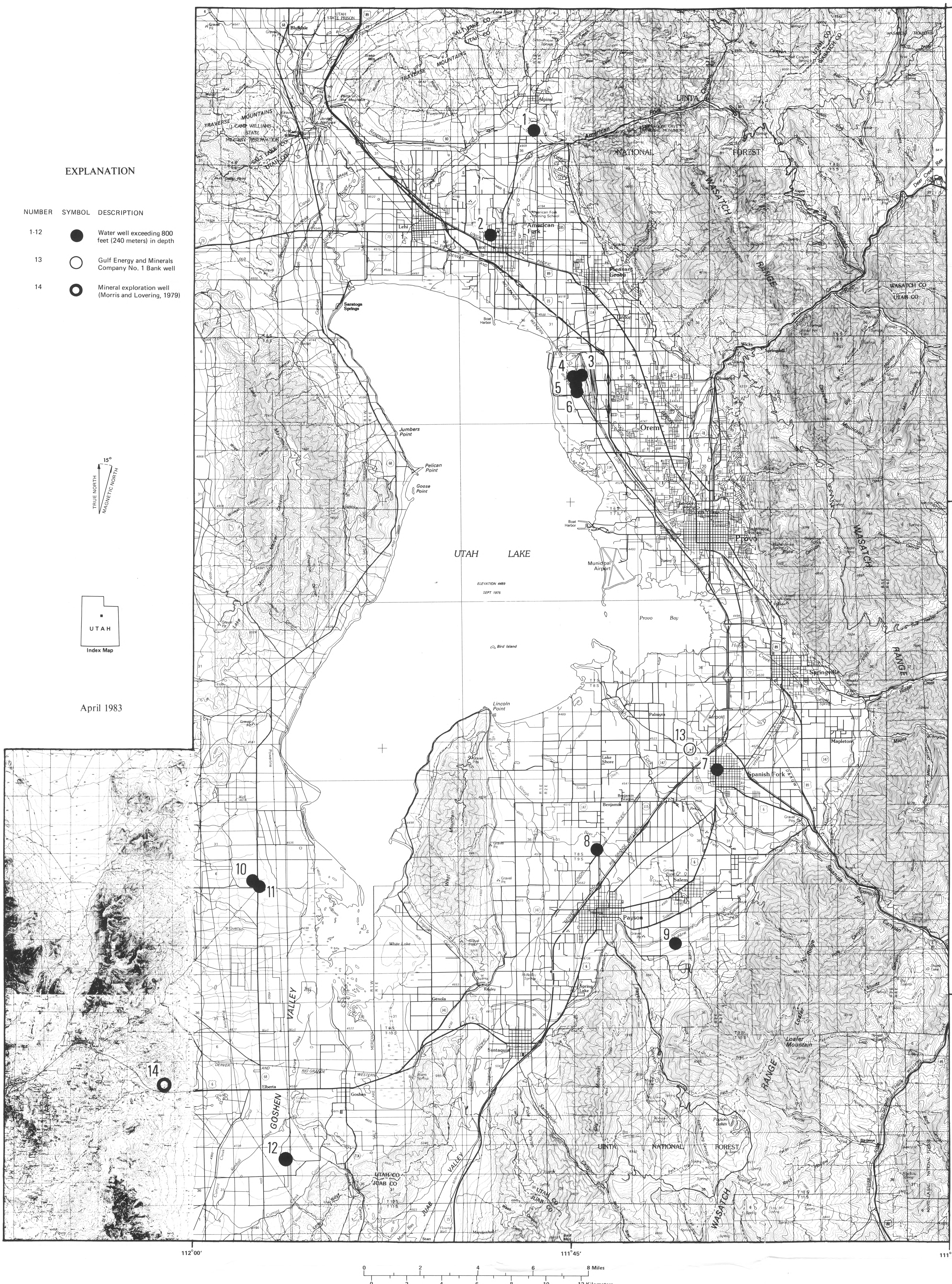

EXPLANATION

NUMBER	SYMBOL	DESCRIPTION
1-12	●	Water well exceeding 800 feet (240 meters) in depth
13	○	Gulf Energy and Minerals Company No. 1 Bank well
14	◎	Mineral exploration well (Morris and Lovering, 1979)

TRUE NORTH
MAGNETIC NORTH
15°

UTAH
Index Map

April 1983

Plate 1

TOPOGRAPHIC MAP OF SURVEY AREA SHOWING WELL LOCATIONS

By Deborah A. Davis and Kenneth L. Cook

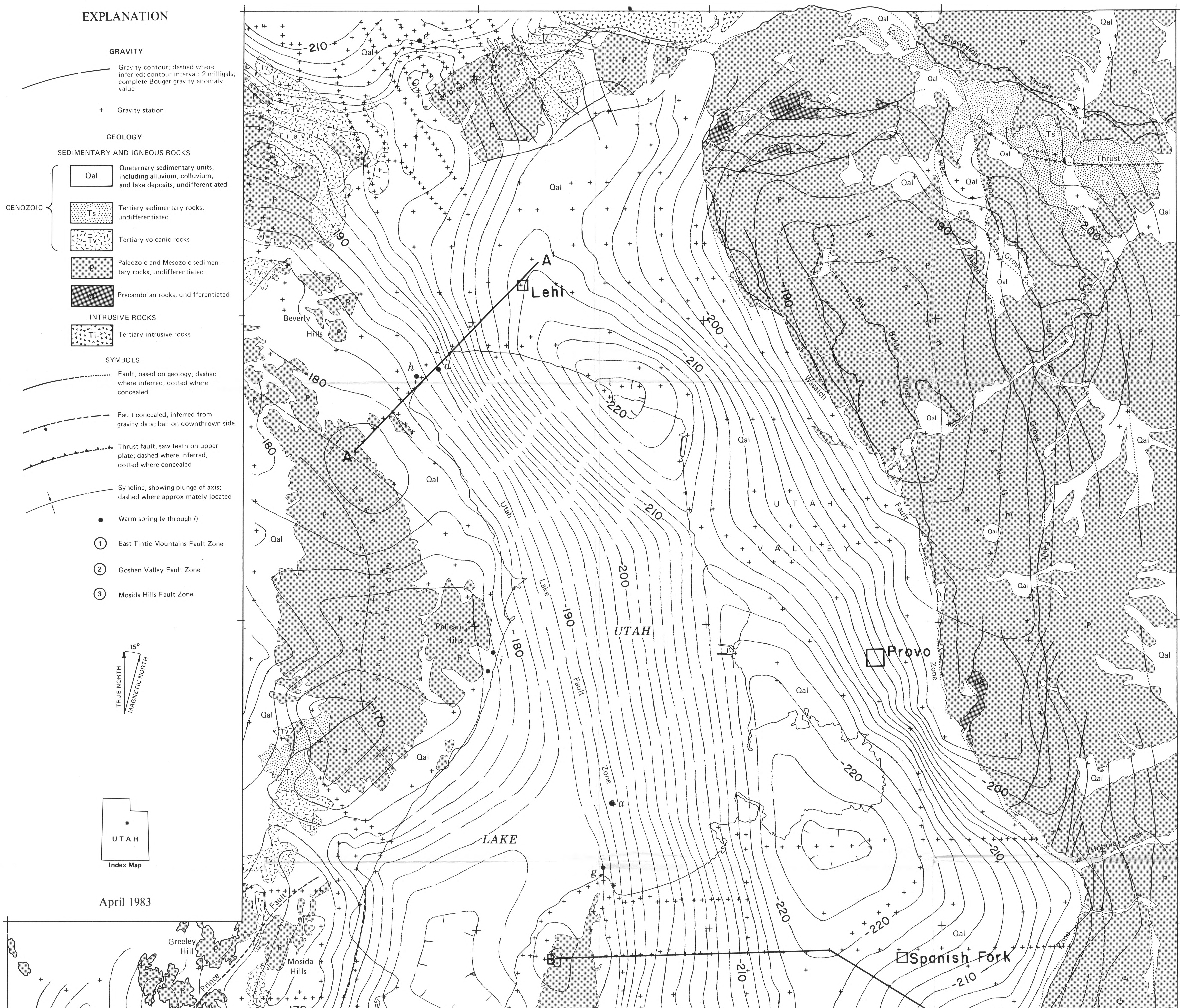

Plate 2

COMPLETE BOUGUER GRAVITY ANOMALY AND GENERALIZED GEOLOGIC MAP OF UTAH AND GOSHEN VALLEYS AND ADJACENT AREAS, UTAH

By Deborah A. Davis and Kenneth L. Cook